

**San Joaquin Valley Drainage Authority**

**San Joaquin River  
Up-Stream DO TMDL Project  
ERP-02D-P63**

**Task 8**

**Linking the San Joaquin River to the Stockton Deep Water  
Ship Channel**

**Draft Final Report**

**April 17, 2008**

Gary M. Litton  
Mark Brunell  
Jordan C. Monroe

Civil Engineering Department  
Department of Biology  
University of the Pacific  
Stockton, CA

Nigel W.T. Quinn

Lawrence-Berkeley National Laboratory  
Berkeley, CA

## **Abstract**

A three-year effort to characterize the presence, transport and fate of algae in the San Joaquin River (SJR) was performed during the summers of 2005 to 2007 as part of a larger study investigating low dissolved oxygen in the Stockton Deep Water Ship Channel (DWSC). Previous investigations show that algae dominate the oxygen demands entering the DWSC during summer months (Lehman et al. 2004). In the present study, the mechanisms controlling algal fate in the San Joaquin River were investigated by characterizing changes in chlorophyll and other water quality parameters and by determining the diversity and abundance of the zooplankton grazing community. Lagrangian monitoring was used to track a parcel of water over a 31 mile non-tidal to tidal reach upstream of the DWSC. A plug-flow reactor model was developed to describe and estimate the relative contribution of potential mechanisms responsible for the decline of algal populations upon entry into the tidal regime of the SJR and the 2 to 3 day travel time to the DWSC. The two dominant mechanisms for the decay of chlorophyll a below Mossdale appear to be zooplankton grazing and the reduction of available light associated with increased river depth. Settling during slack tide periods and dispersion associated with tidal flows may also contribute, but are much less important.

## **Objectives**

The goal of the project is to quantitatively determine the cause of the decrease in chlorophyll and associated oxygen demands between Vernalis and the DWSC. The following objectives are proposed to meet this goal:

- Quantify oxygen demands entering the DWSC.
- Characterize the growth and decay of algae from Vernalis to the DWSC and the dominant mechanisms responsible for there growth and decay.
- Estimate biochemical oxygen demand (BOD) decay and nitrification rates.
- Provide a comprehensive data set for model development and calibration from Vernalis to the DWSC.

While this work seeks to develop a mechanistic understanding of algal processes between Vernalis and the DWSC, utilization of a water quality model may prove necessary to fully explain the generated data. As such, development of a comprehensive data set for model algorithm development and calibration is included as one of the objectives.

Task 9 augments Task 8 by assessing algae grazing and changes in algal populations between Vernalis and the DWSC. A separate interim report has been prepared by Dr. Mark Brunell for Task 9.

## **Background**

The growth and decay dynamics of algae in the San Joaquin River (SJR) reach between Vernalis and the DWSC is poorly characterized despite 2 years of intensive study performed during 2000 and 2001. Contradictory data exist for algal growth and decay between Vernalis and the DWSC (Jones & Stokes 1998; Lehman 2001; Foe, Gowdy, and McCarthy 2002). However, the data do strongly indicate a significant loss of algal biomass downstream of Vernalis and Mossdale (Jones & Stokes 2002; Lehman 2001). Extant DWSC models rely on input data generated at Mossdale, but this model over predicts the chlorophyll entering the DWSC by approximately 3 times and under predicts the dissolved oxygen (DO) by 2 mg/L for 2001 (Jones & Stokes 2002).

The existing monitoring program has been incapable of explaining apparent losses of algal biomass between Mossdale and the DWSC. Estimates were made in 2001 of inflows and diversions to this SJR reach (Quinn and Tullock 2002). However, this work was based on scanty historic information and a boat survey – insufficient to properly characterize the algal dynamics or other mechanisms responsible for the algal decline. The SJR reach between Vernalis and the DWSC is of critical importance since it dictates the loading of live or decaying algae that directly affect oxygen removal from the water column. Tidal effects complicate the dynamics of this reach also and slow the transport of biological material to the DWSC and its passage through the DWSC.

This study will also yield critical input parameters for developing an accurate water quality model of the SJR and DWSC. Continuous monitoring performed over weeklong periods provides information on the diurnal fluctuations in algal loads as well as providing more accurate insight into data noise than has been possible in the past. Previous sampling in this reach has been limited to grab sampling supplemented with continuous monitoring at Mossdale.

## **Approach and Methods**

### *Location of Project*

This component of the 2003 SJR low DO project is located in the SJR downstream of Vernalis and upstream of Channel Point at the DWSC as shown in Figure 1.

### *Approach Overview*

The loss of chlorophyll *a* (chl *a*) may be associated with agricultural diversions, diminished exposure to light as the SJR deepens in the tidal prism of the Delta, dilution (dispersion) of the SJR during flood tides with water from the DWSC that exhibits much lower chl-*a* concentrations, or settling out of the water column. Dye measurements will provide evidence of mass balance and losses and would indicate diversions from the SJR, when used in combination with current and planned flow and water quality monitoring in this reach. Additional self-contained, continuous, monitoring stations will capture additional data including chl-*a*, DO, pH, and water temperature. Light-dark bottle field tests are proposed to quantify algal DO productivity. Long-term BOD bottle tests will quantify DO decay and nitrification rates.

This task is proposed for three years of investigation. The approach is flexible to permit adaptive monitoring within the SJR between Vernalis and the DWSC. During the first year, four monitoring runs will be conducted during each of month from June to September. Only two trials are scheduled for the second year, and one run is proposed for the last year of this study. The monitoring runs are designed to address extant questions about the SJR, but the emphasis on certain study elements will be modified to attempt to resolve new questions that arise as more information becomes available.

Each monitoring run involved four specific tasks:

**Task 8.1:** Deployment of four continuous monitoring sondes at selected locations for approximately 4-5 days while Task 8.2 tasks are performed. The sondes measure water temperature, dissolved oxygen, electrical conductivity, pH, turbidity, chlorophyll *a*, and instrument depth. This subtask will provide a data set for modeling and provide a means for interpreting the results of Task 8.2. The positioning of the monitoring sondes in the SJR is flexible in order to optimize the utility of the data collected. As new data become available, the positioning of the sondes will be tailored to answer specific questions.

**Task 8.2:** Perform Lagrangian monitoring to assess mass losses of a conservative tracer and reactive substances (i.e., algae, BOD, ammonia). Rhodamine WT tracer is released at Vernalis and then followed as this parcel of water flows to the DWSC. In situ measurements of water temperature, dissolved oxygen, electrical conductivity, pH, turbidity, chlorophyll *a*, and rhodamine WT, instrument depth, water depth are collected every 2 seconds and stamped with time and coordinate location. Water samples are collected periodically and analyzed for nitrogen species (NH<sub>3</sub>, NO<sub>2</sub><sup>-</sup>, NO<sub>3</sub><sup>-</sup>, TKN), chlorophyll *a*, pheophytin *a* (ph *a*), total suspended solids (TSS), volatile suspended solids (VSS), and long-term biochemical oxygen demand (BOD), carbonaceous BOD, and nitrogenous BOD.

**Task 8.3:** Augment fieldwork with laboratory assessment of BOD decay and nitrification kinetics. Long-term BOD laboratory trials are performed in a dark, temperature controlled environment.

**Task 8.4:** Field light/dark bottle experiments. Light and dark bottles are suspended at various depths to measure chlorophyll *a* and dissolved oxygen production as a function of light. Light intensity is measured as a function of depth during the deployment of the bottles.

### *Water Quality Measurements*

#### Continuous Water Quality Measurements

Tasks 8.1 and 8.2 were performed with multiparameter sondes manufactured by Hydrolab, Inc. or Yellow Spring Instruments (YSI, Inc.). These instruments were previously described in Task 4: Monitoring. Calibration was performed per standard methods (APHA 1998, APHA 2005) or manufacturer's specifications and checked periodically in the field or at the end of deployment. The data acquisition frequency was set to 15 minutes. Continuous measurements performed from the monitoring boat utilized a YSI 600 XL sonde with separate SCUFA fluorometers for chlorophyll *a* and rhodamine WT. During the 2006 trials, a second YSI 6600 sonde with temperature, EC, pH, DO, chlorophyll fluorescence, and turbidity sensors was also deployed on the boat to serve as a backup.

#### Discrete Water Sample Collection and Analysis

All the tasks will require the collection of water samples for constituent quantification. Sampling will be performed by manual grab methods or peristaltic pumps. Analysis will be performed in accordance with standard methods (APHA 1998, APHA 2005). TSS and VSS will be performed by SMs 2540 D and E, respectively. However, trials will be performed with filters required for chl *a* (SM 10200H) instead of filters required by SMs 2540 D and E to obtain better correlations among VSS, chl *a*, and BOD. Filter pore sizes for TSS and VSS can be significantly larger than pore sizes of filters specified for chl *a* analysis. Chl *a* and pha *a* will be extracted using an acetone/water solution and UV absorption in accord with SM 10200H. Biochemical oxygen tests will be of a long-term nature (SM 5210 C) to facilitate determination of decay rate constants.

### *Detailed Task Descriptions*

#### ***Task 8.1: Deployment of Continuous Recording Sensors***

Four additional monitoring sites on the SJR were instrumented between Vernalis and the DWSC. These locations are flexible and will be changed as new information becomes available. Continuous water quality sondes (Hydrolab 5SDX, Hach Inc., Boulder, CO), measuring chl *a*, turbidity, EC, pH, DO, and water temperature were deployed at four locations for approximately 1 week once a month from May to October. The deployment coincides with the Lagrangian dye tracking measurements. These sondes capture the diurnal patterns of algal growth and decay allowing advective transport of algae to be

separated from tidal transport and more careful mass accounting of algal loading in this SJR reach. These stations also yield important data sets for model calibration.

### ***Task 8.2: Lagrangian Monitoring***

In addition to the in-river, continuous sensors, a slug of rhodamine WT dye will be dispersed uniformly across the SJR and tracked downstream by boat. Monthly injections of dye and deployment of the light-dark bottle experiments are proposed from May to October. In situ measurements of dye concentration, chl *a*, pH, DO, turbidity, water temperature, water depth, and instrument depth will be captured electronically with their GPS coordinate location. Figure 2 presents a photograph of the monitoring boat and a schematic diagram of the equipment required for this task. This system permits the simultaneous collection of all data from five different instruments every second. These data are processed in real-time and displayed graphically using MATLAB (MathWorks, Natick, MA). This system permits accurate accounting of dye mass in the SJR and precise characterization of chl *a*, DO, and other parameters in the SJR. For example, bathymetry measurements will yield water depth information that may be correlated to the growth and decay of chl *a* in the reach between Vernalis and the DWSC.

To augment the continuous monitoring, discrete water quality samples were also collected for quantification of chl *a*, pha *a*, VSS, TSS, BOD, CBOD, and verification of in situ turbidity, DO, pH, chl *a* measurements. As shown on Figure 2, discrete water samples can be collected at a prescribed water depth using 5/16-inch-inner-diameter tubing attached to a peristaltic pump (MasterFlex, Cole-Parmer Instrument Company, Vernon Hills, IL). Mass balance applied to the longitudinal measurements of inorganic solids will be used to assess net losses associated with settling.

These monitoring efforts will be coordinated with other water tracking studies proposed in the river above Vernalis so the same water parcel and associated changes in water quality and algal populations can be followed from the upper San Joaquin River to the DWSC. It is anticipated that each full river dye tracking study will require 4 to 5 continuous days of extensive field work. Water samples collected during these trials will be periodically transported to the laboratory and processed or preserved as appropriate.

### ***Task 8.3: BOD Decay and Nitrification Rates***

The BOD and CBOD tests were performed over 20 days to determine kinetic decay rate constants of BOD, CBOD, and NBOD. The rate of NBOD decay will also be evaluated by monitoring the ammonia and nitrate concentrations when ammonia concentrations exceed 0.5 mg/L. Direct measurements will be made of ammonia oxidation rates as a function of time will be made using Clark-type electrodes. The data from these experiments will be used to determine more accurately the liability of the soluble ammonia in this SJR reach. Understanding and predicting how fast ammonia is oxidized in this region is important to assigning the oxygen demand allocation between algal biomass and ammonia. These tests are scheduled to augment the Lagrangian dye tracking investigations.

#### ***Task 8.4: Light-Dark Bottle Experiments***

As part of the Lagrangian studies, light-dark bottle experiments were also performed to assess whether the apparent decay of algal biomass from Mossdale to the DWSC may be associated with reduced exposure to light as the river channel depth increase within the tidal prism. Previous studies have shown that algae collected in the SJR 1 mile above the DWSC decay extremely rapidly when kept in darkness (Litton 2002). To assess the impact of light reductions, light-dark bottles were suspended from a buoy at various depths while following the dye slug. Light intensity will be measured at each depth periodically. The pH, DO, chl-*a*, and pha-*a* concentrations will be quantified for the light-dark bottle experiments. These tests assess whether light limitation is a significant cause of the chl-*a* decay between Mossdale and the DWSC. These data also yield algal productivity and DO response curves as a function of light intensity, data critical for modeling this SJR reach.

## **Results and Discussion**

### **Status of Work**

The following elements of Task 8 have been initiated or completed.

- Bathymetric survey along the approximate river thalweg from Vernalis to the DWSC.
- Lagrangian and fixed-location sonde water quality monitoring was performed in July, August, September, and October of 2005, July and August, 2006, June, 2007. Near zero low net flows to the DWSC after June, 2007 required that longitudinal measurements be performed every 2 to 4 miles from the DWSC to the HOR instead of the Lagrangian monitoring.
- Light-dark bottle experiments were deployed in all three of the study years.
- Long-term BOD tests were conducted with all the lagrangian and longitudinal monitoring performed from 2005 to 2007.
- Provisional data sets are available for the three years of the study. Final data sets will be available with completion of the final report.
- Development of a numerical model to interpret the results of the Lagrangian water quality trackings has been developed.

A detailed map of the study reach is presented in Figure 3 for the San Joaquin River from Vernalis to the DWSC. Also shown on Figure 3 are the locations of the discrete water and plankton sampling. Table 2 contains sampling dates, times and coordinate data for these locations.

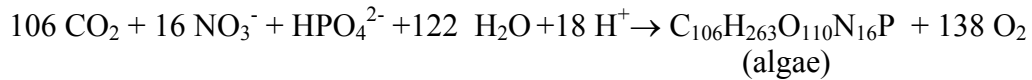
The Task 8 field investigation was scheduled to start in May, 2005. However, extremely high flows in the San Joaquin River postponed the work until July as this condition yields short travel times and data sets that were not representative of the river during periods of critical DO levels in the DWSC. Monitoring was again postponed in 2006 until July due to extremely high flows. Only two trials were performed in 2006 due to the persistent high flows. Resources were conserved in the event that lower, and therefore, more representative flow would return in 2007. The flow conditions of 2007 proved to be more representative than 2005 and 2006. Net flows declined to zero for most of July and August, 2007. A comparison of the 2004, 2005, 2006, and 2007 flows measured at Vernalis are presented in Figure 4 and show that May and June flows were in excess of 10,000 cfs for both 2005 and 2006. The flow during these time periods is often between 1000 and 2000 cfs. Figures 5, 6, and 7 provide a comparison of San Joaquin River flow at Vernalis and at Garwood Bridge for 2005, 2006, and 2007, respectively. The base

river flow entering the DWSC was approximately 1000 cfs in 2005, but exceeded 1500 cfs during most of the summer of 2006. In 2007, the net flow entering the DWSC was approximately 800 cfs, but after July 15 the net flow fluctuated around zero until September. Previous studies have shown that dissolved oxygen concentrations remain above water quality objectives when net flows entering the DWSC exceed 1500 cfs (Foe *et al.*, 2002).

## **Water quality measurements from Vernalis to the DWSC.**

### *Task 8.1 Deployment of Continuous Recording Sensors*

Four water quality sondes were deployed at the Vernalis, Midway, Mossdale, and Brandt Bridge stations shown previously in Figure 1. Examples of the dissolved oxygen, pH, and chlorophyll *a* results are shown in Figures 8 and 9 for the Midway and Brandt Bridge stations, respectively. Algal productivity is clearly shown in the diel variations of chlorophyll *a*. During daylight hours chlorophyll *a* levels increase until approximately 4:00 PM and then decrease during the night. The dissolved oxygen and pH also respond to this algal production and respiration. Shown in the chemical representation below, the production of algae will yield higher DO and pH levels in the water.



The pH increases from the consumption of 18 hydronium ions for each algal cell produced. A quantitative analysis of the production of algae and dissolved oxygen and the consumption of carbonate minerals has been initiated with all the data sets collected for 2005, 2006, and 2007. An approach similar to that presented later in this report for light-dark bottle data analysis will be used with the algal-zooplankton model to better interpret data sets and assist with water quality modeling efforts. The data from the fixed sondes augments the results of the Lagrangian monitoring completed as Task 8.2. Data sets of all fixed sondes deployed in conjunction with the Lagrangian monitoring have been made available.

### *Task 8.2 Lagrangian monitoring*

Five trials have been performed to track a water parcel from Vernalis to the DWSC in 2005 and 2006. A sixth trial started at the Head of Old River (HOR) instead of Vernalis in August, 2006 due to the abnormally high flows. This trial focused on assessing spatial temporal variations in zooplankton populations. Details of the results of the plankton measurements are contained in the Task 9 annual report. The flows of 2007 were much lower than those observed in the previous two years. One lagrangian tracking was conducted from Vernalis to the DWSC in June, 2007. The near zero net flow below the HOR prevented additional lagrangian trials for the remainder of the summer as the travel

time exceeded 10 days. Instead, longitudinal monitoring was performed in July, August, and September during slack tide periods from the DWSC to the HOR.

### *Lagrangian tracking results*

The lagrangian monitoring was initiated by dispersing Rhodamine WT dye into the San Joaquin River and tracking it to the DWSC with a fluorometer collecting data at regular intervals (2 to 60 sec). In July 2005, the travel time to the DWSC was approximately 32 hours at a Vernalis flow rate of approximately 4500 cfs. The San Joaquin River flow splits at the Head of Old River, with approximately 1800 cfs continuing to the DWSC as measured at the Garwood Bridge USGS station (station code SJG at [cdec.water.ca.gov](http://cdec.water.ca.gov)). These flows are much higher than flows observed during drier water years and yield a relatively fast travel times. The river mile associated with the sample locations and collection times are presented in Table 2. The low net flows observed during 2007 prevented implementation of the Lagrangian monitoring in July, August, and September, as it would take theoretically an infinite amount of time to travel from the HOR to the DWSC. During these months, longitudinal monitoring was performed every 2 miles from the HOR to the DWSC to assess water quality changes. The 2007 schedule of monitoring events is presented in Table 3.

Dispersion attenuates the peak tracer concentration as the dyed water moves downstream. In addition, approximately 60 percent of the water dyed at Vernalis flowed down Old River and never reached the DWSC. As such, for each lagrangian trial starting at Vernalis, the tracer plume was replenished below the Head of Old River.

The response of chlorophyll *a* in the dyed parcel of water that flowed to the DWSC is shown in Figure 10 for the July, 2005 trial. Similar to the chlorophyll *a* data measured by the fixed sondes, these data also exhibit a diel pattern where chlorophyll *a* increases during the day and decreases by night. Figure 9 also contains chlorophyll *a* data measured in the laboratory from discrete water samples. The pH and DO data are also consistent with the chlorophyll results behavior. The pH and DO increase or decrease with chlorophyll production or respiration. As with the fixed sonde data, additional analyses will be performed to evaluate whether chemical stoichiometry and light intensity can be used to simulate these responses in DO and pH.

Figure 11 plots the extracted pigment concentrations of chlorophyll *a* and pheophytin *a*. Also presented is the fraction of chlorophyll *a* relative to the sum of these two pigments. As shown in Figure 11, the chlorophyll *a* fraction remains high throughout the transport to the deep water ship channel, indicating that the algal community is in excellent physiological condition. This was not the case for the months of August, September and October, 2005 shown in Figures 12-17. Similar data sets have been generated during the monitoring performed in July and August, 2006 are shown in Figures 18-21.

As shown in Figures 18 and 19, the July, 2006 chlorophyll *a* data was not consistent with that observed in 2005 for July. Chlorophyll *a* concentrations decreased from about 70  $\mu\text{g/L}$  at Mossdale to 40  $\mu\text{g/L}$  at the DWSC. The total pigment concentration remained

relatively constant in the study reach, but the chl *a* to total pigment ratio decreased from about 0.7 above Mossdale to 0.4 at the DWSC indicating the deteriorating physiological state of the algae. This deterioration was not as pronounced in August, 2006 for the trial started at the Head of Old River (HOR). The chl*a*/total pigment ratio was fairly uniform at 0.8 from the HOR (RM 53.6) to the DWSC (RM 40) and chlorophyll *a* values exhibited the typical increase during the day and decline during night. These data sets will be further analyzed with the algae-zooplankton model presented later in this report.

Even though river flows were relatively high in 2005 and 2006, some patterns observed between Vernalis and Mossdale in past years emerged. As shown earlier in Figure 10 for the July monitoring, chlorophyll *a* concentrations exhibited a strong diel signal with dramatic increases observed during daylight hours followed by significant declines at night. A highly correlated response was observed in pH and dissolved oxygen data. As presented in Figures 12, 14 and 16 for 2005 trials, diel fluctuations decreased with each successive month as the chlorophyll *a* concentrations decreased from a maximum of 70 µg/L in July to less than 5 µg/L in October. For example, dissolved oxygen concentration varied from about 7 to 12 mg/L from early morning to late afternoon in July above Mossdale Crossing. In contrast, less than 1 mg/L of variation of DO was observed in October.

With the exception of July 2005 and August 2006, each dye tracking trials measured a decay of chlorophyll *a* below Mossdale. As shown in Figures 10 and 11, chlorophyll *a* concentrations remained relatively constant and above 50 µg/L during the July tracking. In August, a decrease from 35 to 20 µg/L was observed between Vernalis and the DWSC (Figures 12 and 13). September and October trials yielded similar results with a decline from about 15 to 5 µg/L as shown in Figures 13 to 16. Dissolved oxygen and pH exhibited similar trends. Observations in July, 2006 exhibited a similar decline in chl *a* in route to the DWSC below Mossdale.

In addition to the decrease in chlorophyll *a* observed below Mossdale, the physiological health of the algal community also significantly declined in this reach during all months, except July, 2005 and August, 2006. Using chlorophyll *a* and pheophytin *a* pigment concentrations as a guide to assess the productive condition of the algae, the fraction of chlorophyll *a* to the total pigment concentration also decreased significantly below Mossdale. As shown in Figure 13 for August, 2005 the chlorophyll *a* fraction decreased from 0.9 to 0.6. During September and October the decline was more dramatic, the chlorophyll *a* fraction was approximately 0.75 at Vernalis and only 0.3 at the DWSC (Figures 15 and 17). In addition to the decline of chlorophyll *a* below Mossdale, the total pigment concentration also decreases significantly as exhibited in Figures 10 through 17. With the exception of July, these observations show significant losses in the size and health of the algal community while flowing from Mossdale to the DWSC. The June, 2007 lagrangian monitoring results for chlorophyll and dissolved oxygen are presented in Figure 22. The travel time to the DWSC from Vernalis was over 65 hours for this trial. Diel effects were strongest in the upper river, but evident throughout the 31 mile reach. For example, chlorophyll *a* concentrations increased from approximately 40 to 80 µg/L from 8:30 in the morning to sunset on June 12. Also shown in Figure 22 was

the effect on dissolved oxygen associated with algal productivity during the day and respiration at night. The previously discussed increase in chlorophyll a on June 12 yielded a rise in dissolved oxygen from 10 to 15 mg/L. As shown throughout the June, 2007 tracking, the rise and fall of chlorophyll and dissolved oxygen are well correlated with diel influences. Figure 23 is presented to illustrate the effect of increased water depth to measured chlorophyll a and pheophytin a concentrations. Above Mossdale the average water depth is often about 5 ft, this corresponds with the depth of the photic zone, defined as the depth at which 1 percent of the incident light penetrates the water column. Below Mossdale, the average river depth increases from about 10 ft to 15 ft over 14 miles. The river then transitions from depths of 15 ft to 40 ft in the DWSC. With the deepening of the well-mixed San Joaquin River above the DWSC, the algae spend less time in the photic zone, an observation that appears to influence the reduced production of chlorophyll a and oxygen during the daylight periods. In Figure 23, the chlorophyll a decay product, pheophytin a, is also observed to increase, suggesting that light limitation in deeper waters is adversely effecting the physiological health of the algal community.

This effect is better shown in Figure 24 where the chlorophyll a to total pigment ratio is plotted for the June, 2007 tracking from Vernalis to the DWSC. In this plot the decline in the pigment ratio approximately parallels the average water depth of the San Joaquin River. While light limitation associated with increased river depth appears to influence the algal community, the decline in the pigment ratio is also associated with the rise in the zooplankton population as presented in Figure 25. Approximately exponential growth of the zooplankton concentration appear to be strongly correlated to the decline in the chlorophyll and the increase in the pheophytin concentration. Zooplankton microcosm experiments presented later will show that algal losses due to grazing yields increases in pheophytin. These June, 2007 observations provide some of the best evidence that light limitation and zooplankton grazing are dominant mechanisms controlling the algal community while it is being advectively transported below Mossdale to the DWSC.

As discussed earlier, longitudinal monitoring of the San Joaquin River at discrete locations between Mossdale and the DWSC were performed in July, August, and September of 2007 when the net flow fluctuated around 0 cfs. For these flow conditions, the advective transport of algae and other oxygen demanding substance is effectively zero and dispersive transport mechanisms dominate. The dissolved oxygen, ultimate BOD, extracted chlorophyll a, and the pigment ratio are presented in Figures 26 and 27 for the longitudinal monitoring performed during slack tide periods. These results exhibit a linear change in concentration from the HOR to the DWSC that is characteristic in dispersion dominated waters. For example, the dissolved oxygen decreased from about 11 mg/L at the HOR to 5 mg/L at the DWSC. The variation in the concentration at a fixed location is influenced by tidal flows and the time of day. Note that higher concentrations of DO were measured in early evening and the lowest concentration were observed in early morning. The changes in BOD shown in this figure will be discussed later with Task 8.3 results.

As shown in Figure 27, the chlorophyll a concentration declines dramatically below the SBC site, located approximately 5 miles above the DWSC. These data suggest that the extent of tidal excursion up the San Joaquin River from the DWSC is about 5 miles. Ebb flows push the high chlorophyll a levels to rm44 while the flow reversal occurring with flood tide provide low chlorophyll a water coming from the DWSC up to rm 46. The effect on the physiological health of the algae community, as measured by the pigment ratio, also exhibits a decline between the HOR and the DWSC. Pigment ratios decrease from 0.8 to 0.4 over this 14 mile reach of the San Joaquin River. While not shown here, this drop in chlorophyll a and the pigment ratio has been shown to be correlated to peak concentrations in the zooplankton population (Litton and Brunell, 2008).

The longitudinal monitoring was also performed in August and September and the results are displayed in Figures 29 to 31. The behavior in observed with dissolved oxygen, chlorophyll a, and pigment ratio during these months was similar to that observed and discussed for the July, 2008 longitudinal monitoring.

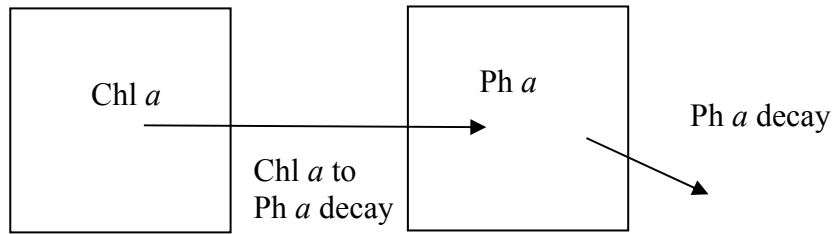
To further quantify the effect of zooplankton grazing on the algae community, two zooplankton microcosm experiments were performed in late September and early October. The results shown in Figure 32 indicate that concentrated zooplankton populations can dramatically reduce the chlorophyll a concentration and rise the pheophytin a levels. These microcosms were maintained in the photic zone for 4.5 hours prior to remeasurement. The control microcosm received no additional zooplankton and after 4.5 hours the chlorophyll a concentration had doubled from 65 to 130 ug/L. However, the microcosm seeded with a high concentration of zooplankton exhibited a net decrease in chlorophyll of approximately 20 ug/L. These tests also suggest that the consumption of algae by zooplankton results in a transformation of chlorophyll a to pheophytin a, and some of the pheophytin pigment survives the digestive processes of the zooplankton.

Figure 33 presents more results of microcosm tests performed on October 3, 2007. In this test the chlorophyll a and pheophytin a was monitored every 1.5 hours by removing 2 microcosm bottles (with and without zooplankton seed) from the water column and sampling for chlorophyll a and pheophytin a. For these tests algal productivity was inhibited by placing the bottle below the photic zone. These experiments indicated that the zooplankton were responsible for decreasing the chlorophyll a concentration from approximately 50 to 35 ug/L after 6 hours. During this time the pheophytin a concentration increased from 20 to 40 ug/L. These tests also support the observation that chlorophyll a is transformed to pheophytin when ingested and excreted by zooplankton. The kinetic rates estimated with these experiments for zooplankton grazing were used later in the modeling efforts used to assess the relative contribution of grazing on the chlorophyll a decline below the HOR.

Laboratory microcosm tests were also performed to assess chlorophyll a and pheophytin a decay when algae are subjected to darkness. These experiments were performed with water collected from Mossdale (MSD), Brandt Bridge (BDT), Stockton Brick Company (SBC), and the Outfall Pier (OP) on August 1, 2007. Each sample was maintained in

darkness at 20°C for 13 days. Periodically, the samples were collected from the microcosms and measured for chlorophyll *a*, pheophytin *a* and algal fluorescence. The algal fluorescence was best correlated to chlorophyll *a* and not total pigment concentrations (chlorophyll *a* plus pheophytin *a* concentrations). As such the chlorophyll fluorescence was calibrated with the extracted chlorophyll *a* concentrations and plotted in Figures 34 to 37 with the extracted pigment concentrations. These data shown a rapid decline in chlorophyll *a* when subjected to extended darkness.

To assess the kinetic rates of chlorophyll *a* and pheophytin *a* a simple mass balance conceptual model for the water samples appears below for the concentration of chlorophyll *a* and pheophytin *a*. In box 1, chlorophyll *a* decays to pheophytin *a* according to an assumed first-order rate law. In box 2, the pheophytin *a* concentration is influenced by the rate of decay of chlorophyll *a* to pheophytin *a* (increases the pheophytin *a* concentration) and the decay of pheophytin *a*. Pheophytin *a* is also assumed to decay at a first-order rate.



Governing

Equations: 
$$\frac{d(Chla)}{dt} = -k_c Chla \qquad \frac{d(Pha)}{dt} = A_{c \rightarrow p} \frac{d(Chla)}{dt} - k_p Pha$$

Solutions:

$$Chla = (Chla_0)e^{-k_c t} \qquad \text{(eq. 1)}$$

$$Pha = (Chla_0)A_{c \rightarrow p} \frac{k_c}{k_p - k_c} [e^{-k_c t} - e^{-k_p t}] + (Pha_0)e^{-k_p t} \qquad \text{(eq. 2)}$$

Where:

- Chla* = chlorophyll *a* concentration at time *t*
- Chla*<sub>0</sub> = initial concentration of chlorophyll *a*
- Pha* = pheophytin *a* concentration at time *t*
- Pha*<sub>0</sub> = initial concentration of pheophytin *a*
- A*<sub>*c*→*p*</sub> = chlorophyll *a* to pheophytin *a* mass conversion factor (set to 1)
- k*<sub>*c*</sub> = first-order decay rate of chlorophyll *a*
- k*<sub>*p*</sub> = first-order decay rate of pheophytin *a*

Samples in excellent physiological conditions are considered to contain no pheophytin *a* (APHA 1998, 2005). Chlorophyll *a* is converted to pheophytin *a* upon loss of the

magnesium atom. Regression expressions for the spectrophotometric determination of chlorophyll *a* indicate that 1 µg/L of pure chlorophyll *a* is converted to 1 µg/L of pure pheophytin *a* upon complete loss of its magnesium atom (APHA 1998, 2005). Therefore,  $A_{c \rightarrow p}$ , was set to 1 for the analysis presented here.

The samples collected from the San Joaquin River exhibited aging upon collection as indicated by the presence of pheophytin *a*. To adjust for this deterioration before reaching the DWSC, the time was adjusted by  $\Delta t$ , in the modified solutions for chlorophyll *a* and pheophytin *a* concentrations:

$$\text{Chl } a = \text{Chl } a_0^a \exp(-k_c t + \Delta t) \quad (\text{eq. 3})$$

$$\text{Ph } a = k_c \text{Chl } a_0^a A_{c \rightarrow p} / (k_p - k_c) [ \exp(-k_c(t + \Delta t)) - \exp(-k_p(t + \Delta t)) ] \quad (\text{eq. 4})$$

Where,  $\text{Chl } a_0^a$  is the estimated concentration of chlorophyll *a* when the population was in excellent physiological condition. Under this condition the initial pheophytin *a* concentration,  $\text{Ph } a_0$ , is zero. The data for the two decay rate experiments performed with water collected from the San Joaquin River are shown in Figures 34 to 37. Decay constants of  $0.55 \text{ d}^{-1}$  for  $k_c$  and  $0.27^{-1}$  for  $k_p$ , were found to provide a reasonable fit of the model to both sets of experimental data in past studies (Litton, 2002). These constants were subsequently used in modeling efforts presented later.

### ***Task 8.3: BOD Decay and Nitrification Rates***

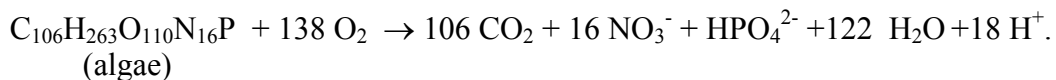
During the tracer transport to the DWSC samples were also collected to assess the biochemical oxygen demand of the water. Nitrification rate kinetic experiments were also scheduled if ammonia concentrations exceeded 0.5 mg/L as N. All ammonia concentrations were measured below the detection limit of 0.05 mg/L, except at the City of Stockton outfall which is only one mile above the DWSC. Thus, nitrification rate tests were not performed with the samples collected in 2005, 2006 and 2007.

Long-term BOD experiments were performed at selected sample stations between Vernalis and the DWSC. The carbonaceous component of the BOD was measured by inhibiting nitrifying bacteria with 2-chloro-6-(trichloro methyl) pyridine (TCMP). The nitrogenous BOD was determined by subtracting the CBOD from the BOD. An example of the BOD test results are shown in Figure 38. The individual BOD and CBOD results from all three years are presented in Appendix A. Correlations with an approximate first-order fitting equation were generally excellent as most regression coefficients were greater than 0.95. A comparison of the  $\text{BOD}_{10}$  with the estimated  $\text{BOD}_{\text{ult}}$  is shown in Figure 39. Plots of the 20-d BOD measured from water samples collected between Vernalis and the DWSC during 2005 and 2006 are presented in Figure 40 and show little change in the 31-mile reach suggesting that the decay of algae below Mossdale has a limited effect on the exertion of the associated BOD. However, the relatively high flows encountered in the field investigation to date may best explain the uniformity of the

BOD results. The 20-d BOD data for 2006 are also approximately twice the concentration measured in 2005.

The ultimate BOD results of the June, 2007 lagrangian tracking indicate that the BOD is correlated to the chlorophyll a data presented earlier in Figure 25. Between Vernalis and rm62 the BOD<sub>ult</sub> increased from approximately 7.5 to 13 mg/L. In this same reach the chlorophyll a increased from about 40 to 80 mg/L. Beyond rm 62 both the BOD<sub>ult</sub> and the extracted chlorophyll reached a plateau at about 12 mg/L and 70 mg/L, respectively. Approaching the DWSC, the BOD and the chlorophyll declined sharply within 1 mile of the DWSC. This correlation is also evident in the longitudinal profiles shown earlier in Figures 27-31.

The data also suggest that about 30 percent of the BOD is nitrogenous as presented in Table 4 for the July, 2005 lagrangian monitoring. However, total ammonia was undetected during the transport to the DWSC as shown in Table 4. These results were typical of BOD results observed throughout the study as shown in Appendix A. The NBOD appears to originate from the algae that decay during the BOD test. A common chemical expression of algae decomposition provides estimates of its associated CBOD and NBOD:



Thus, each mg/L of algae will yield a theoretical oxygen demand of 1.2 mg/L. Of this 1.2 mg/L, approximately 25 percent is nitrogenous.

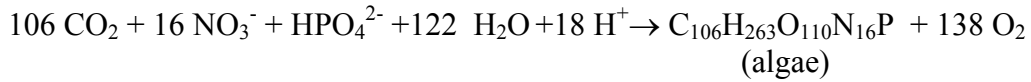
#### ***Task 8.4: Light-Dark Bottle Experiments***

Light-dark bottle tests were conducted during the lagrangian monitoring performed in 2005, 2006, and 2007 during daylight and night time periods and during the longitudinal monitoring conducted from July to September, 2007. The results of these experiments can be integrated into the water quality analytical model independently of Task 8. The data presented for July, 2005 is typical of other trials performed in subsequent months and years.

Light-dark bottle experiments were performed by suspending 2-L BOD bottles or 1-L polycarbonate bottles at depths of 1-ft intervals from a buoy. A dark bottle was also suspended to evaluate algal respiration. A filtered water sample was also placed in darkness to correct for the dissolved oxygen uptake associated with soluble oxygen demanding substances. Data collected in July for an experiment performed below Vernalis is presented in Table 5. The bottles were incubated for approximately 4.5 hours during midday. Chlorophyll *a* concentrations increased from 54 to 88 ug/L for the bottle placed at a depth of 1 ft. Photosynthesis occurring in this microcosm resulted in an increase of the dissolved oxygen from 8.6 to 14.3 mg/L. Consumption of carbonate minerals also increased the pH over 1 unit. In contrast, the bottle maintained in darkness exhibited a decrease in chlorophyll *a*, DO and pH due to algae respiration and decay.

The light intensity was also measured as a function of depth. Combining the light intensity measurements with the data presented in Table 5 yields a productivity-intensity (PI) curve that can be used to estimate DO production. Figure 42 presents the PI curve generated for the July light-dark bottle trial.

The production of chl a can also be estimated from the chemical representation for the growth of algae.

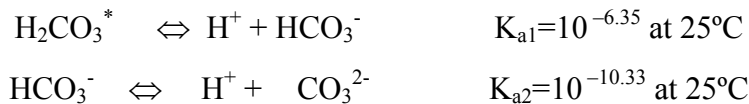


The production of algae will yield an increase in dissolved oxygen and pH, and a decrease in the total carbonate species concentration. Total carbonates,  $C_{T,\text{CO}_3}$ , is the sum of dissolved carbon dioxide gas ( $\text{CO}_2$ ), carbonic acid ( $\text{H}_2\text{CO}_3$ ), bicarbonate ( $\text{HCO}_3^-$ ), and carbonate ( $\text{CO}_3^{2-}$ ). The total carbonate concentration was calculated from the total alkalinity and the pH of the solution.

The change of the pH is also regulated by the following carbonate species that serve to buffer the pH of water when acids or bases are added. The sum of these species concentration is the total carbonate concentration,  $C_T$ .

$$C_T = [\text{CO}_{2(aq)}] + [\text{H}_2\text{CO}_3] + [\text{HCO}_3^-] - [\text{CO}_3^{2-}]$$

Since  $\text{CO}_{2(aq)}$  is approximately 1000 times greater than  $\text{H}_2\text{CO}_3$  it is common to combine these species as  $\text{H}_2\text{CO}_3^*$  yielding the following chemical equilibrium.



When alkalinity is dominated by the presence of carbonate species, the initial alkalinity and pH of the water can be used to calculate the initial total carbon concentration.

$$\text{alkalinity} = C_T (\alpha_1 + 2\alpha_2) + [\text{OH}^-] - [\text{H}^+] \quad (2),$$

where,  $\alpha_1$  and  $\alpha_2$  are the ionization fractions for  $\text{HCO}_3^-$  and  $\text{CO}_3^{2-}$ :

$$\alpha_1 = \frac{K_{a1}[H^+]}{[H^+]^2 + K_{a1}[H^+] + K_{a1}K_{a2}},$$

$$\alpha_2 = \frac{K_{a1}K_{a2}}{[H^+]^2 + K_{a1}[H^+] + K_{a1}K_{a2}}.$$

The equilibrium constants,  $K_{a1}$  and  $K_{a2}$ , are dependent on the ionic strength and temperature of the water. Temperature correction for the equilibrium constants were performed with Van't Hoff's equation.

$$\ln \frac{K_{25}}{K_i} = \frac{\Delta H^\circ}{R} \left( \frac{1}{T_i} - \frac{1}{T_{25}} \right)$$

Where,  $\Delta H^\circ$  is the standard change of enthalpy for the specific chemical reaction,  $R$  is the universal gas constant,  $T_i$  and  $T_{25}$  are the absolute temperatures at temperature  $i$  and 25°C, and  $K_{25}$  and  $K_i$  are the equilibrium constants at 25°C and temperature  $i$ .

The salinity of water will also affect chemical equilibrium. The ionic strength,  $\mu$ , of water can be estimated from the specific conductance or total dissolved solids (SC; Russell, 1976; Lind, 1970).

$$\mu = 1.6 \times 10^{-5} \times \text{SC } (\mu\text{mho/cm})$$

$$\mu = 2.5 \times 10^{-5} \times \text{TDS (mg/L)}$$

The SC of the San Joaquin River typically ranges from 600 to 900  $\mu\text{mho/cm}$  and the TDS varies from approximately 250 to 650 mg/L. A value of 600  $\mu\text{mho/cm}$  yields an ionic strength of approximately 0.01, a level at which the equilibrium constants should be adjusted. The adjustment is achieved with the activity coefficient of each species in the solution. For example, a pH electrode measures the hydronium ion activity in water:

$$\{\text{H}_3\text{O}^+\} \equiv \{\text{H}^+\} = \gamma_{\text{H}^+}[\text{H}^+],$$

where,  $\{\text{H}^+\}$  is a shorthand notation for the hydronium activity,  $[\text{H}^+]$  is the molar hydrogen ion concentration, and  $\gamma_{\text{H}^+}$  is the activity coefficient for the hydrogen ion.

For ionic strengths less than 0.1, the Güntelberg approximation provides reasonable estimates for the activity coefficient,

$$-\log \gamma_i = \frac{0.5Z_i^2 \mu^{1/2}}{1 + \mu^{1/2}},$$

where,  $Z_i$  is the valance of ion  $i$ . Ionic strength effects can be incorporated into chemical equilibrium calculations by developing a corrected equilibrium constant. As an example, consider the dissociation of water at 25°C.



$$K_w = \{\text{H}^+\} \{\text{OH}^-\} = \gamma_{\text{H}^+} [\text{H}^+] \gamma_{\text{OH}^-} [\text{OH}^-]$$

Thus the corrected equilibration constant,  $K_w^c$ , is computed from the activity constants and  $K_w$ :

$$K_w^c = \frac{K_w}{\gamma_{\text{H}^+} \gamma_{\text{OH}^-}} = [\text{H}^+] [\text{OH}^-].$$

Similar adjustments were also performed for the other equilibrium equations.

Aqueous solutions are electrically neutral. This balance of positive and negative charges yields the following equation for the San Joaquin River:

$$\text{alkalinity} + [\text{H}^+] = [\text{HCO}_3^-] + 2[\text{CO}_3^{2-}] + [\text{OH}^-],$$

and after substitution, the concentration of carbonate minerals,  $C_{\text{T,CO}_3}$ , before and after the light-dark bottle incubation period is computed from:

$$\text{alkalinity} + [\text{H}^+] = \alpha_1 C_{\text{T,CO}_3} + 2\alpha_2 C_{\text{T,CO}_3} + [\text{H}^+]/K_w^c$$

These chemical equations and calculations were used to estimate chl  $a$  production based on increases in DO and pH. The alkalinity was also measured before and after the light exposure. Chlorophyll  $a$  was assumed represent 1% of the total algal biomass. The predictions for the each of the bottles are shown in Figure 43. Estimations of chlorophyll  $a$  production from DO or pH data are reasonably good and exhibit the same trend as the measured chlorophyll  $a$  values. These analyses suggests that common chemical representations of algae and equilibrium calculations may be adequate to describe algal productivity and decay in the San Joaquin River. Dissolved oxygen uptake and pH response associated with algal processes could be incorporated in the algae-zooplankton models independent of Task 8.

A number of causes for the decline of the algal community below Mossdale have been identified by inspecting the data sets. These appear to include zooplankton grazing, the reduction of available light associated with increased river depth below Mossdale, and dispersion associated with tidal flows. No single mechanism is dominant in the 2005, 2006 and 2007 data sets; however, light limitation and zooplankton grazing appear to be the primary causes for the decline in chlorophyll  $a$  concentrations below the HOR. Light

has been identified as the limiting factor for algal productivity in the San Joaquin River because available nutrient concentrations are typically very high (Lehman, 2002). Figure 21 shows the approximate thalweg bathymetry of the San Joaquin River from Vernalis to the DWSC and illustrates the relative depth of the river above and below Mossdale. Above Mossdale the average river depth is almost entirely within the photic zone. However, below Mossdale the average depth increases from 5 to 20 ft. Thus algae in the well-mixed San Joaquin River above the DWSC may be in then 5 ft thick photic zone only 25 percent of time for a river depth of 20 ft. A more comprehensive analysis follows.

### Data interpretation with a numerical model

The development of a numerical water quality model was initiated to assess the contribution of depth and zooplankton grazing on the algae concentrations. Below Mossdale, the depth of the San Joaquin River increases steadily from about 5 ft to 20 ft at the Port of Stockton (RM 39.0) as shown in Figure 21. The dyed parcel of water tracked during the Lagrangian measurements (Task 8.2) was considered to be well-mixed from Vernalis to the DWSC, a characteristic supported by water quality parameter vertical profiles. Except during brief 15 to 30-minute periods when tidal flows reverse direction a well-mixed water profile appears valid.

A relatively simple numerical model was developed to assist with the interpretation of the Lagrangian monitoring results. The concentration of chl *a*, ph *a*, and zooplankton were simulated along the 31 mile reach between Vernalis and the DWSC. The governing ordinary differential equations appearing below were solved simultaneously with Matlab (The Mathworks, Inc.).

$$\frac{dChla}{dt} = k_g Chla - k_{da} Chla - k_{gz} Chla$$

$$\frac{d(Pha)}{dt} = -A_{c \rightarrow p} k_{da} Chla - k_{gz} Pha - k_{dp} Pha$$

$$\frac{dZoo}{dt} = A_{ca} \eta \frac{Chla}{k_{sa} + Chla} C_{gz} (Chla + Pha) \cdot Zoo - k_{dz} Zoo$$

Where:

- Chla* = the chlorophyll *a* concentration,
- Pha* = the pheophytin *a* concentration,
- Zoo* = the zooplankton concentration in the dyed water,
- $k_g$  = the algal growth rate, a function of temperature, light and nutrients,
- $k_{da}$  = the algal decay rate,
- $k_{gz}$  = the zooplankton grazing rate on the algae,
- $A_{c \rightarrow p}$  = the conversion factor of ch *a* to ph *a* when ch *a* decays to ph *a*,
- $k_{dp}$  = the pheophytin *a* decay rate,

$A_{ca}$  = is the ratio of carbon to chlorophyll *a*,  
 $\eta$  = is the grazing efficiency,  
 $C_{gz}$  =zooplankton grazing rate, and  
 $k_{dz}$  =the zooplankton decay rate.

The algal growth rate constant is a function of temperature, light, and nutrients. Temperature corrections to  $k_g$  were performed with:

$$k_{g,T}(temp, nutrients, light) = k_{g,20} \phi_{nutrients} \phi_{light},$$

$$k_{g,T} = k_{g,20} 1.066^{T-20},$$

and  $\phi_{nutrients}$  and  $\phi_{light}$  are attenuation factors associated with nutrient and light inhibition on the growth rate. For nutrients, a Michaelis-Menten term is used to reduce growth relative to the limiting nutrient of the system,

$$\phi_{nutrients} = \frac{C_{LN}}{k_{s,LN} + C_{LN}},$$

where  $C_{LN}$  and  $k_{s,LN}$  are the concentration of the limiting nutrient and half-saturation constant for the limiting nutrient (e.g., carbon, nitrogen (5-20  $\mu\text{gN L}^{-1}$ ), phosphorus (1-5  $\mu\text{gP L}^{-1}$ ), silica(20-80  $\mu\text{gSi L}^{-1}$ )), respectively. For the simulations presented here, measured concentrations in the San Joaquin River between Vernalis and the DWSC are generally well above the half-saturation concentrations (Lehman, 2001) and therefore are not expected to significantly limit algal growth in the study reach. Monitoring of these nutrients during 2007 again exhibited high non-limiting concentrations.

The influence of light was simulated to be dependent on the,

1. growth rate dependence on light intensity,
2. diurnal surface-light variation,
3. light attenuation with depth.

To account for algal growth inhibition at high intensities, the light intensity attenuation factor,  $\phi_{light}$  is expressed in terms of the intensity  $I$  (Steele, 1965),

$$\phi\{I(z, t)\} = \frac{I(z, t)}{I_s} e^{-\frac{I(z, t)}{I_s} + 1},$$

where  $I_s$  is the optimal light level. The intensity,  $I$ , is a function of the time and the depth in the water column,  $z$ .

Suspended particles, including algae, attenuate the light intensity exponentially with depth,

$$I(z) = I_0 e^{-k_e h},$$

where,  $I_0$  is the light intensity at the water surface, and  $k_e$  is the exponential extinction coefficient, which can be approximated by the Secchi-disk depth (SD),

$$k_e = \frac{1.8}{SD}.$$

Substituting the light extinction equation into the growth equation:

$$\phi\{I(h,t)\} = \frac{I_0(t)e^{-k_e h}}{I_s} e^{-\frac{I_0(t)e^{-k_e h}}{I_s} + 1},$$

A plot of  $\phi\{I(z,t)\}$  is presented in Figure 45 and exhibits the sensitivity of the algal growth attenuation factor, and therefore, the algal growth rate, to the depth in the water. This profile was generated with a Secchi-disk depth of 2 ft; measurements are frequently less than 2 ft in the Task 8 study reach. The plot suggests that the algal growth rate is less than 5 percent of the optimum rate at depths below 5 ft between Vernalis and the DWSC.

Integrating with respect to the total water depth, H,

$$\phi_L = \frac{2.718}{k_e H} (e^{-\alpha_1} - e^{-\alpha_0})$$

$$\alpha_0 = \frac{I_0(t)}{I_s}$$

$$\alpha_1 = \frac{I_0(t)}{I_s} e^{-k_e H}$$

yields an expression for evaluating the influence of the attenuated light in the water column (Chapra, 1997). The effect on the growth rate with respect to the total water depth is presented in Figure 46.

The light intensity, I, will also vary during the day, and was characterized with the half-sinusoid,

$$I(t) = I_{\max} \sin[w(t - t_r)]$$

$$t_r \leq t \leq t_s,$$

where  $t_r$  is the time of sunrise and  $t_s$  is the time of sunset.  $I(t) = 0$  during the night. The angular frequency is a function of the photoperiod and the daily period,

$$w = \frac{\pi}{fT_p},$$

where  $f$  is fraction of the photoperiod for the day and  $T_p$  is the daily period (e.g., 24 hr, 1 d). An approximation for the half-sinusoid was represented using a Fourier series (O'Connor and Di Toro, 1970)

$$I(t) = I_m \left( \frac{2f}{\pi} + \sum_{n=1}^{\infty} b_n \cos \left[ \frac{2\pi n}{T_p} \left( t - \frac{fT_p}{2} \right) \right] \right)$$

$$b_n = \cos(n\pi f) \frac{4\pi / f}{(\pi / f)^2 - (2\pi n)^2}.$$

The advantage of using the Fourier series was that it was not necessary to manually turn the light on and off when solving the three governing equations simultaneously. Twenty terms were used to calculate the Fourier series approximation. An example of the series used in the simulations is shown in Figure 24 for a 24-hr day with a photoperiod fraction of 0.6.

### Grazing

Losses due to zooplankton grazing are a function of the algae and zooplankton concentrations,

$$k_{gz} = C_{gz} Zoo,$$

where,  $C_{gz}$  and  $Zoo$ , are the grazing rate and zooplankton concentration respectively. Adjusting for temperature,

$$k_{gz} = k_{gz,20^\circ C} \theta_{gz}^{T-20},$$

adding a Michaelis-Menten term to account for the observed leveling off of the grazing rate at high chlorophyll  $a$  concentrations (Chapra, 1997) yields and adjusting for temperature yields,

$$k_{gz} = \frac{Chla}{K_{sa} + Chla} C_{gz} \theta_{gz}^{T-20} ZooChla$$

The overall formulation for the zooplankton grazing rate incorporates the grazing efficiency,  $\eta$ , zooplankton decay,  $k_{dz}$ , and algal biomass carbon to chlorophyll  $a$  mass ratio,  $A_{ca}$ , yielding a final equation for simulating the effect of zooplankton grazing on algae,

$$\frac{dz}{dt} = A_{ca} \eta \frac{Chla}{k_{sa} + Chla} C_{gz} ZooChla - k_{dz} Zoo.$$

Table 6 contains the parameters introduced above and representative values.

Figure 48 shows the sensitivity of algal productivity as a function of river depth in the absence of zooplankton grazing. The simulation was conducted for a 50-hour travel time from Vernalis to the DWSC, similar to flow conditions observed in September, 2005. The initial concentrations of chlorophyll *a*, pheophytin *a* and zooplankton were assumed to be 100  $\mu\text{g/L}$ , 0  $\mu\text{g/L}$ , and 3.0  $\mu\text{gC/L}$ , respectively. Two of the simulations assume the river is of fixed depth at either 5 or 20 ft. At a constant 5 ft depth, chlorophyll *a* concentrations remain high, with growth during the day and decay during the night. However, if the San Joaquin River were of a constant 20 ft depth, chl *a* concentrations continue to decline from Vernalis to the DWSC. Using the actual mid-river depth for the simulation yields an increase in the chl *a* concentration for the first 9 hours of daylight. As shown previously in Figure 44, the average river depth is about 5 ft during this time. After 20 hours, the water parcel is beyond Mossdale, CA, the point at which river depth increases and tidal flows become more significant. From 20 to 50 hours the chl *a* continues to decline due to the effect of increased river depth on the algal growth rate.

The potential effect of zooplankton grazing is shown in Figure 49. The two upper curves simulate depth effects without grazing as shown previously in Figure 25. The lower curve simulates the additional reduction in chl *a* associated with zooplankton grazing. These simulations suggest that river depth and zooplankton effects can account for the 50 percent reduction in chl *a* that is commonly observed between Mossdale and the DWSC during periods of low net flow. Measurements presented in the Task 9 interim report indicate that relatively low concentrations of zooplankton are present above Mossdale, but populations were observed to increase dramatically as the water approached the DWSC. The zooplankton population growth is also simulated by the model as shown in Figure 50. These modeling efforts appear to support the general observed trends in chl *a*, pheophytin *a* and zooplankton shown earlier for the lagrangian monitoring conducted in 2005, 2006, and 2007.

The observed concentrations of extracted chlorophyll *a* and pheophytin *a*, and zooplankton are presented in Figure 51 for August 2005. The model simulations are superimposed as solid lines on the graph. Simulations yield reasonable but not perfect fits to the observed data. Algal concentrations increase during daylight hours, and decrease at night. However, beyond 25 hours (rm50) the chl *a* concentrations attenuate from approximately 40 to 20  $\mu\text{g/L}$ . The last sharp decline in chl *a* is probably associated with dispersion of low chl *a* water from the DWSC mixing with higher chl *a* water entering from the San Joaquin River. The model developed here doesn't consider dispersion and therefore, may be incapable of accurately simulating algal pigment concentrations with approximately 1 mile of the DWSC. A corresponding increase in pheophytin *a*, the degradation product of chl *a*, occurs during this decline. Zooplankton concentrations also increase dramatically below rm50, suggesting that grazing is a significant mechanism for algal decline. Measured concentrations of algal pigments and zooplankton are again compared with model simulations for the June, 2007 lagrangian tracking. The simulation yields good fits to the observed chlorophyll *a* and pheophytin *a* concentrations, and a reasonable simulation to most of the zooplankton measurements. The numerical model presented here was not developed as a predictive tool, but instead to quantitatively estimate the contribution of light attenuation and zooplankton grazing to

the behavior of algae being transported by flow to the DWSC. The simulations shown here support the conclusion that light attenuation and zooplankton grazing can account for most of the algal dynamics above the DWSC. This exercise may also assist in developing accurate algorithms for a more comprehensive model of the San Joaquin River. These algorithms could be incorporated into a comprehensive water quality management model to evaluate land use practices, pollutant control strategies, and water routing operations in the San Joaquin River watershed.

### **Summary and Conclusions**

A three-year field study has been completed to evaluate algal productivity and decay between Vernalis and the Stockton DWSC. A monitoring approach that relies on measuring parameters at fixed locations while simultaneously tracking water quality and algal changes in a dyed parcel of water during transport to the DWSC has been employed. Oxygen demands, algal productivity and decay, and zooplankton grazing were also characterized with isolated batch microcosm experiments. Task 9 augments this work by identifying and enumerating phytoplankton populations for assessing changes in species composition within the study reach. In addition, Task 9 identifies and quantifies zooplankton and bi-valve populations to evaluate the impacts of grazing on algae flowing to the DWSC and South Delta

High flows in the San Joaquin River during 2005 and 2006 delayed the start of major field components until July of each year. The resources originally assigned for May and June were rescheduled to later months or years when lower, more representative flows occurred. Eight dye tracking field trials were performed in 2005, 2006 and 2007. When the net flow entering the DWSC approached zero, the lagrangian monitoring approach was no longer feasible and an additional four longitudinal monitoring schemes was conducted in July, August, and September of 2007.

A number of causes for the decline of the algal community below Mossdale have been identified by inspecting the data sets, developing a algal growth and decay model and conducting model simulations. Two of the dominant mechanisms appear to be zooplankton grazing and the reduction of available light associated with increased river depth below Mossdale. Biochemical oxygen demands entering the DWSC were correlated to the chlorophyll a concentration in 2007, but not in 2005 and 2006. Net flows to the DWSC in 2005 and 2006 were abnormally high and may be one of the causes for the poor correlation of algal biomass to the BOD. Improved treatment of wastewater effluent discharged to the San Joaquin River from the City of Stockton in 2007 may also influence the improved BOD correlation to chlorophyll a. These observations emphasize the importance of including the two dominant mechanisms that impact chlorophyll a concentrations entering the DWSC, light limitation associated with increased river depth and zooplankton grazing, in dissolved oxygen simulation models of the San Joaquin River below Mossdale.

The light-dark bottle experiments suggest that algal productivity can be predicted with either pH or dissolved oxygen measurements using chemical stoichiometry and equilibrium calculations. This approach is being applied to the river data and combined with light intensity measurements to simulate the algal productivity and respiration between Vernalis and the DWSC. In addition, zooplankton populations and algal settling near the DWSC also suggest a synergistic effect where zooplankton grazing efficiency may increase with slack water conditions. Experiments and monitoring was performed for quantifying the grazing rates, determine the spatial distribution of zooplankton, assess algal setting in the river and better quantify the influence of mixing and dispersion when close to the DWSC. These activities have also yielded important data sets for developing and calibrating a comprehensive numerical model of the upper San Joaquin River and the DWSC.

### **Acknowledgements**

The study team gratefully acknowledges the California Bay-Delta Authority for project funding.

## References

APHA, 2005. Standard Methods of the Examination of Water and Wastewater, 21<sup>th</sup> Edition. 2005. American Public Health Association, Washington, DC.

APHA, 1998. Standard Methods of the Examination of Water and Wastewater, 20<sup>th</sup> Edition. 1998. American Public Health Association, Washington, DC.

Bowie, G.L., Mills, W.B., Porcella, D.B., Campbell, C.L., Pagenkopf, J.R., Rupp, G.L., Johnson, K.M., Chan, P.W.H., Gherini, S.A. and Chamberlin, C.E. 1985. Rates, Constants, and Kinetic Formulations in Surface Water Quality Modeling. U.S. Environmental Protection Agency, ORD, Athens, GA, ERL, EPA/600/3-85/040.

Carslaw H.S. and J.C. Jaeger, 1959. Conduction of Heat in Solids. 2<sup>nd</sup> edition. Oxford University Press, London.

Chapra, 1997. *Surface Water–Quality Modeling*, McGraw-Hill: New York.

Dumont, H. T., van de Velde, I., and Dumont, S. (1975) The dry weight estimate of biomass in a selection of Cladocera, Copepoda, and Rotifera from the plankton, periphyton, and benthos of continental waters. *Oecologia* **19**, 225-246.

Fick A. 1855. On Liquid Diffusion. *Philso. Mag.* 4(10), 30-39.

Fischer H.B., E.J. List, R.C.Y. Koh, J. Imberger and N. H. Brooks, 1979. Mixing in Inland and Coastal Waters. Academic Press Inc.

Foe, C., M. Gowdy, and M. McCarthy, 2002. Draft Strawman Allocation of Responsibility Report, California Regional Water Quality Control Board, Central Valley Region, January, Sacramento, CA.

Fourier J.B.J. 1922. *Theorie Analytique de la Chaleur*. Didot, Paris.

Godfrey R.G. and Frederick, B.J. 1970. Dispersion in Natural Streams. US. Geological Survey Professional Paper, 433-B.

Holley E.R. and G. Abraham. 1973. Laboratory Studies on Transverse Mixing in Rivers. *J. Hydraul. Res.* 11, 219-253.

- Jackman A.P. and Yotsukura N. 1977. Thermal Loading of Natural Streams. U.S. Geological Survey Professional paper 991.
- Jones & Stokes, 2002. Evaluation of Stockton Deep Water Ship Channel Model Simulations of 2001 Conditions: Loading Estimates and Model Sensitivity, Prepared for the CALFED Bay-Delta Program 2001 Grant 01-N61, Sacramento, CA
- Jones & Stokes, 2001. "City of Stockton Year 2000 Field Sampling Program Data Summary", Prepared for the City of Stockton, Sacramento, CA.
- Jones & Stokes, 1998. *Potential solutions for achieving the San Joaquin River dissolved oxygen objectives*. Prepared for the City of Stockton Department of Municipal Utilities, Sacramento, CA.
- Mackay. J.R. 1970. Lateral Mixing of the Liard and Mackenzie Rivers Downstream from their Confluence. *Can. J. Earth Sci.* 7, 111-124.
- Lehman, P. 2001. "The Contribution of Algal Biomass to Oxygen Demand in the San Joaquin River Deep Water Channel", Final Draft Report, San Joaquin River Dissolved Oxygen TMDL Steering Committee, Department of Water Resources, Central District, Sacramento, CA.
- Lehman, P. W., Sevier, J., Giulianotti, J., and Johnson, M. (2004) Sources of Oxygen Demand in the Lower San Joaquin River, California. *Estuaries* **27**(3), 405-418.
- Lind, C.J. 1970. U.S. Geological Survey Professional Paper 700D, pp. D272-D280.
- Litton, G.M., 2002. "Sediment Deposition Rates and Oxygen Demands in the Deep Water Ship Channel of the San Joaquin River, Stockton, CA", Prepared for CALFED Bay-Delta Program 2001 Grant 01-N61-005, University of the Pacific, Stockton, CA.
- Pace, M. L. and Orcutt, Jr., J. D. (1981) The relative importance of protozoans, rotifers, and crustaceans in a freshwater zooplankton community. *Limnology and Oceanography* **26**(5), 822-830.
- O'Connor, D.J. and Di Toro, D.M. 1970. Photosynthesis and Oxygen Balance in Streams. *J. San. Engr. Div. ASCE* 96(2), 547-571.
- Quinn N. W. T. and A. Tullock, 2002. "San Joaquin River Diversion Data Assimilation, Drainage Estimation and Installation of Diversion Monitoring Stations. Prepared for the CALFED Bay-Delta Program 2001 Grant 01-N61.
- Russell, L.L. 1976. Chemical Aspects of Groundwater Recharge with Wastewaters, Ph.D. Thesis, University of California, Berkeley, December.

Snoeyink, V.L. and D. Jenkins, 1980. *Water Chemistry*. Wiley & Sons, New York, 463p.

Steele, J.H. 1965. Notes on Some Theoretical Problems in Production Ecology. In *Primary Production in Aquatic Environments*, C.R. Goldman, ed., University of the California Press, Berkeley, CA.

Stumm W. and J.J. Morgan, 1996. *Aquatic Chemistry*, 3<sup>rd</sup> ed., Wiley & Sons: New York.

U.S. Army Corps of Engineers. 1984. San Joaquin River, Stockton to the Merced River, Aerial Atlas. U.S. Army Corps of Engineers Sacramento District, Water Resources Planning Branch Investigations Section, Sacramento, CA.

Yotsukura, N. H.B. Fischer and W.W. Sayre 1970. Measurement of Mixing Characteristics of the Missouri River between Sioux City, Iowa and Plattsmouth, Nebraska. US Geological Survey Water Supply Paper 1899-G.

## **Appendix A**

Tabular and graphical BOD and CBOD data and figures are contained in this appendix

## **Electronic Appendices**

The following data has been made available as an electronic appendix to this report.

1. Fixed sonde data from fixed instruments deployed during the lagrangian tracking events.
2. Lagrangian monitoring data captured *insitu* or measured with laboratory methods
3. Algal productivity and zooplankton grazing microcosm experimental results

Table 1: Dates and locations of the Lagrangian tracking trials performed during 2005, 2006 and 2007.

Dates	Start Location/ Time	End Location/Time	Total Travel Time (hr)
July 13-14, 2005	VNS 12:12	DWSC 18:30	30.5
August 16-18, 2005	VNS 13:35	DWSC 13:58	48.4
Sept. 15-17, 2005	VNS 9:39	DWSC 11:54	50.2
October 13-15, 2005	VNS 9:10	DWSC 00:15	38.6
July 19-21, 2006	VNS 18:10	DWSC 10:06	40.0
August 9-10, 2006	HOR 9:04	DWSC 10:48	25.8
June 12-15, 2007	VNS 8:39	DWSC 2:15	65.5
July 19-20, 2007	VSN 10:45	MSD 9:30	22.8

VRN: Vernalis (SJR River Mile 71.9)

MSD: Mossdale boatramp (SRJ River Mile 56.7)

HOR: Head of Old River (SJR River Mile 54.0)

DWSC: Stockton Deep Water Ship Channel (SJR River Mile 39.8)

Table 2: Discrete water sample locations during 2005 and 2006.

July 2005

	map	River mi	River km	time	Time run	date
SJR 1	J5-1	68.4	110.0	13:00	0	7/13/05
SJR 2	J5-2	65.8	105.8	15:20	140	7/13/05
SJR 3	J5-3	61.4	98.9	17:48	288	7/13/05
SJR 4	J5-4	58.9	94.8	19:55	415	7/13/05
SJR 5	J5-5	55.6	89.5	23:45	645	7/13/05
SJR 6	J5-6	53.1	85.4	3:00	840	7/14/05
SJR 7	J5-7	53.1	85.4	4:55	955	7/14/05
SJR 8	J5-8	51.1	82.2	8:00	1140	7/14/05
SJR 10	J5-9	44.1	70.9	14:05	1505	7/14/05
SJR 11	J5-10	42.9	69.1	16:00	1620	7/14/05
SJR 12	J5-11	40.6	65.4	18:30	1770	7/14/05

August 2005

	map	rm	rk	time	Time run	date
SJR 1	A5-1	71.5	115.06495	13:00	0	8/16/05
SJR 2	A5-2	69.5	111.84635	15:00	120	8/16/05
SJR 3	A5-3	66.8	107.50124	16:50	230	8/16/05
SJR 4	A5-4	64.3	103.47799	18:40	340	8/16/05
SJR 5	A5-5	62.4	100.42032	20:20	440	8/16/05
SJR 6	A5-6	57.66	92.792238	0:50	710	8/17/05
SJR 7	A5-7	56.6	91.08638	3:30	870	8/17/05
SJR 8	A5-8	56	90.1208	5:49	1009	8/17/05
SJR 9	A5-9	53.84	86.644712	9:30	1230	8/17/05
SJR 10	A5-10	52.2	84.00546	12:00	1380	8/17/05
SJR 11	A5-11	48.2	77.56826	15:00	1560	8/17/05
SJR 12	A5-12	48.1	77.40733	17:50	1730	8/17/05
SJR 13	A5-13	46.7	75.15431	21:11	1931	8/17/05
SJR 14	A5-14	44.8	72.09664	0:00	2100	8/17/05
SJR 15	A5-15	47	75.6371	7:05	2525	8/18/05
SJR 16	A5-16	46.7	75.15431	9:00	2640	8/18/05
SJR 17	A5-17	42.6	68.55618	12:30	2850	8/18/05
SJR 18	A5-18	39.8	64.05014	13:55	2935	8/18/05

Sept 2005

	map	rm	rk	time	Time run	date
SJR1	S5-1	71.7	115.38681	9:45	0	9/15/05
SJR2	S5-2	67.9	109.27147	12:30	165	9/15/05
SJR3	S5-3	64.3	103.47799	14:30	285	9/15/05
SJR4	S5-4	60.5	97.36265	17:40	475	9/15/05
SJR5	S5-5	58.6	94.30498	19:50	605	9/15/05
SJR6	S5-6	56.7	91.24731	22:50	785	9/15/05
SJR7	S5-7	56	90.1208	0:00	855	9/16/05
SJR8	S5-8	56	90.1208	2:00	975	9/16/05
SJR9	S5-9	56	90.1208	4:00	1095	9/16/05
SJR10	S5-10	56	90.1208	6:00	1215	9/16/05
SJR11	S5-11	52.08	83.812344	9:07	1402	9/16/05
SJR12	S5-12	49.3	79.33849	12:15	1590	9/16/05
SJR13	S5-13	46.8	75.31524	13:10	1765	9/16/05
SJR14	S5-14	43	69.1999	0:45	2340	9/17/05
SJR15	S5-15	42.4	68.23432	2:00	2415	9/17/05
SJR16	S5-16	42.4	68.23432	3:00	2475	9/17/05
SJR17	S5-17	42.4	68.23432	4:00	2535	9/17/05
SJR18	S5-18	42.4	68.23432	5:00	2595	9/17/05
SJR19	S5-19	42.4	68.23432	6:00	2655	9/17/05
SJR20	S5-20	42.4	68.23432	7:00	2715	9/17/05
SJR21	S5-21	44.154	71.057032	7:56	2771	9/17/05
SJR22	S5-22	40.9	65.82037	11:00	2955	9/17/05
SJR23	S5-23	39.9	64.21107	12:00	3015	9/17/05

Oct 2005

	map	rm	rk	time	Time run	date
SJR1	O5-1	71.9	115.70867	9:35	0	10/13/05
SJR2	O5-2	68.07	109.54505	12:00	145	10/13/05
SJR3	O5-3	64.3	103.47799	15:15	340	10/13/05
SJR4	O5-4	60.2	96.87986	18:45	550	10/13/05
SJR5	O5-5	57.46	92.470378	22:00	745	10/13/05
SJR6	O5-6	55.8	89.79894	1:10	935	10/14/05
Isco7	O5-7	55.8	89.79894	2:00	985	10/14/05
Isco8	O5-8	55.8	89.79894	4:00	1105	10/14/05
SJR7	O5-9	51.05	82.154765	8:05	1350	10/14/05
SJR8	O5-10	47.7	76.76361	11:05	1530	10/14/05
SJR9	O5-11	45	72.4185	14:00	1705	10/14/05
SJR10	O5-12	45	72.4185	17:00	1885	10/14/05
SJR11	O5-13	44.1	70.97013	20:35	2100	10/14/05
SJR12	O5-14	40	64.372	23:55	2300	10/14/05

Jul 2006

	map	rm	rk	time	Time run	date
SJR1 3'	J6-1	71.91	115.72476	18:05	0	7/19/06
SJR2 4'	J6-2	67.3	108.30589	21:00	175	7/19/06
SJR3 8'	J6-3	63.3	101.86869	0:00	355	7/20/06
SJR4	J6-4	59.42	95.624606	3:00	535	7/20/06
SJR5	J6-5	55.68	89.605824	6:00	715	7/20/06
SJR6	J6-6	52.66	84.745738	9:00	895	7/20/06
SJR7	J6-7	49.67	79.933931	12:35	1110	7/20/06
SJR8ave	J6-8	48.05	77.326865	15:00	1255	7/20/06
SJR9 13'	J6-9	46.35	74.591055	19:20	1515	7/20/06
SJR10	J6-10	44.27	71.243711	21:00	1615	7/20/06
SJR11	J6-11	45.2	72.74036	0:55	1850	7/21/06
SJR12 15'	J6-12	46.11	74.204823	3:30	2005	7/21/06
SJR13ave	J6-13	44.32	71.324176	6:50	2205	7/21/06
SJR14 20'	J6-14	41.06	66.077858	9:40	2375	7/21/06
DWSCave	J6-15	39.7	63.88921	11:20	2475	7/21/06

Aug 2006

	map	rm	rk	time	Time run	date
SJR1ave	A6-1	53.6	86.25848	8:20	0	8/9/06
SJR2ave	A6-2	51.35	82.637555	11:00	160	8/9/06
SJR3ave	A6-3	47.8	76.92454	14:00	340	8/9/06
SJR4ave	A6-4	46	74.0278	15:50	450	8/9/06
SJR5ave	A6-5	45.3	72.90129	17:50	570	8/9/06
SJR6ave	A6-6	44.58	71.742594	20:15	715	8/9/06
SJR7ave	A6-7	43.88	70.616084	21:55	815	8/9/06
SJR8ave	A6-8	41.7	67.10781	23:55	935	8/9/06
SJR9ave	A6-9	40.32	64.886976	1:55	1055	8/10/06
SJR10ave	A6-10	42.42	68.266506	5:35	1275	8/10/06
SJR11ave	A6-11	42.56	68.491808	7:50	1410	8/10/06
SJR12ave	A6-12	40.07	64.484651	10:05	1545	8/10/06
SJR13ave	A6-13	39.7	63.88921	10:50	1590	8/10/06

Table 3. Schedule of longitudinal monitoring runs and lagrangian tracking or tracer release events for 2007.

Date	Vernalis Flow (cfs)	Net Flow to DWSC <sup>1</sup> (cfs)	Range of Longitudinal Profiles SJR River Miles	Tide conditions	Zooplankton collected	Date and time of dye release
6/12/2007 to 6/15/2007	2223 1858	873 652	Lagrangian tracking from rm71.9 (Vernalis) to rm 39.8 (DWSC)	n/a	yes	6/12/2007 (8:37)
7/16/2007 7/17/2007	1100 997	15 7.3	rm39.8 (7/16 22:49) to rm 54 (0:51)  rm39.8 (7/17 3:49) to rm 54 (7/17 6:00)  rm39.8 (7/17 8:45) to rm 54 (7/17 10:52)  rm39.8 (7/17 15:36) to rm 54 (7/17 17:55)	flood  ebb  flood  ebb	yes  yes  yes  yes	n/a
7/19/2007 7/20/2007	989 968	0	Lagrangian tracking rm71.9(Vernalis) to rm56.7 (Mossdale)	n/a	yes	7/19/2007 10:45
8/14/2007 8/15/2007	1002 919	60 -51	rm39.8 (8/14 21:12) to rm 56.7 (23:45)  rm39.8 (8/15 1:07) to rm 56.7 (8/15 3:10)  rm39.8 (8/15 8:47) to rm 56.7 (8/15 11:08)  rm39.8 (8/15 15:27) to rm 56.7 (8/15 17:53)	flood  ebb  flood  ebb	yes  yes  yes  yes	n/a
9/6/2007	993	21	rm34 (8:32) to rm56.7 (11:23)	ebb	no	n/a
9/19/2007 9/20/2007	939 926	246	rm34 (9/19 21:20) to rm56.7 (9/20 1:45)  39.6 (9/20 7:45) to 56.7 (9/20 10:30)	flood  ebb	yes	9/20/2007 2:05

<sup>1</sup>Measured at the USGS Garwood Bridge Station (CDEC Station: SJG)

Table 4: BOD results for July 13-14, 2005 along the San Joaquin River.

Location	Sample No.	20 day results		
River Mile		BOD	CBOD	NBOD
68.4	SJR 1	6.0	4.0	2.0 / 33%
61.4	SJR 3	7.0	4.5	2.5 / 36%
55.6	SJR 5	7.0	4.5	2.0 / 29%
53.1	SJR 6	7.0	4.8	2.2 / 31%
46.7	SJR 9	6.2	4.3	1.9 / 31%
42.9	SJR 11	7.0	4.6	2.4 / 34%

Table 5: Initial and final DO, pH, and chlorophyll a July light-dark bottle experiment results.

Depth (ft)	Elapsed Time (hr)	DO (mg/L)		pH		Chlorophyll <i>a</i> (ug/L)	
		Start	End	Start	End	Start	End
1	4:45	8.63	14.32	7.92	9.05	54.1	88.0
2	4:40	8.60	13.38	7.92	8.94	54.1	85.4
3	4:30	8.59	10.5	7.97	8.43	54.1	70.9
dark	4:55	8.50	8.03	7.94	7.91	54.1	51.9

Table 6: Parameters used for numerical model simulations (Bowie, 1985, Chapra, 1997).

Parameter	Description	Units	Range	Common values	Simulation value
$k_{g,20}$	maximum algal growth rate	$d^{-1}$		2	2
$k_{da}$	algal decay rate	$d^{-1}$	0.01-0.5	0.1-0.2	0.36
$A_{ca}$	carbon-chlorophyll a ratio	$gC\ gChl^{-1}$	10-100	40	40
$k_{dp}$	pheophytin decay rate	$d^{-1}$	NR	NR	0.27
$A_{c \rightarrow p}$	Chlorophyll pheophytin ratio		NR	NR	1
$C_{gz}$	zooplankton grazing rate	$L\ mgC^{-1}\ d^{-1}$	0.5-5	1 - 2	0, 1.5
$k_{dz}$	zooplankton decay rate	$d^{-1}$	0.001-0.1	0.01-0.05	0.1
$K_{sa}$	zooplankton half-saturation	$\mu gChl\ L^{-1}$	2-25	5-15	10
$\eta$	grazing efficiency		0.4-0.8		0.5
$I_s$	optimal light intensity	$ly\ d^{-1}$		100-400	100

NR: none reported, simulation value based on measured losses and model fit by Litton (2002).



Figure 1: The San Joaquin River between Vernalis and the Stockton Deep Water Ship Channel.

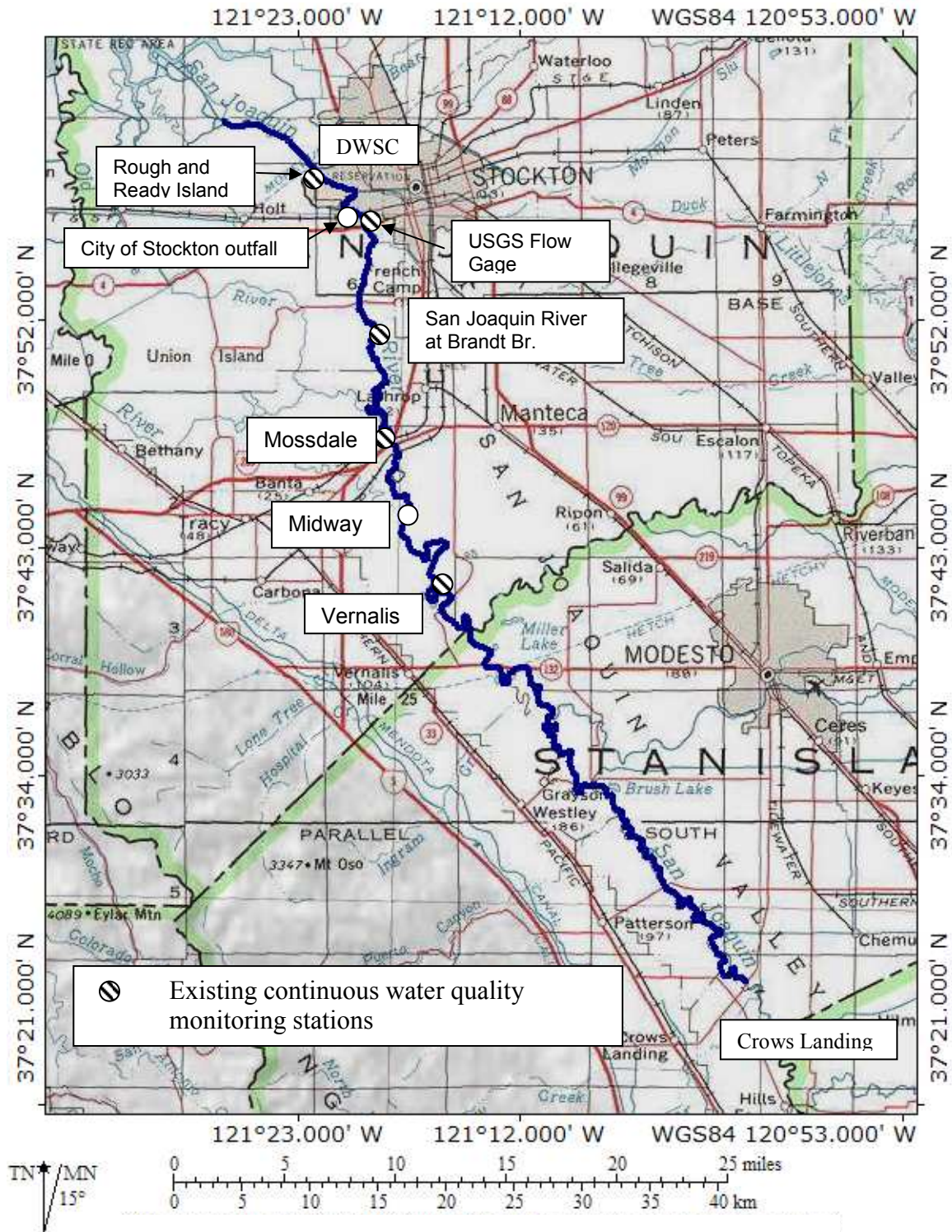
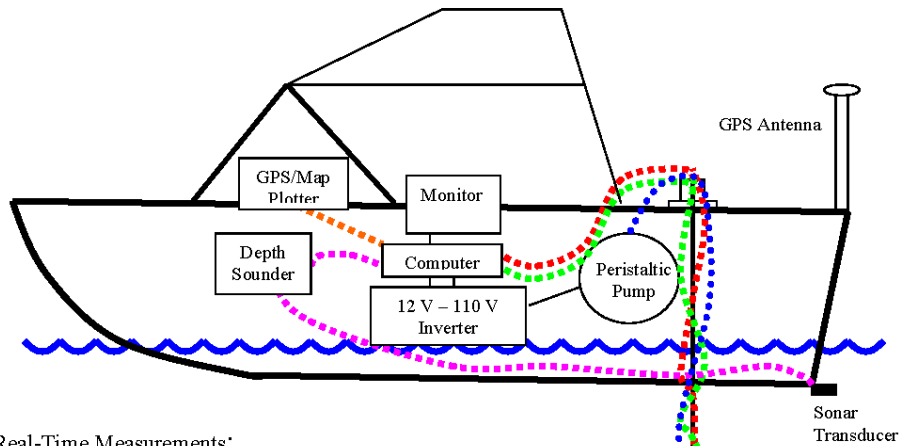


Figure 2: Monitoring boat and data acquisition system.



Real-Time Measurements:

- Coordinate location
- Water depth
- Instrument depth
- Water temperature
- Electrical conductance
- Dissolved oxygen
- pH
- Chlorophyll a
- Rhodamine WT dye
- Turbidity
- Position tracked on navigation chart

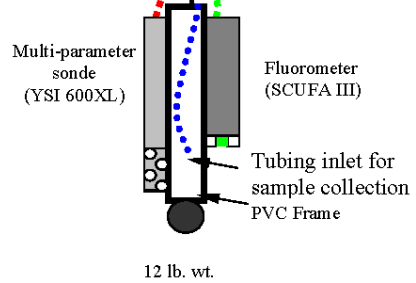


Figure 3: Study reach and discrete sampling locations during 2005 and 2006. The sampling locations are identified in Table 2.

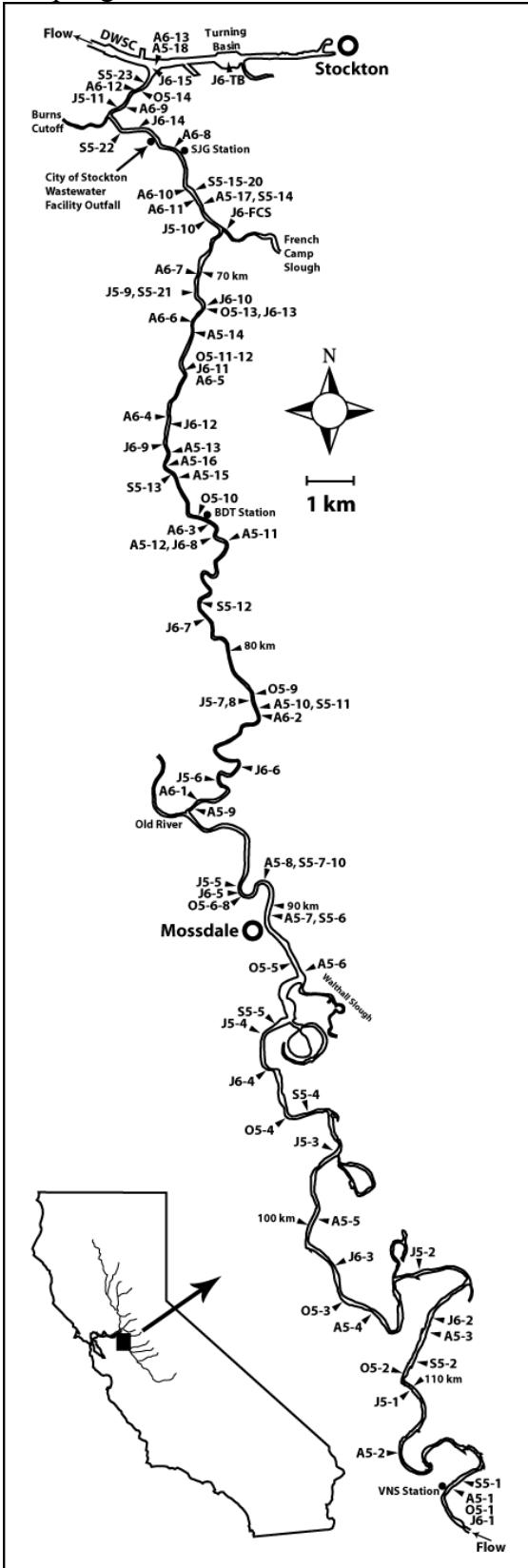


Figure 4: San Joaquin River Flow at Vernalis for 2004 through 2007, and the Task 8 lagrangian monitoring trials performed during 2005, 2006, and 2007.

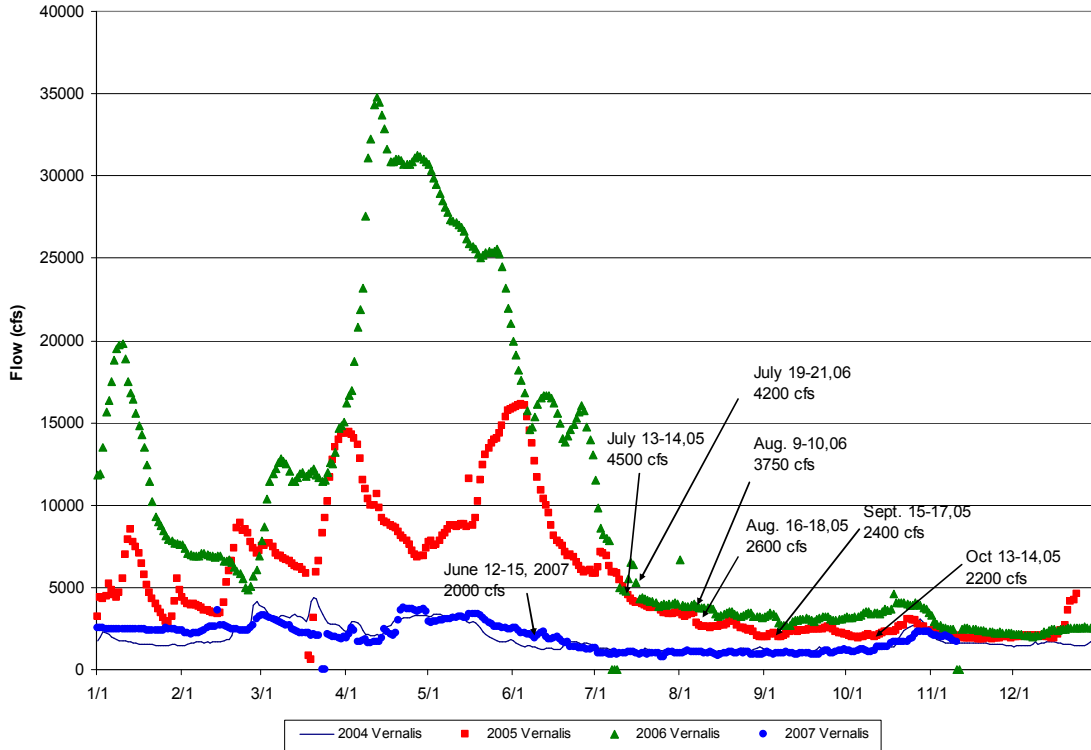


Figure 5: San Joaquin River flow at Vernalis and entering the DWSC (San Joaquin River at Garwood Bridge) during the 2005 monitoring.

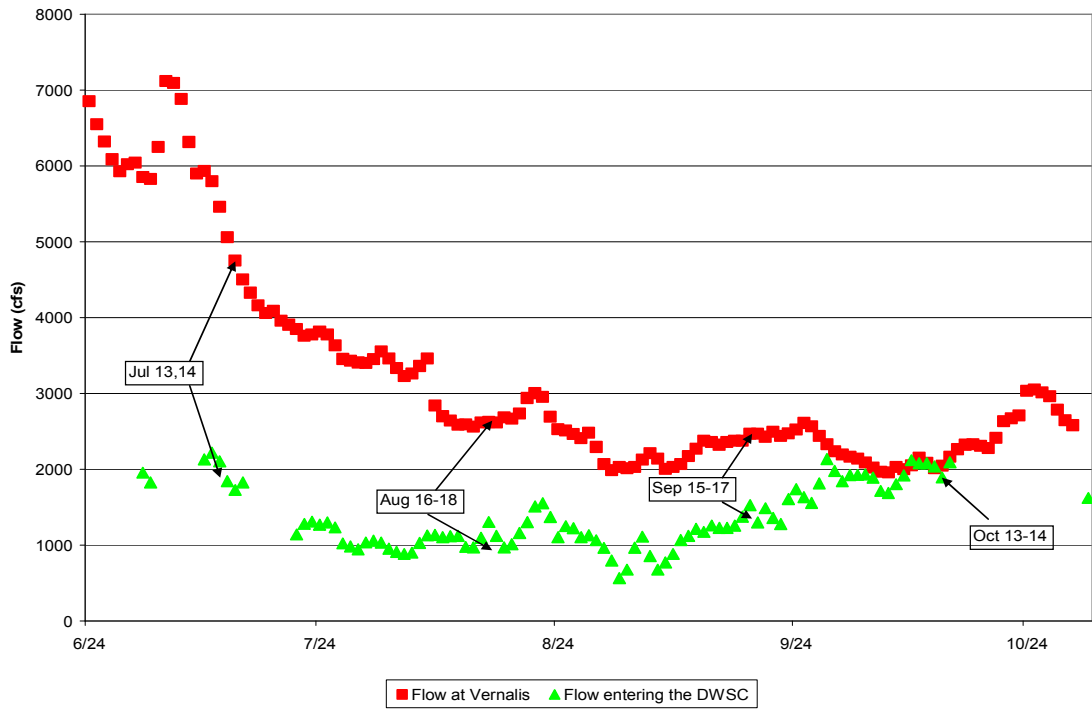


Figure 6: Flows at Vernalis and entering DWSC (measured at the Garwood Bridge station) during the 2006 monitoring.

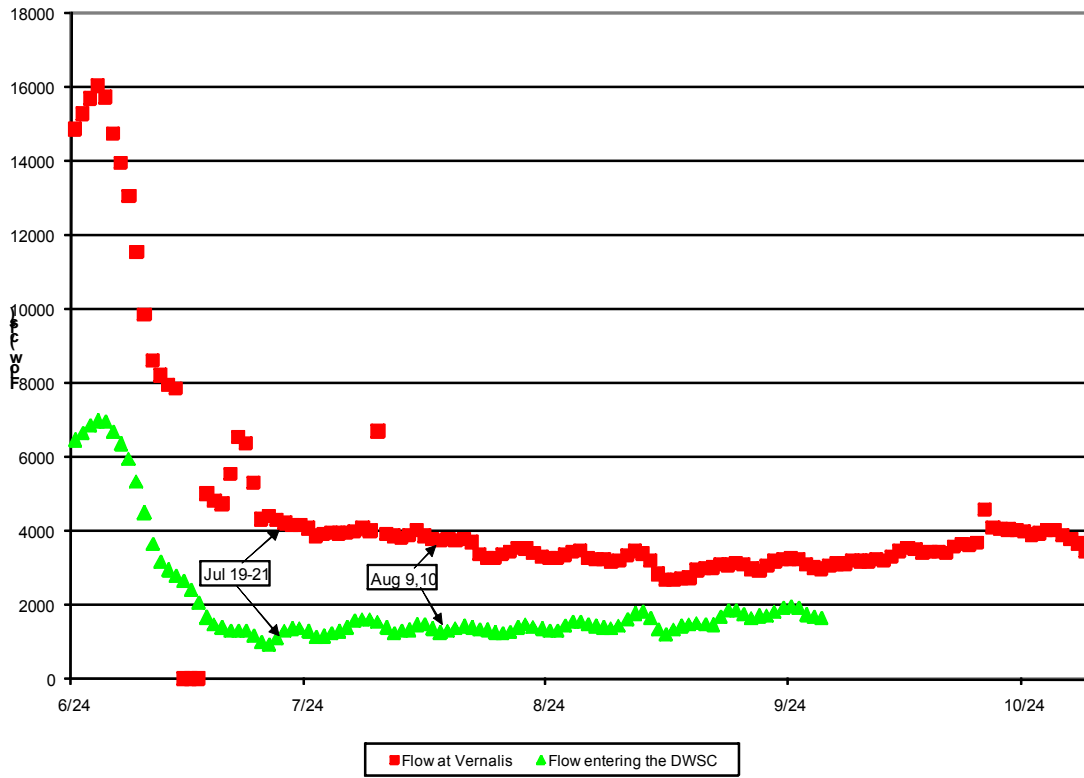


Figure 7: Flows at Vernalis and entering DWSC (measured at the Garwood Bridge station) during the 2007 monitoring. Lagrangian and longitudinal monitoring trails are also shown.

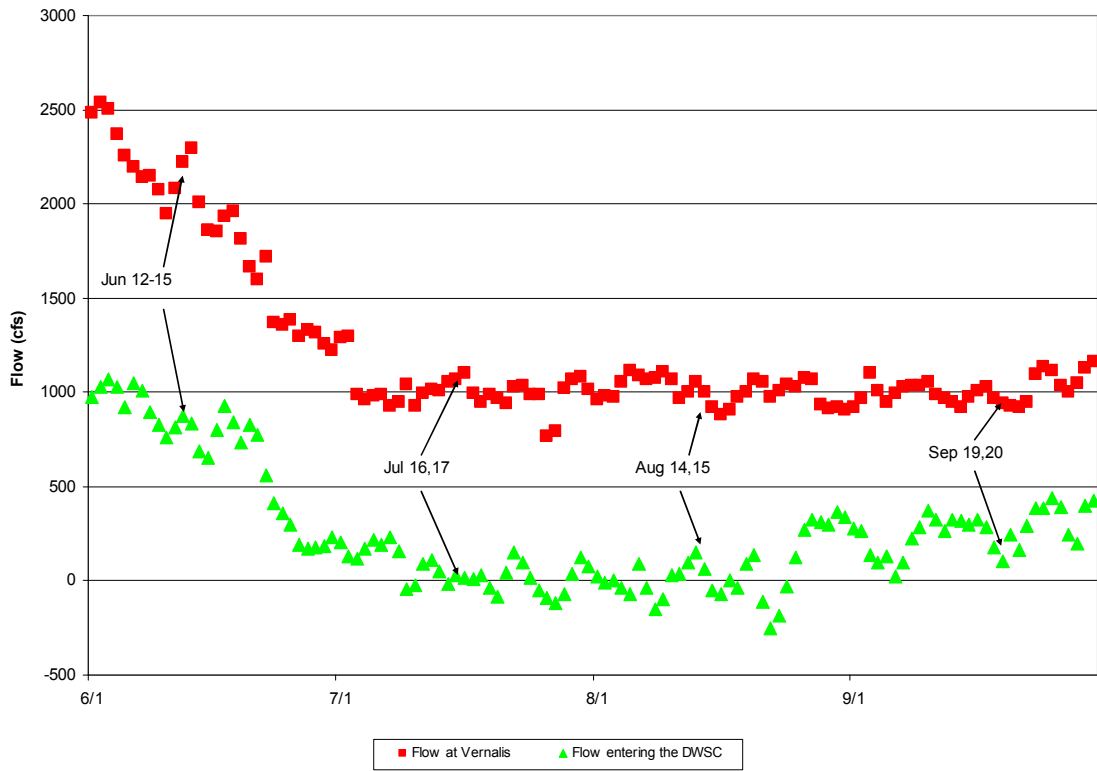


Figure 8: Dissolved oxygen, pH, and chl a measured midway between Vernalis and Mossdale on the San Joaquin River, July 11-15, 2005.

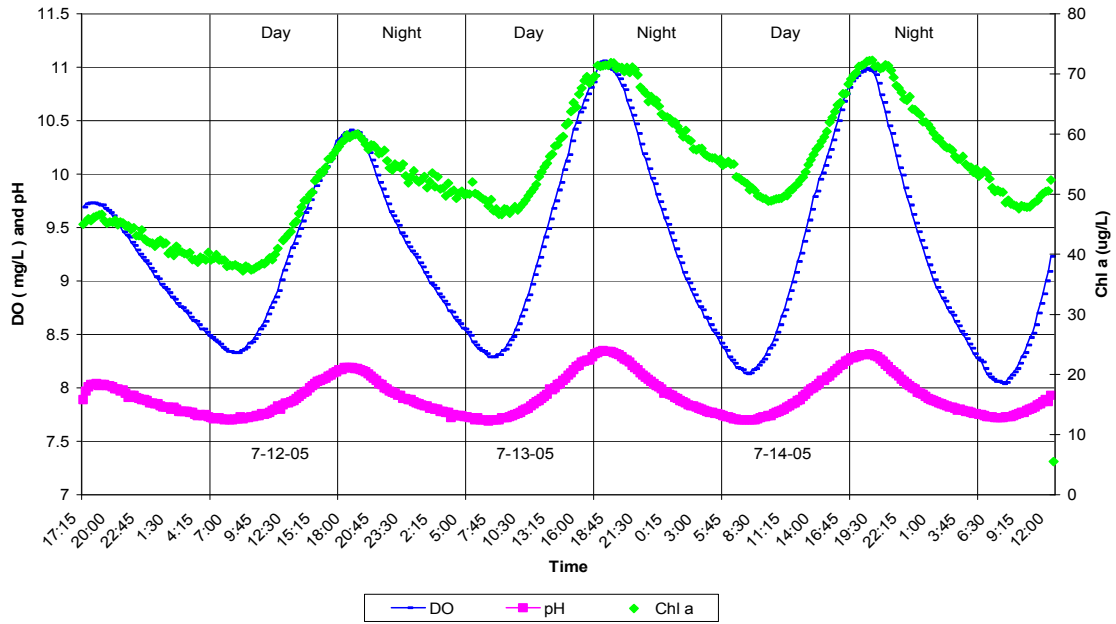


Figure 9: Dissolved oxygen, pH, and Chl a measured at Brandt Bridge on the San Joaquin River, July 11-15, 2005.

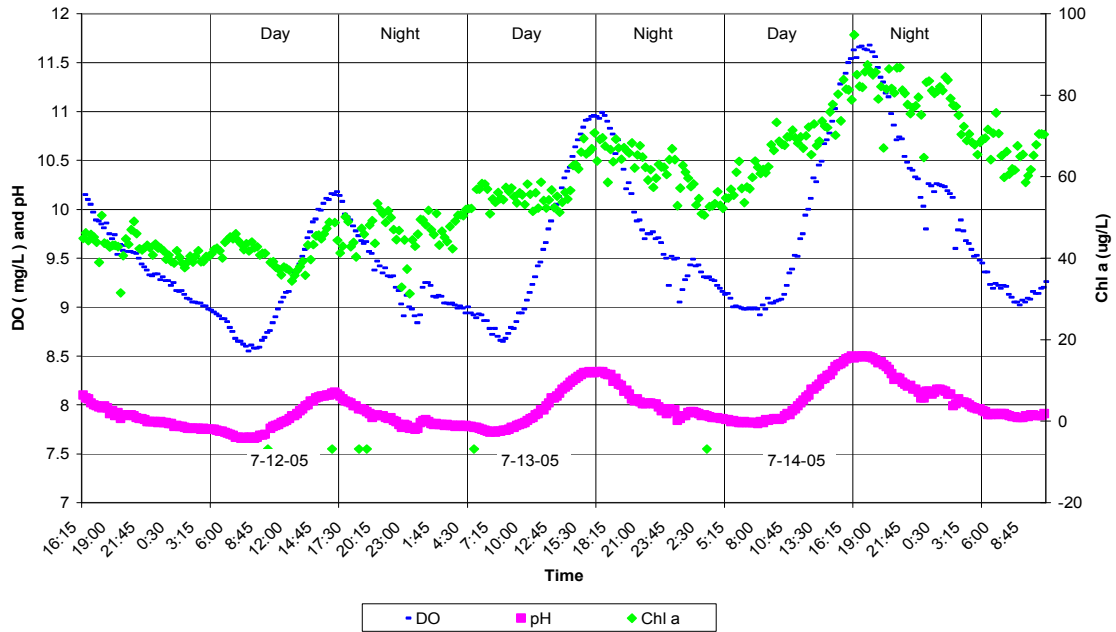


Figure 10: Pigment concentrations, dissolved oxygen, and pH within the rhodamine WT plume flowing from Vernalis to the DWSC, July 13-14, 2005.

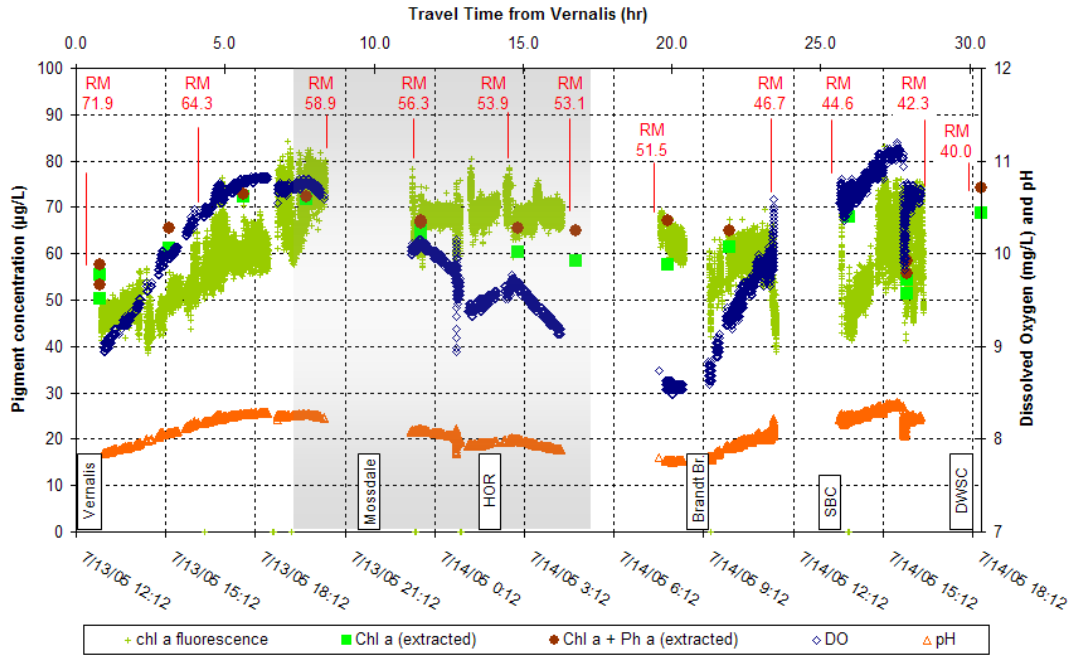


Figure 11: Extracted pigment concentration and the  $chl\ a/(chl\ a + ph\ a)$  fraction within the rhodamine WT plume flowing from Vernalis to the DWSC, July 13-14, 2005.

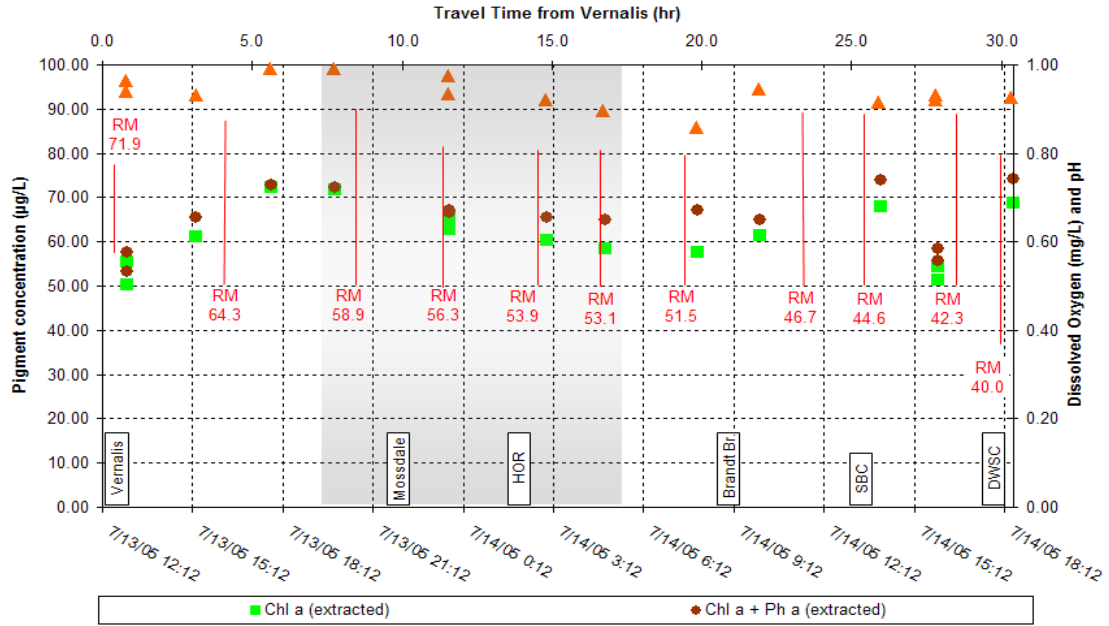


Figure 12: Pigment concentrations, dissolved oxygen, and pH within the rhodamine WT plume flowing from Vernalis to the DWSC, August 16-18, 2005.

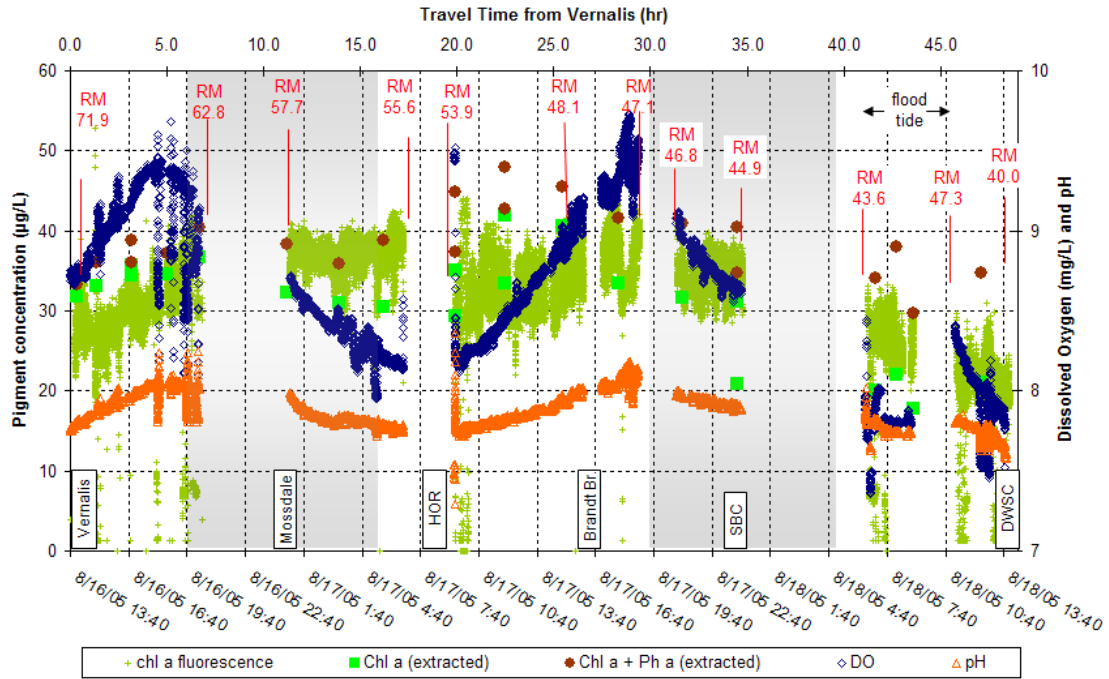


Figure 13: Extracted pigment concentration and the chl a/(chl a + ph a) fraction within the rhodamine WT plume flowing from Vernalis to the DWSC, August 16-18, 2005.

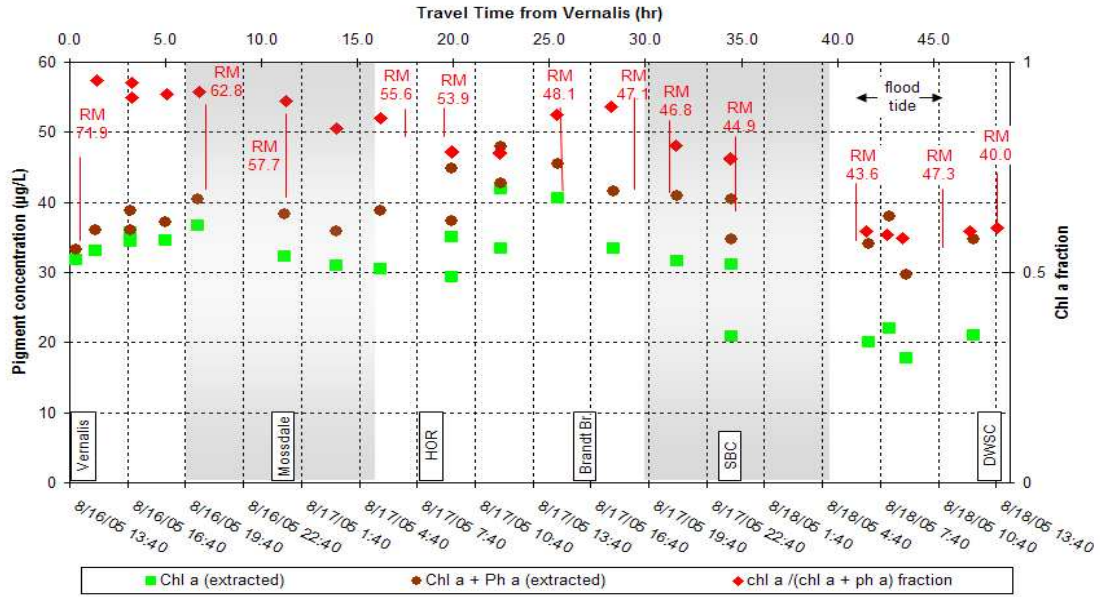


Figure 14: Pigment concentrations, dissolved oxygen, and pH within the rhodamine WT plume flowing from Vernalis to the DWSC, September 15-17, 2005.

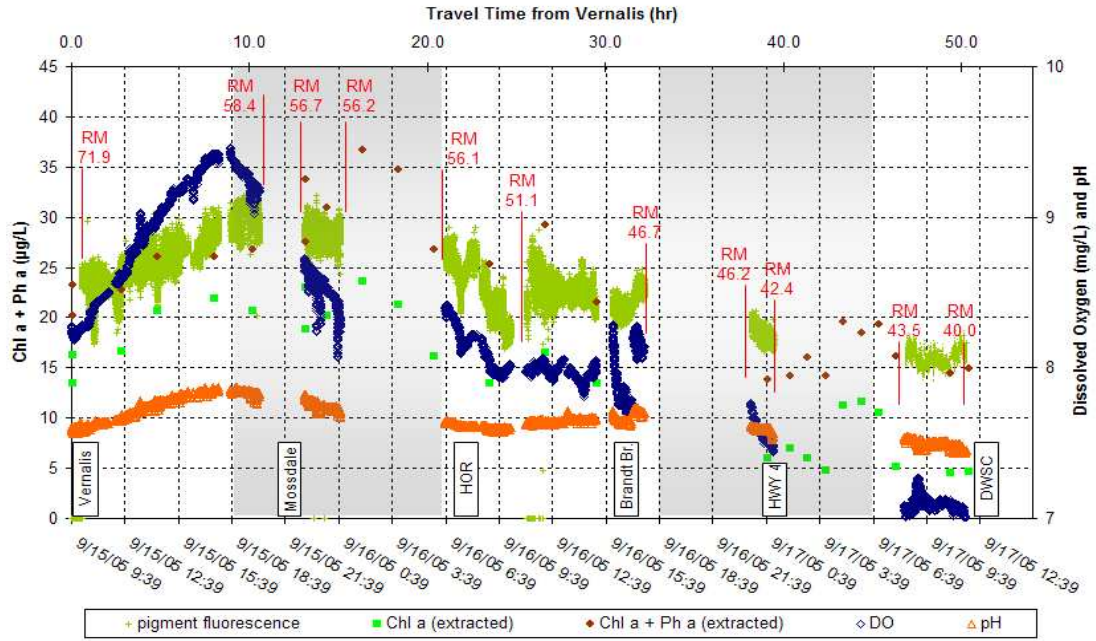


Figure 15: Extracted pigment concentration and the chl a/(chl a + ph a) fraction within the rhodamine WT plume flowing from Vernalis to the DWSC, September 15-17, 2005.

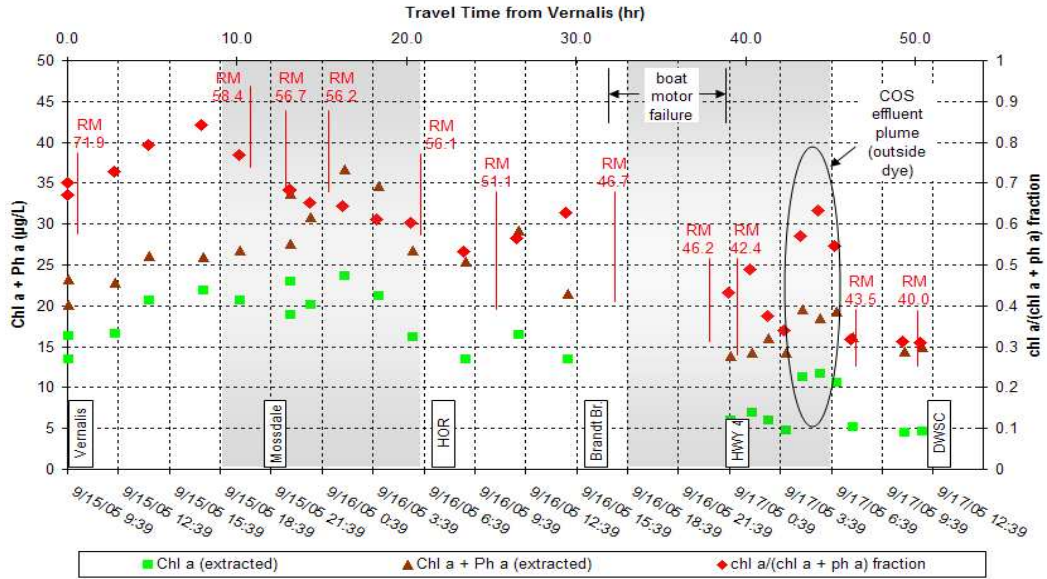


Figure 16: Pigment concentrations, dissolved oxygen, and pH within the rhodamine WT plume flowing from Vernalis to the DWSC, October 13-14, 2005.

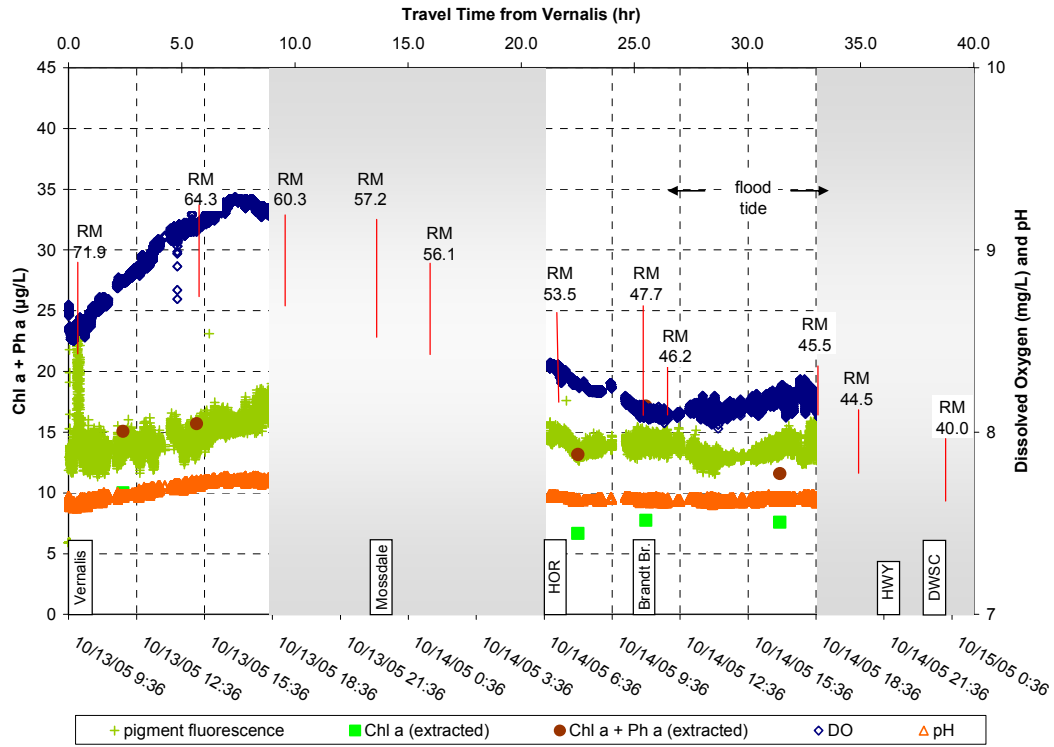


Figure 17: Extracted pigment concentration and the chl a/(chl a + ph a) fraction within the rhodamine WT plume flowing from Vernalis to the DWSC, October 13-14, 2005.

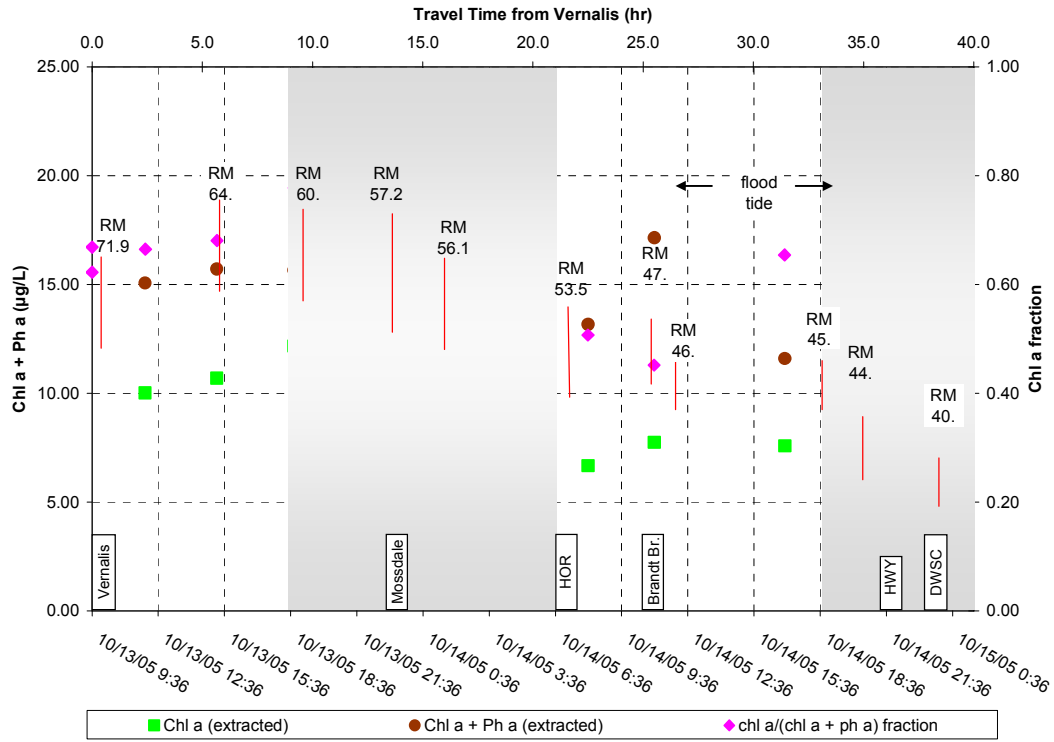


Figure 18: Pigment concentrations, dissolved oxygen, and pH within the rhodamine WT plume flowing from Vernalis to the DWSC, July 19-21 2006.

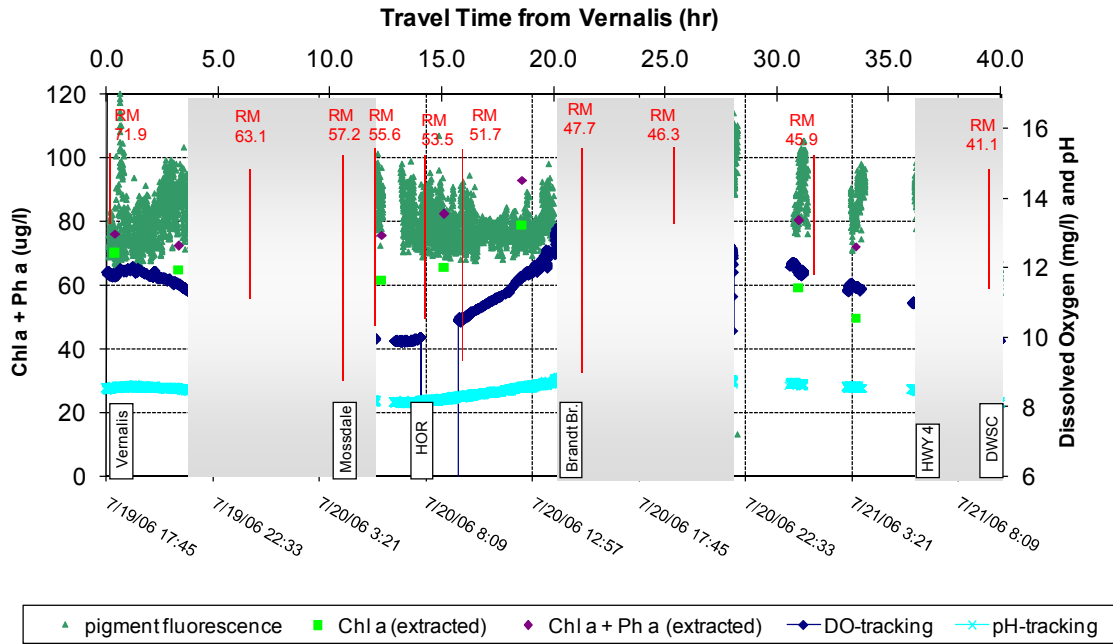


Figure 19: Extracted pigment concentration and the chl a/(chl a + ph a) fraction within the rhodamine WT plume flowing from Vernalis to the DWSC, July 19-21 2006.

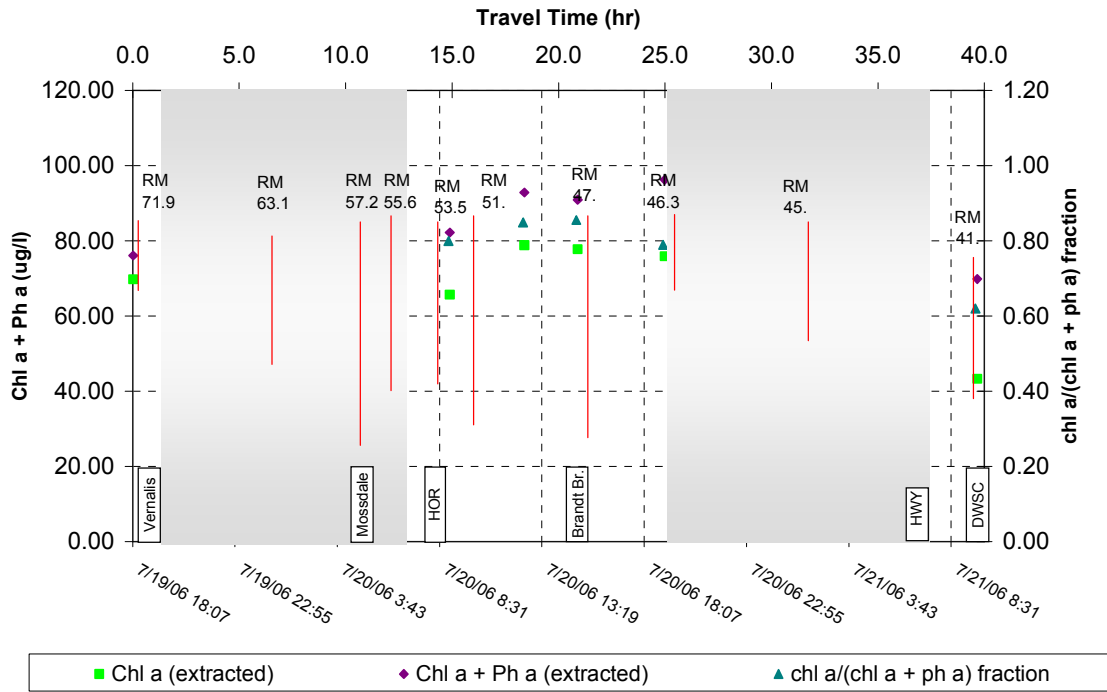


Figure 20: Pigment concentrations, dissolved oxygen, and pH within the rhodamine WT plume flowing from Vernalis to the DWSC, August 9, 10 2006.

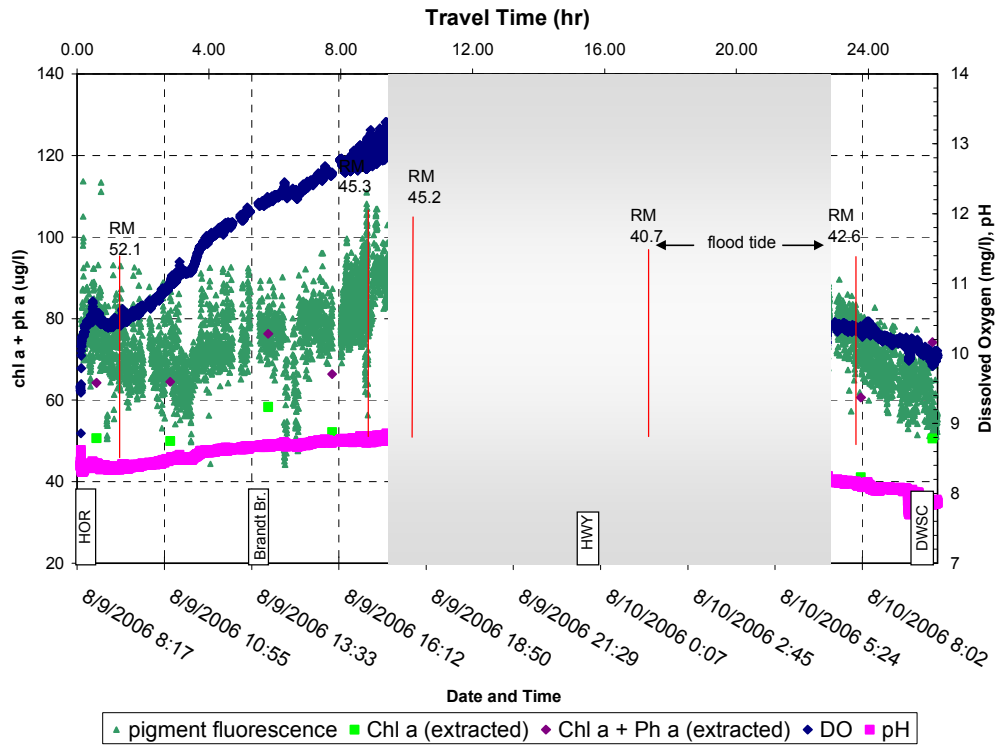


Figure 21: Extracted pigment concentration and the chl a/(chl a + ph a) fraction within the rhodamine WT plume flowing from Vernalis to the DWSC, August 9, 10 2006.

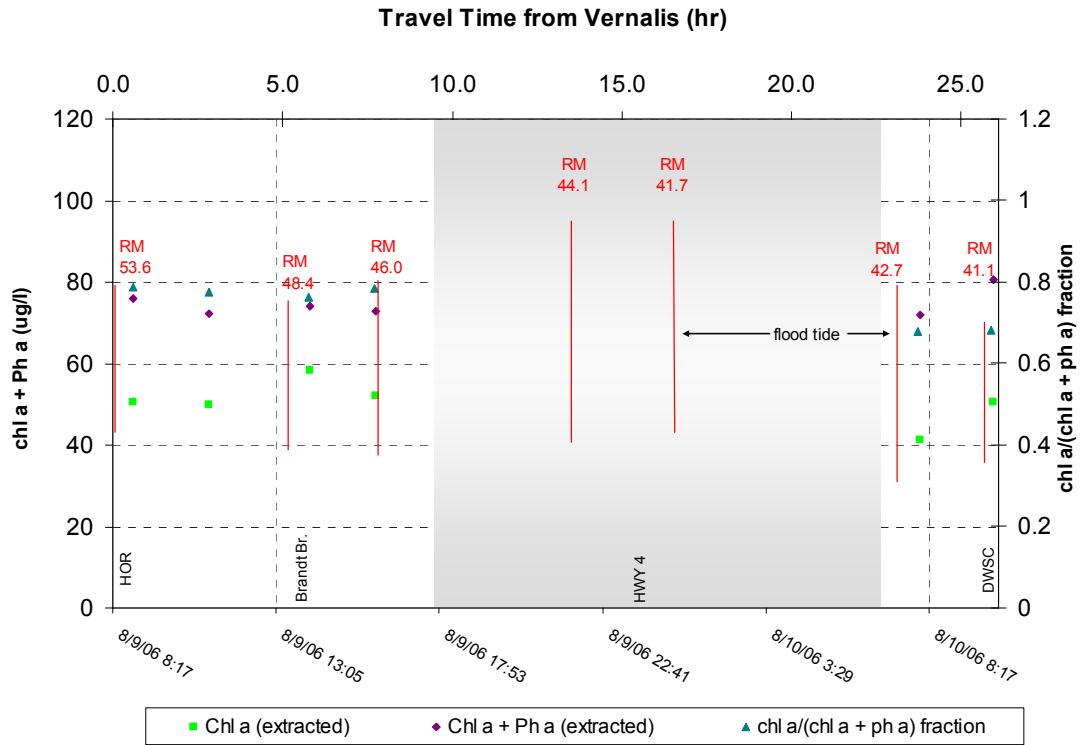


Figure 22: Extracted chlorophyll *a*, chlorophyll fluorescence and dissolved oxygen for the June 12-15, 2007 lagrangian tracking event.

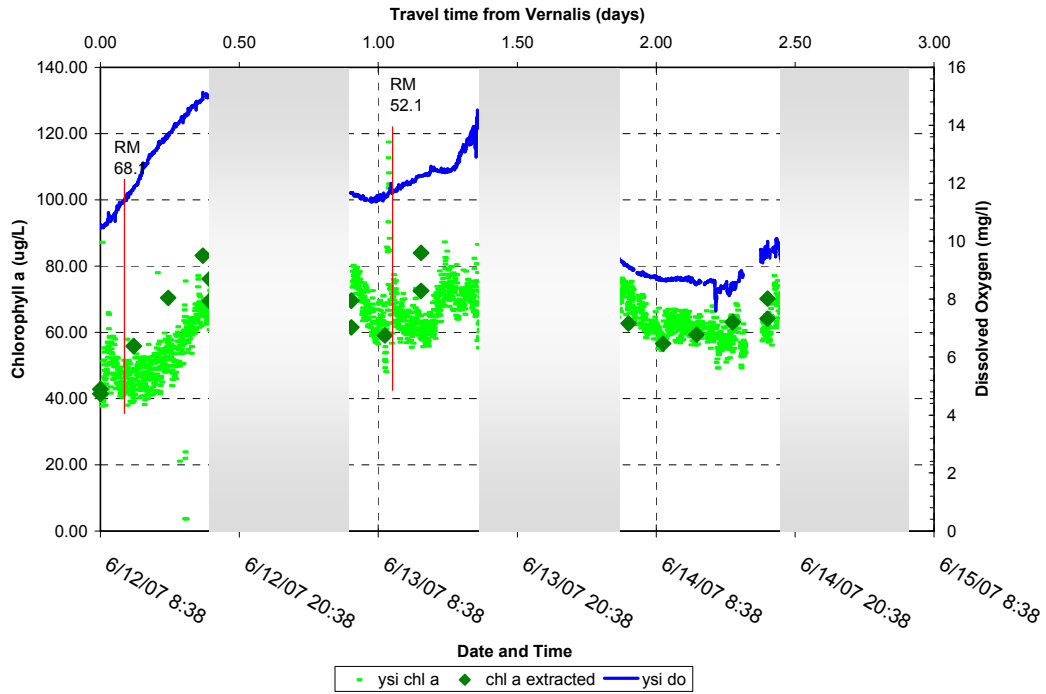


Figure 23: Extracted chlorophyll a and pheophytin a concentrations during lagrangian tracking performed on June 12-15, 2007.

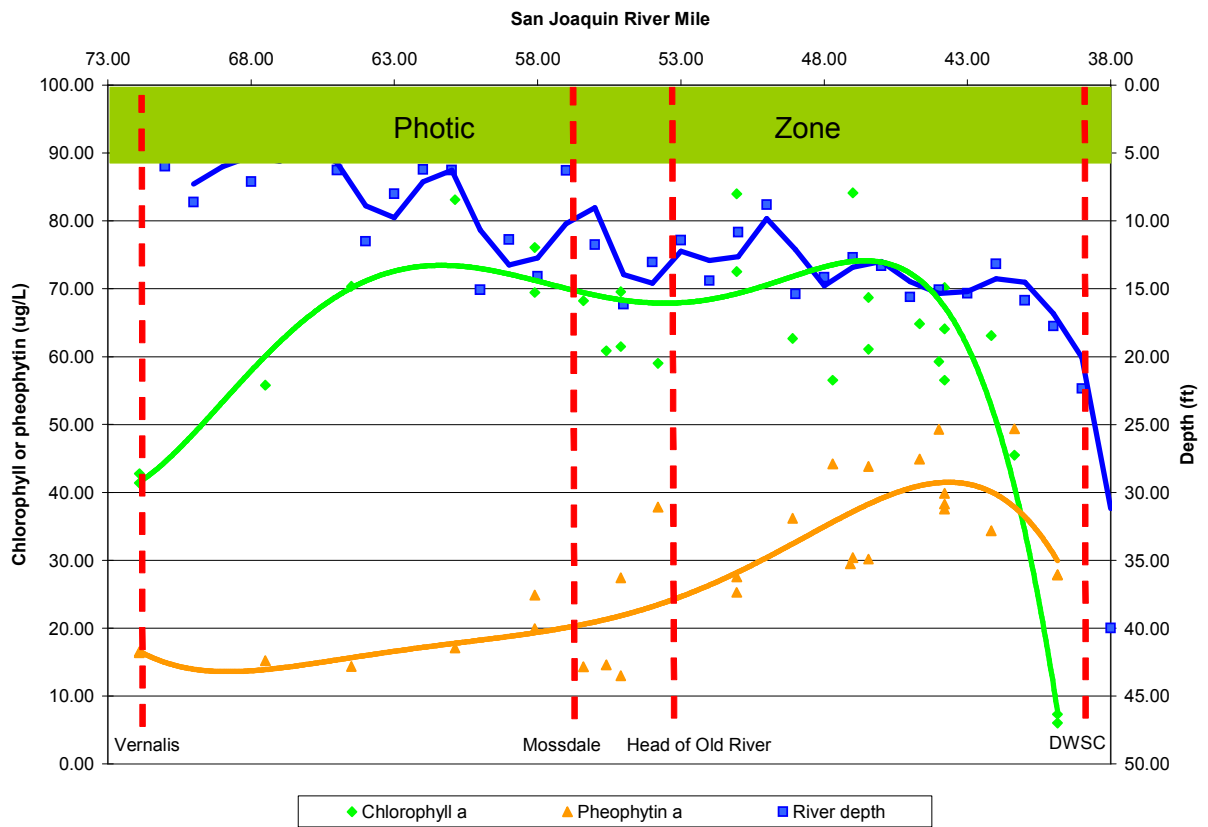


Figure 24: Chlorophyll a to total pigment ratio compared with the water depth during the June 12-15, 2007 lagrangian tracking.

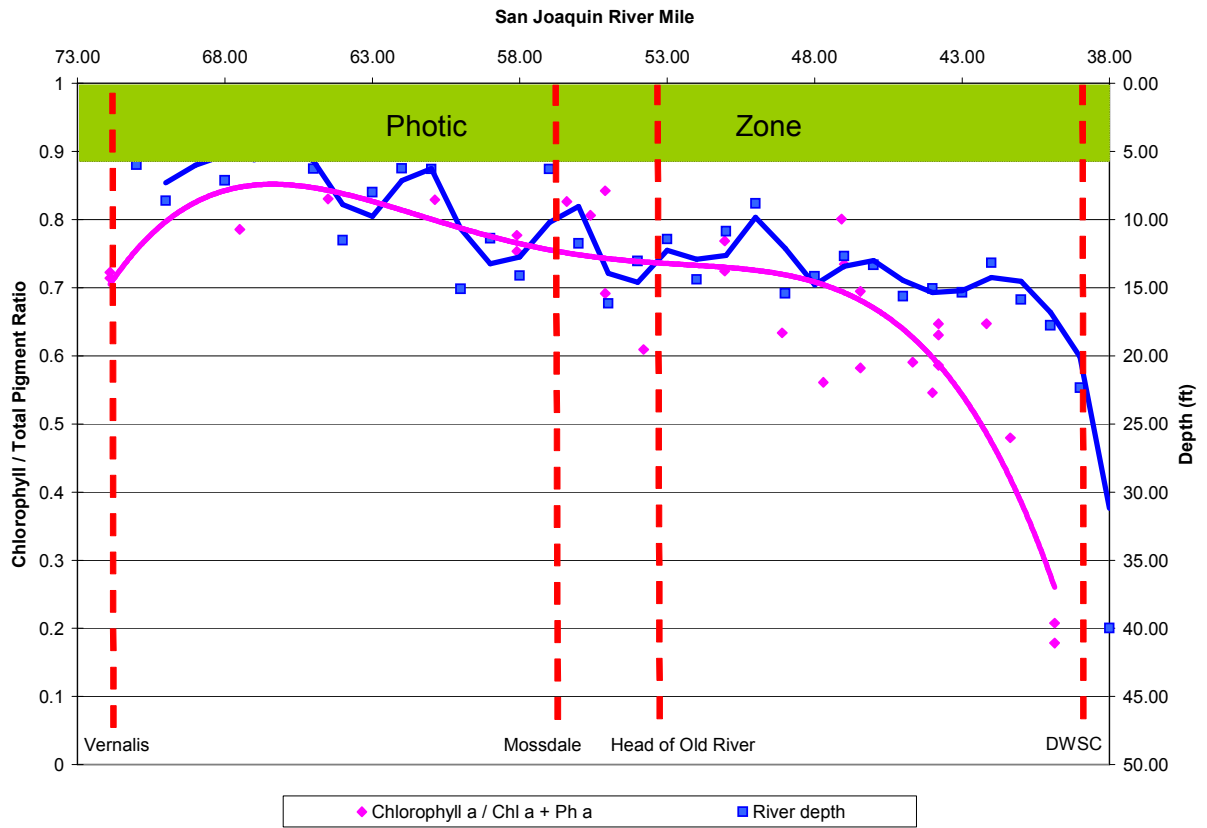


Figure 25: Chlorophyll a, pheophytin a, and zooplankton concentrations during the June 12-15, 2007 lagrangian tracking from Vernalis to the DWSC.

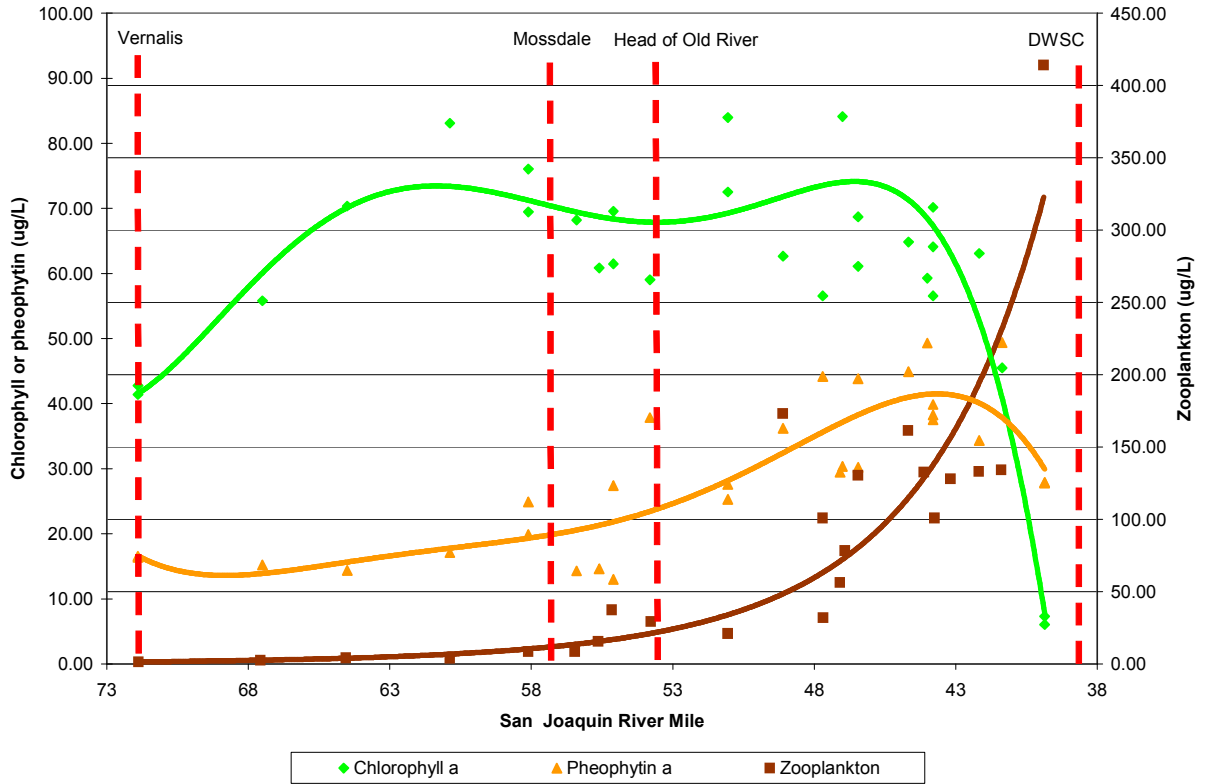
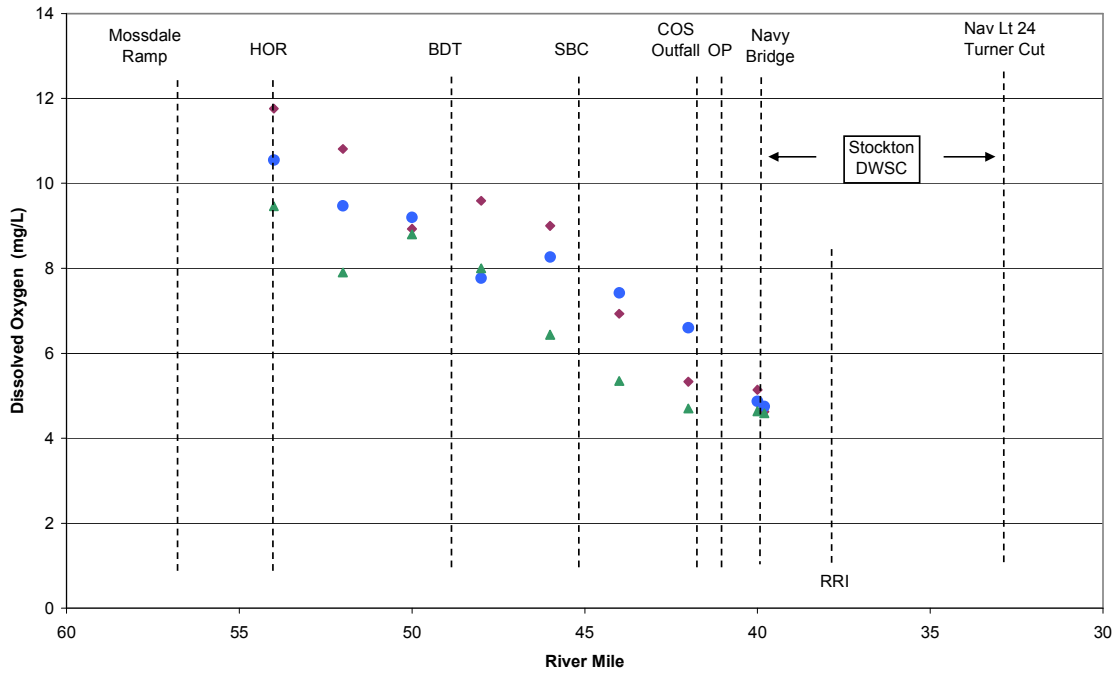
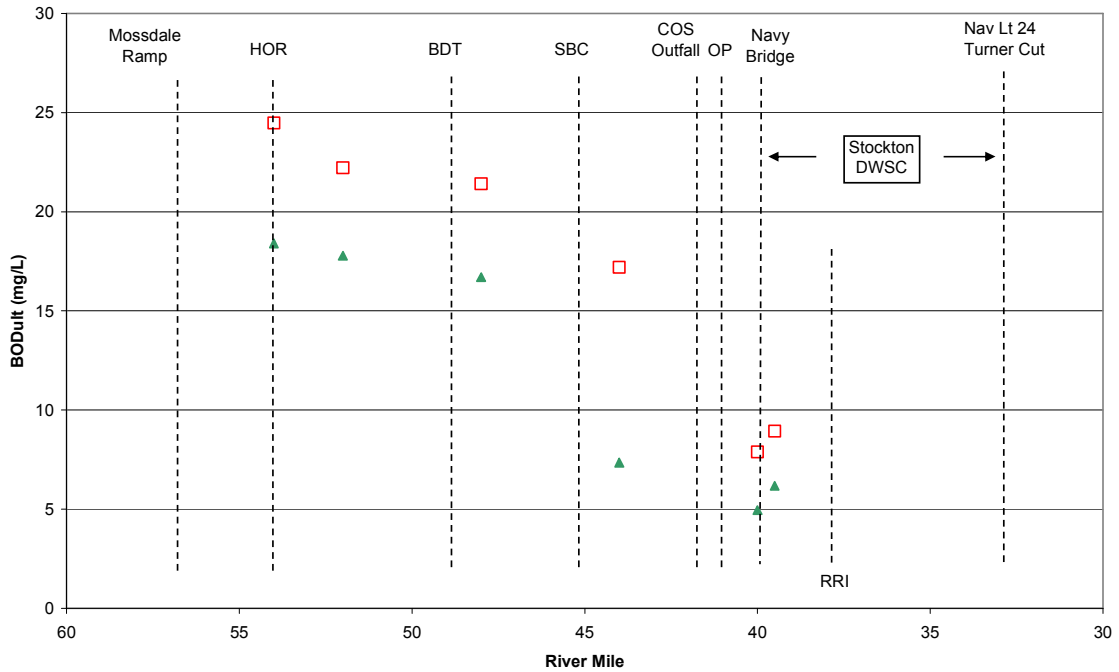


Figure 26: Longitudinal profiles of dissolved oxygen and ultimate BOD during slack tides on July 14 and 15, 2007.

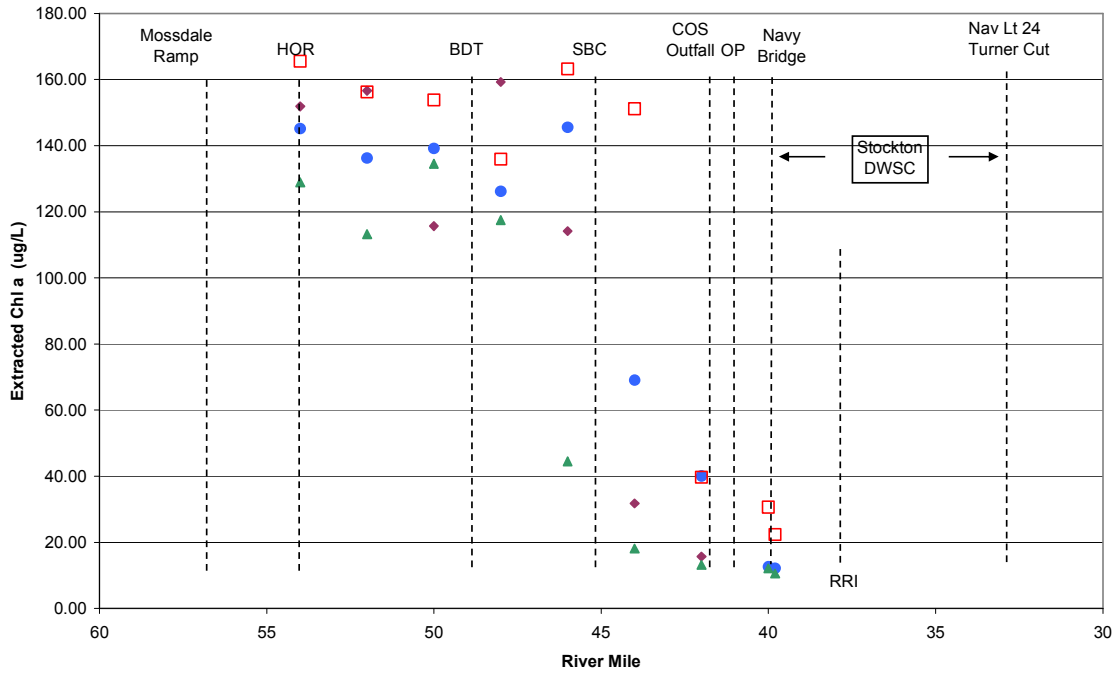


◆ LH tide 7/16 22:49 to 00:51    ● HL tide 7/17 3:49 to 6:00    ▲ HH tide 7/17 8:45 to 10:52    ◻ LL tide 7/17 15:36 to 17:55 (temp. sensor failure)

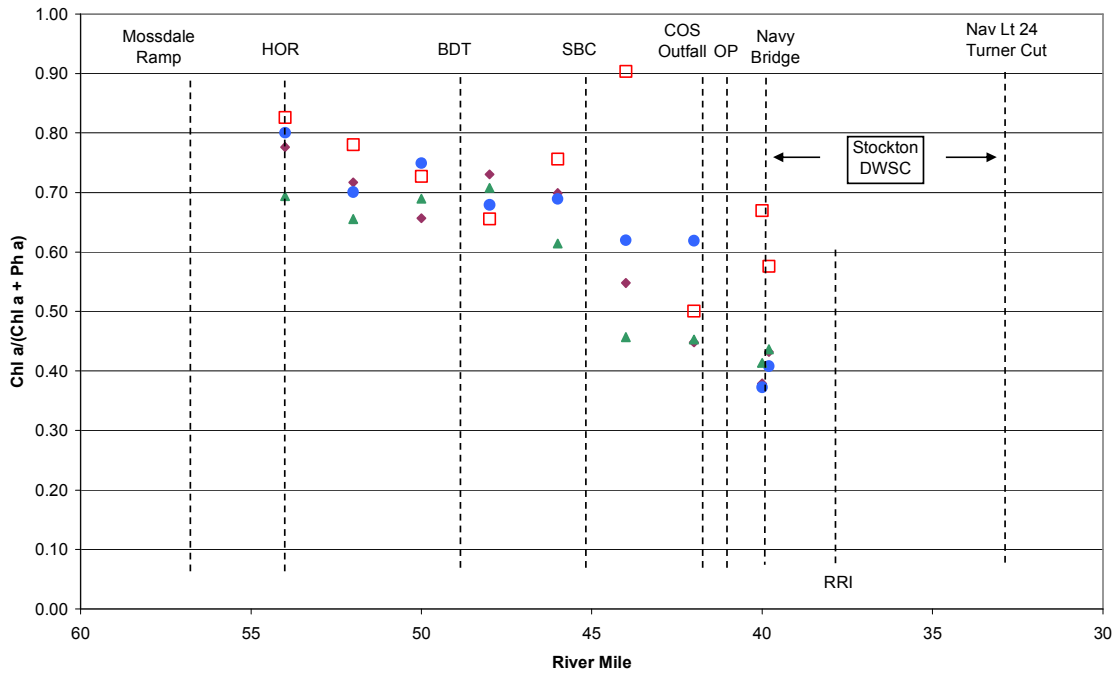


▲ HH tide 7/17 8:45 to 10:52    ◻ LL tide 7/17 15:36 to 17:55 (temp. sensor failure)

Figure 27: Longitudinal profiles of extracted chlorophyll a and and pigment ratio during slack tides on July 14 and 15, 2007.



◆ LH tide 7/16 22:49 to 00:51    ● HL tide 7/17 3:49 to 6:00    ▲ HH tide 7/17 8:45 to 10:52    ◻ LL tide 7/17 15:36 to 17:55 (temp. sensor failure)



◆ LH tide 7/16 22:49 to 00:51    ● HL tide 7/17 3:49 to 6:00    ▲ HH tide 7/17 8:45 to 10:52    ◻ LL tide 7/17 15:36 to 17:55 (temp. sensor failure)

Figure 28: Longitudinal profiles of dissolved oxygen and ultimate BOD during slack tides on August 14 and 15, 2007.

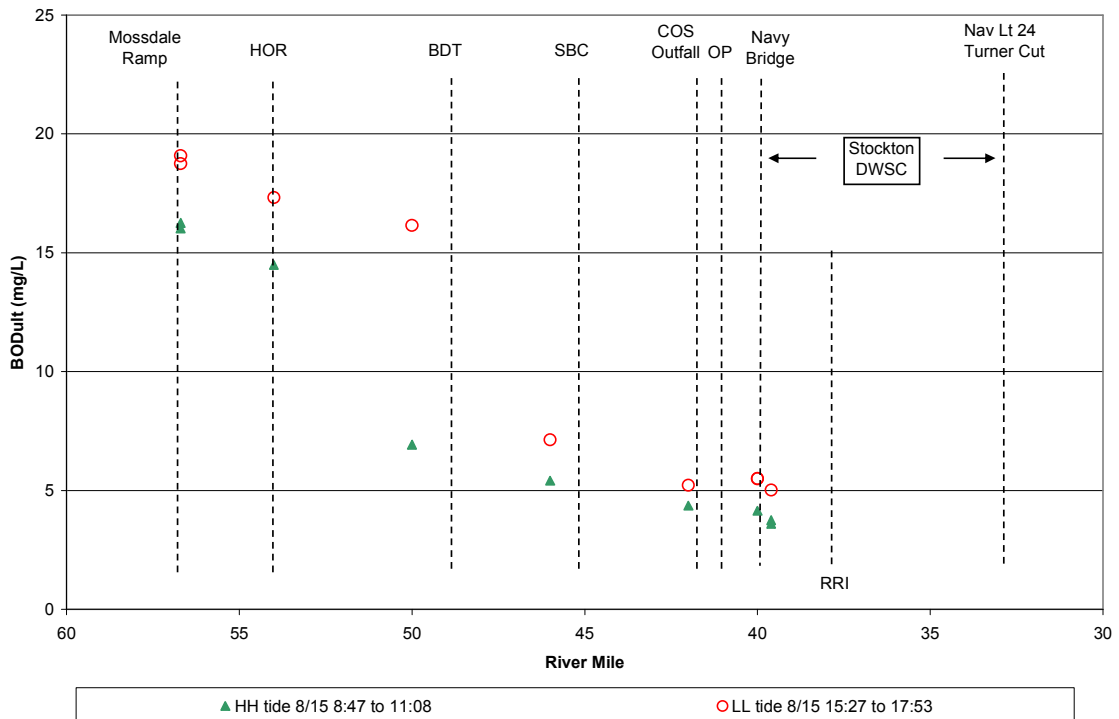
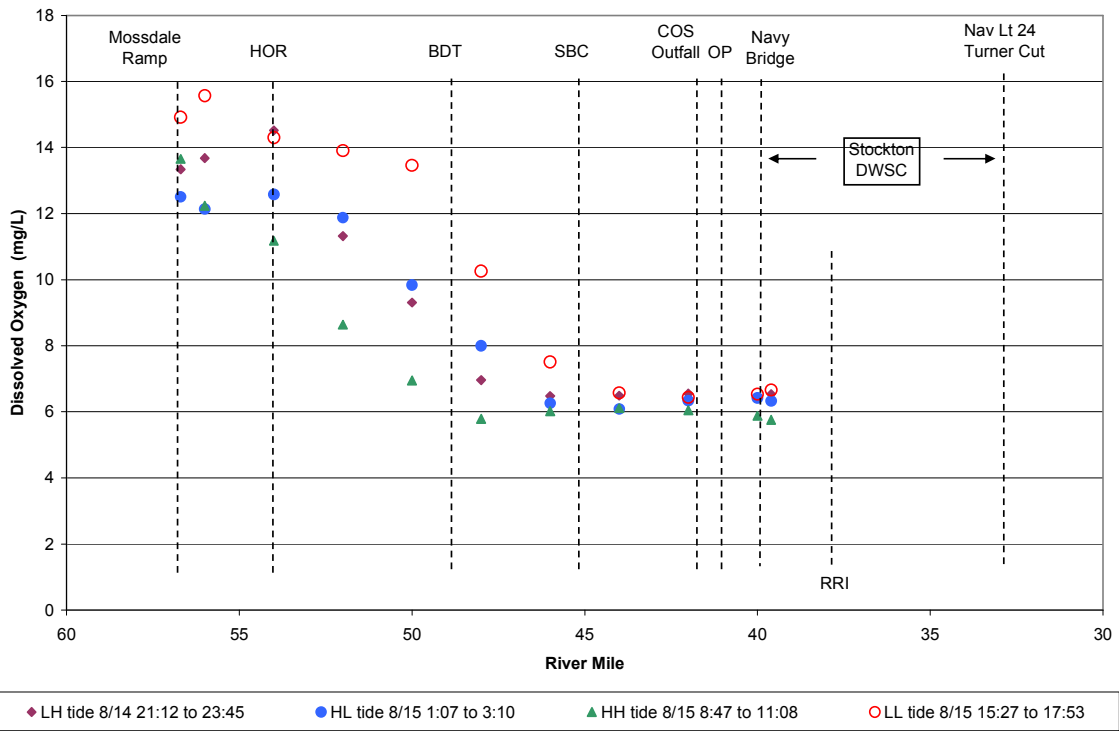


Figure 29: Longitudinal profiles of extracted chlorophyll a and and pigment ratio during slack tides on August and 15, 2007.

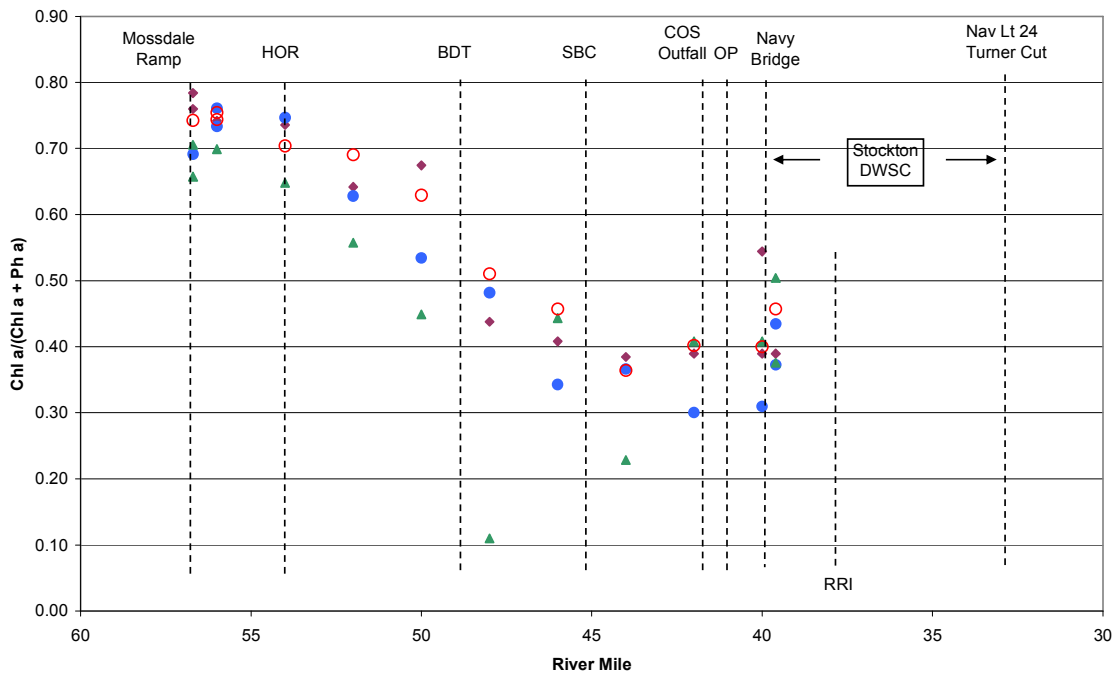
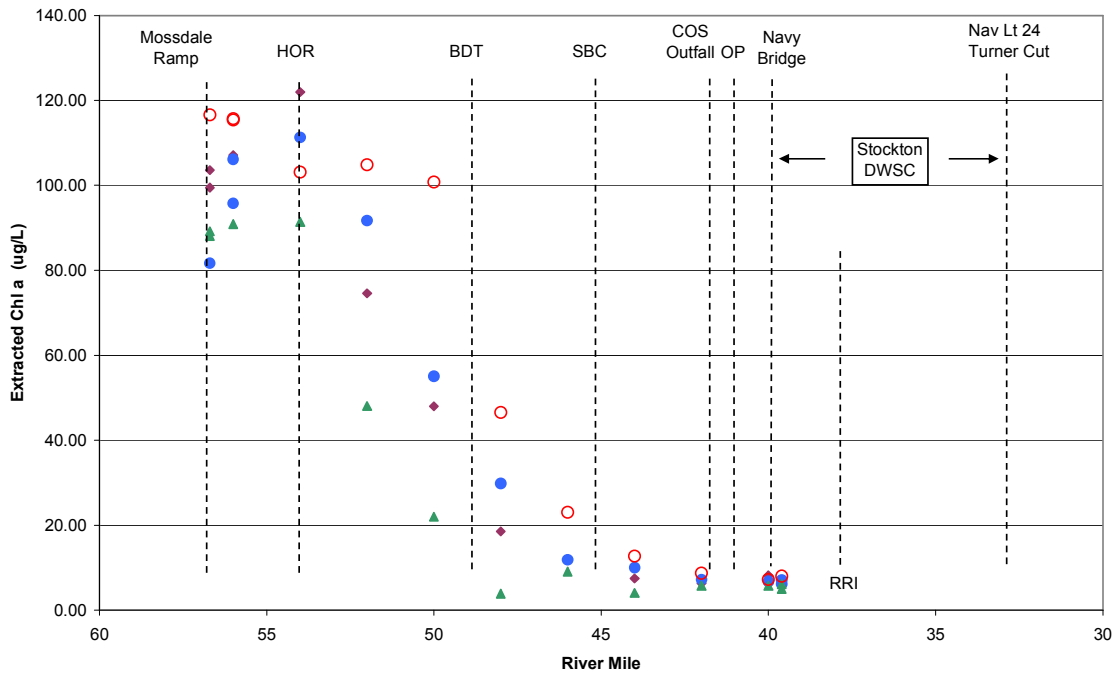


Figure 30: Longitudinal profiles of extracted chlorophyll a and and pigment ratio during slack tides on September 19 and 20, 2007.

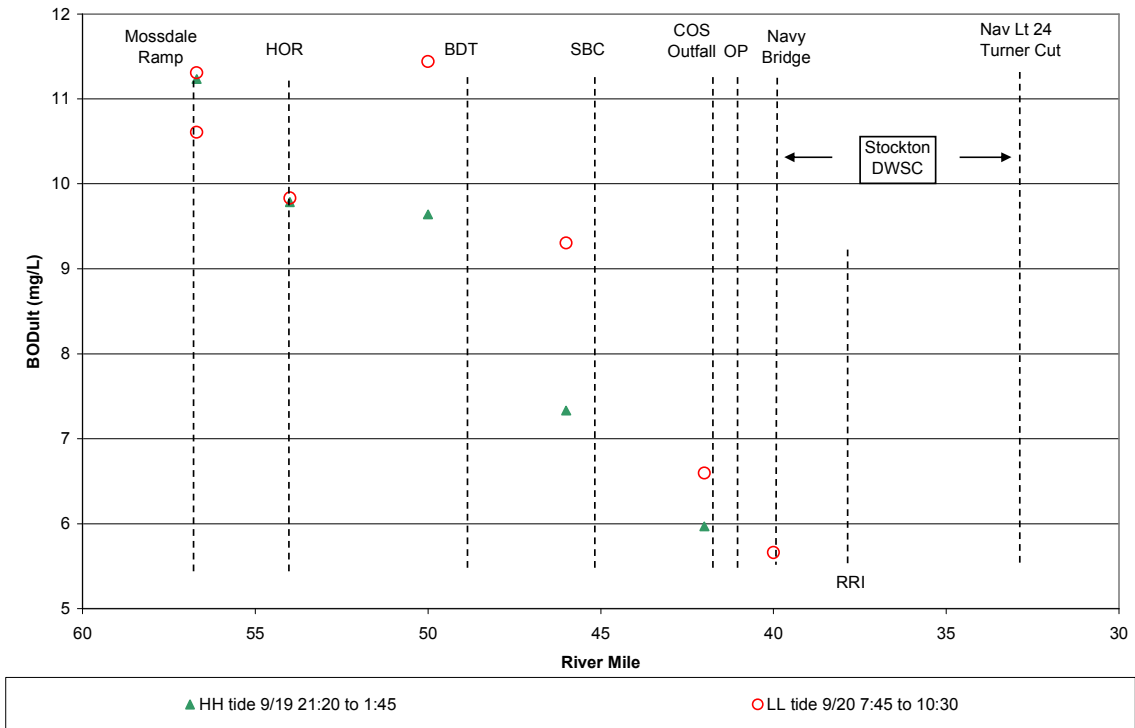
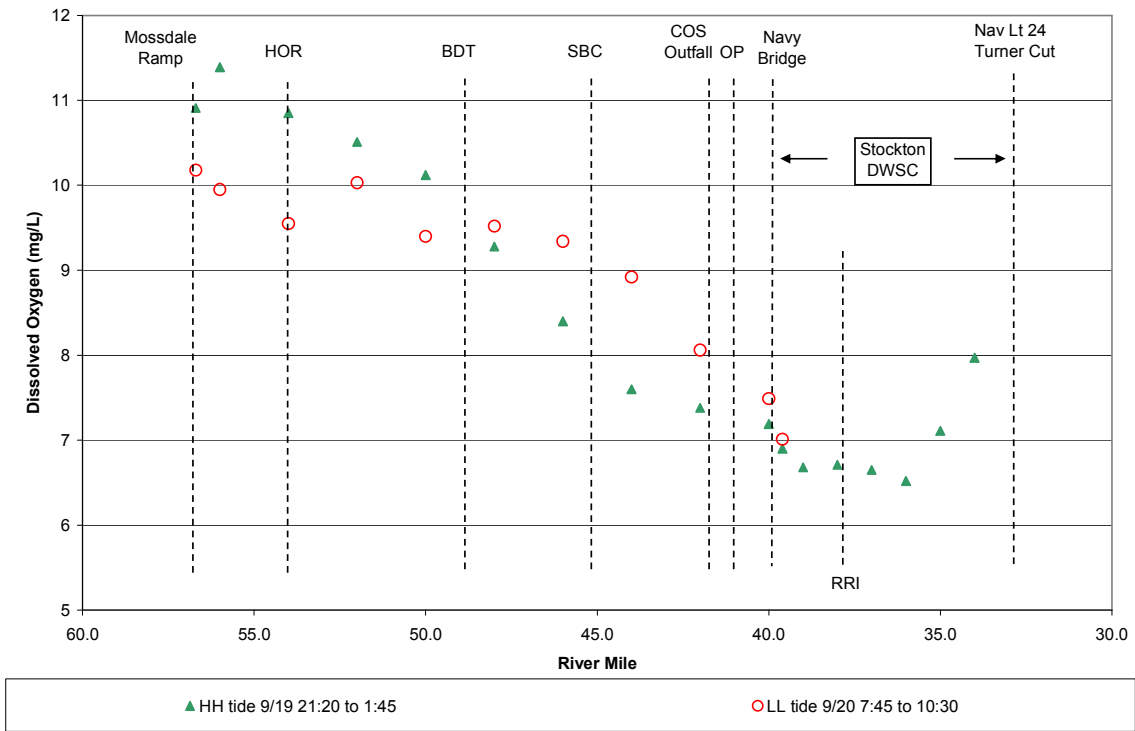


Figure 31: Longitudinal profiles of extracted chlorophyll a and and pigment ratio during slack tides on September 19 and 20, 2007.

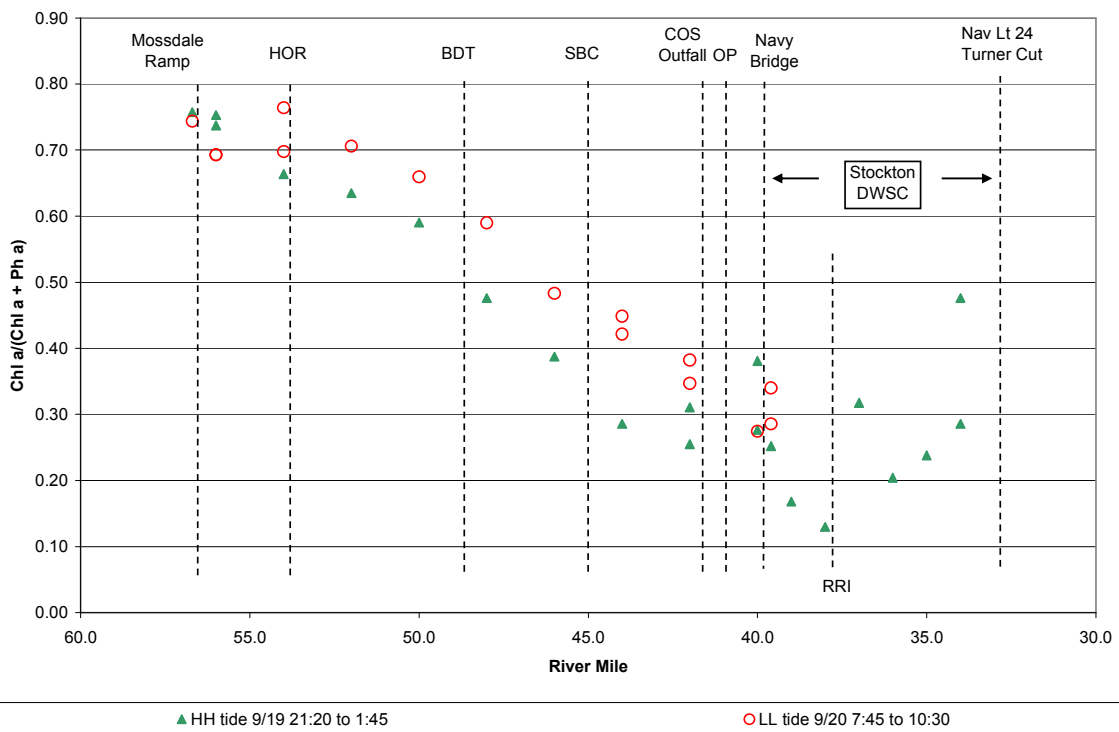
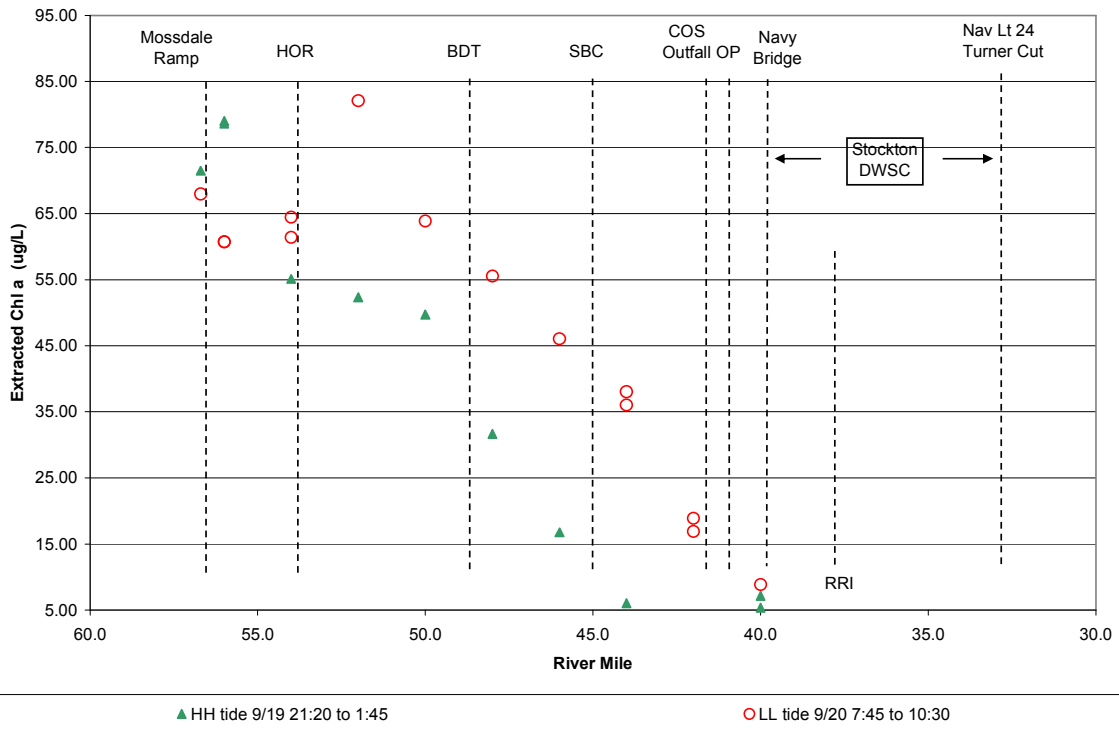


Figure 32: Zooplankton grazing for increasing initial concentrations of Zooplankton after 4.5 hours in the photic zone (approximately 2 ft depth) on September 27, 2007.

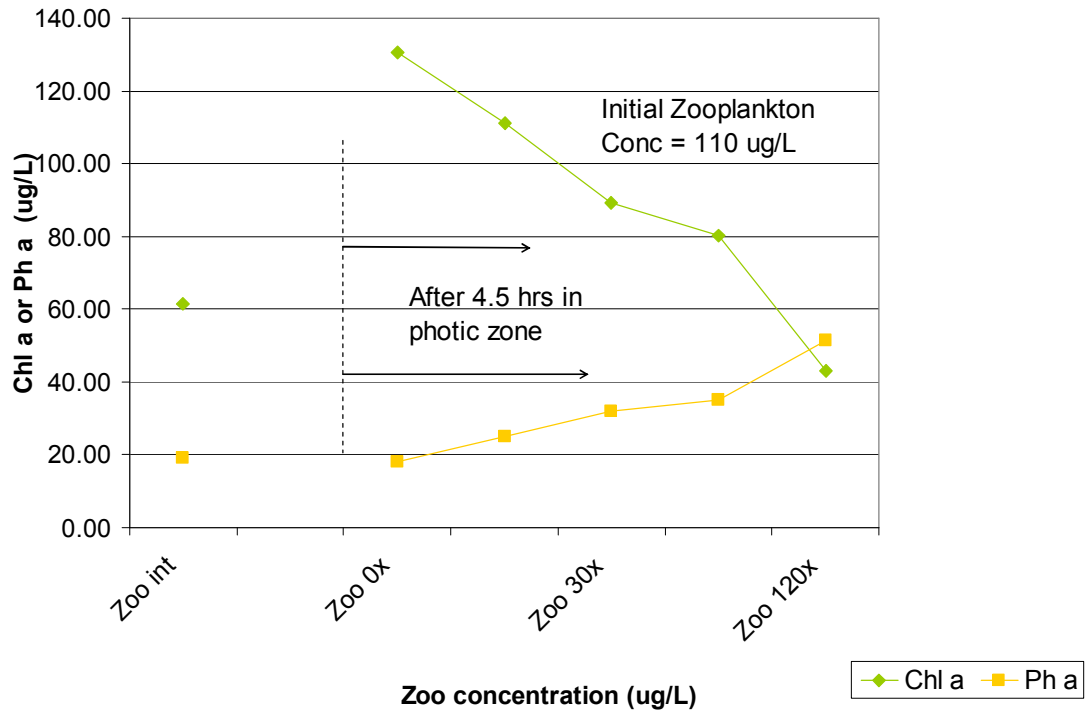


Figure 33: The response of chlorophyll *a* and pheophytin *a* in microcosms with and without concentrated zooplankton measured on October 3, 2007.

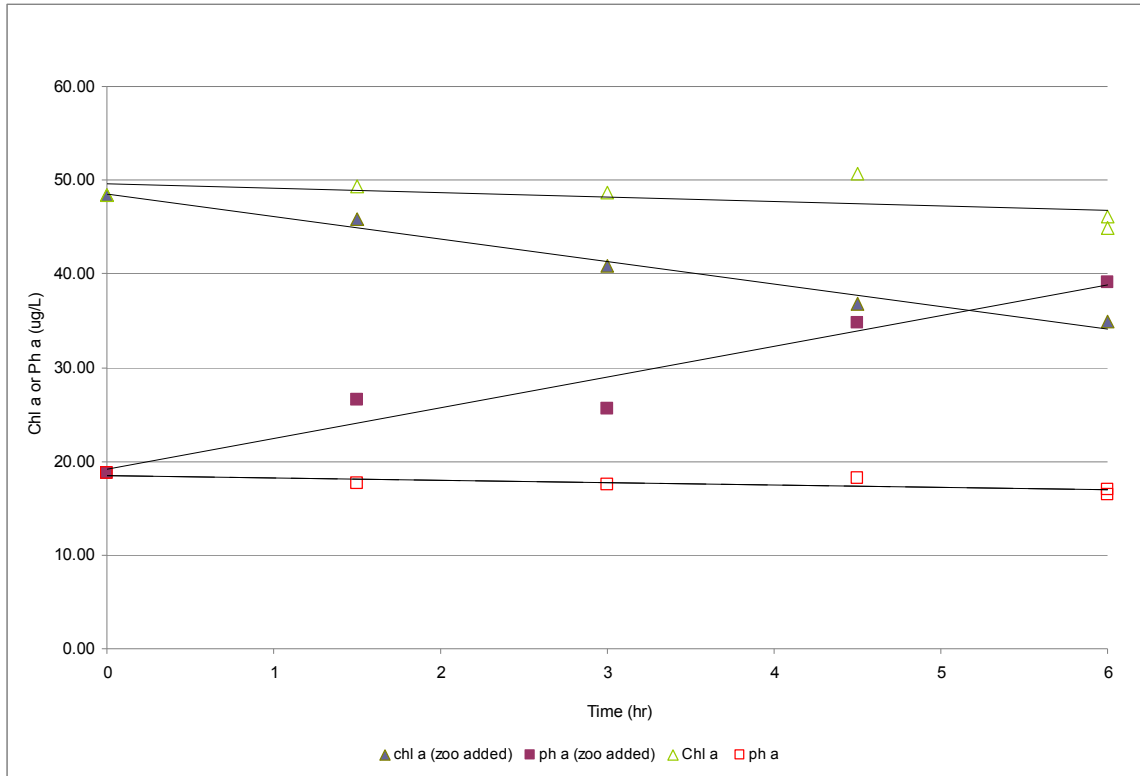


Figure 34: Chlorophyll decay experiment results for water collected at Mossdale (rm56.7) on August 1, 2007 and monitored in the lab for two weeks.

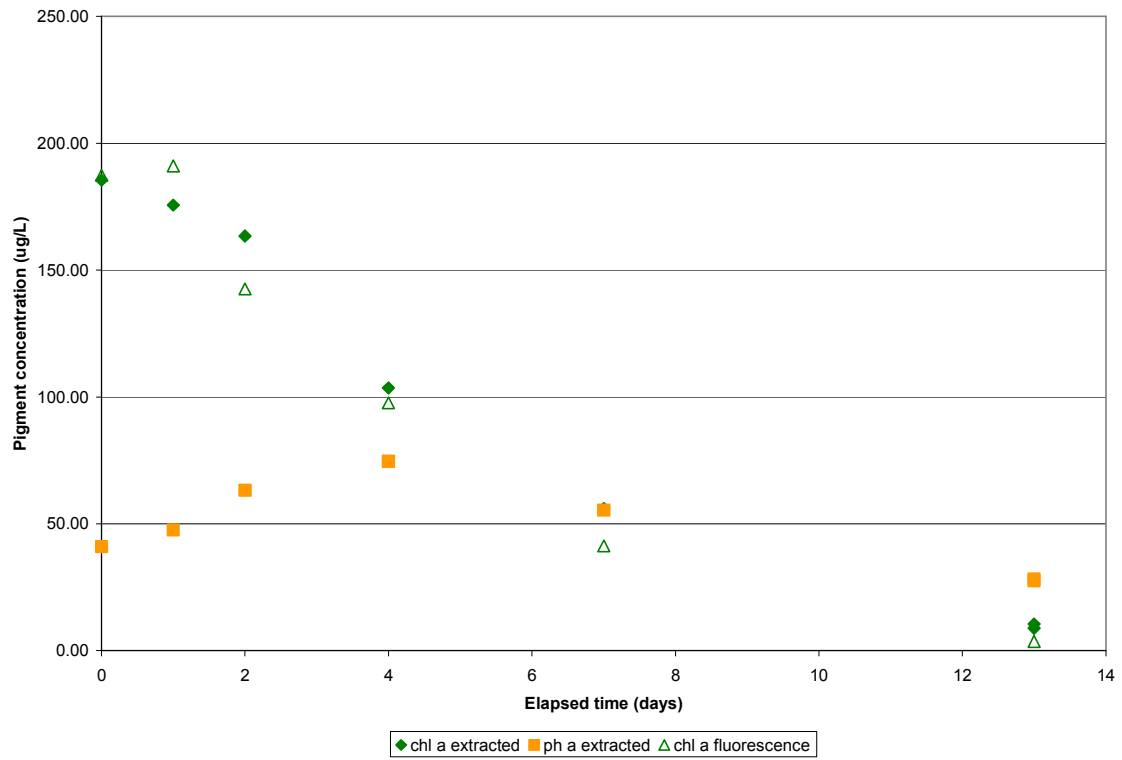


Figure 35: Chlorophyll decay experiment results for water collected at the Brandt Bridge Station (rm48) on August 1, 2007 and monitored in the lab for two weeks.

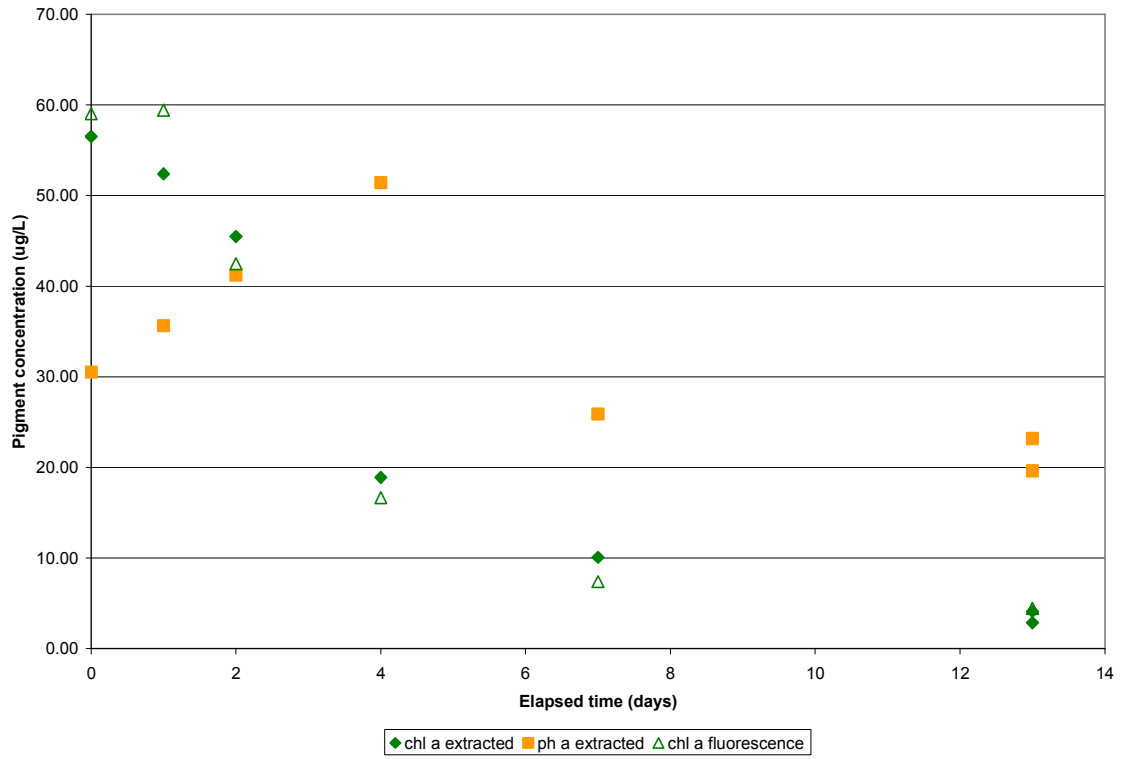


Figure 36: Chlorophyll decay experiment results for water collected at the Stockton Brick Company (SBC) Station (rm45) on August 1, 2007 and monitored in the lab for two weeks.

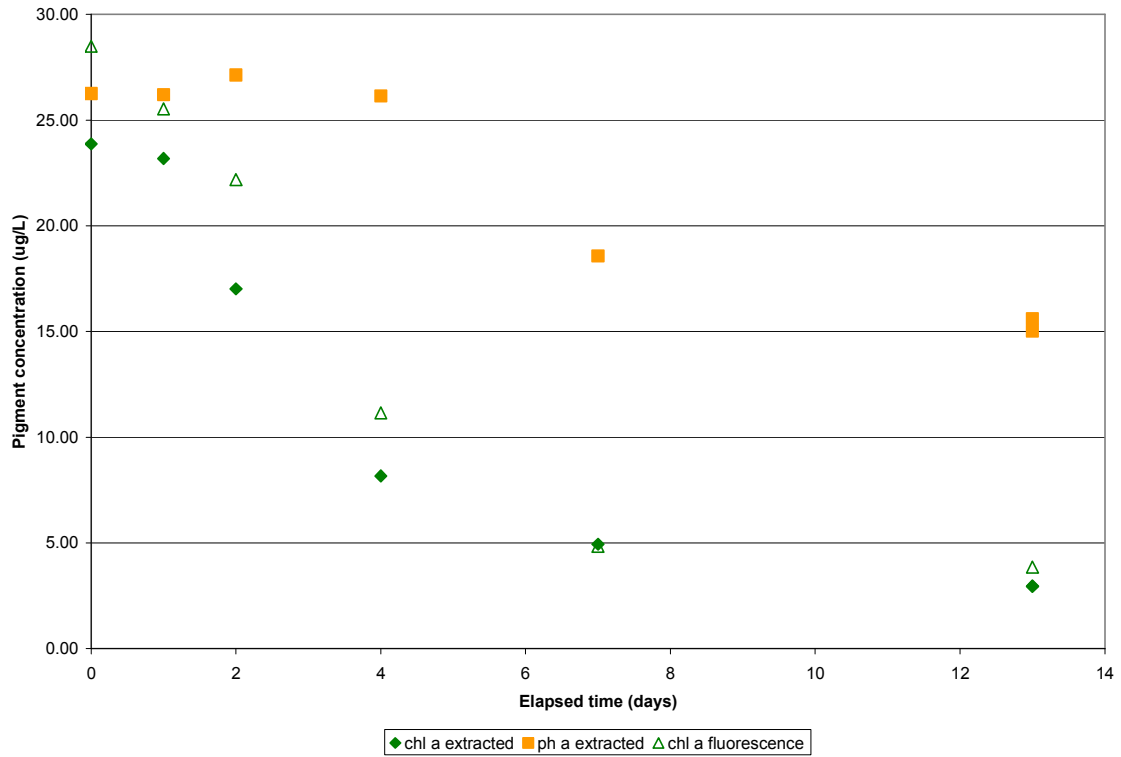


Figure 37: Chlorophyll decay experiment results for water collected at the Outfall Pier (OP) Station (rm41) on August 1, 2007 and monitored in the lab for two weeks.

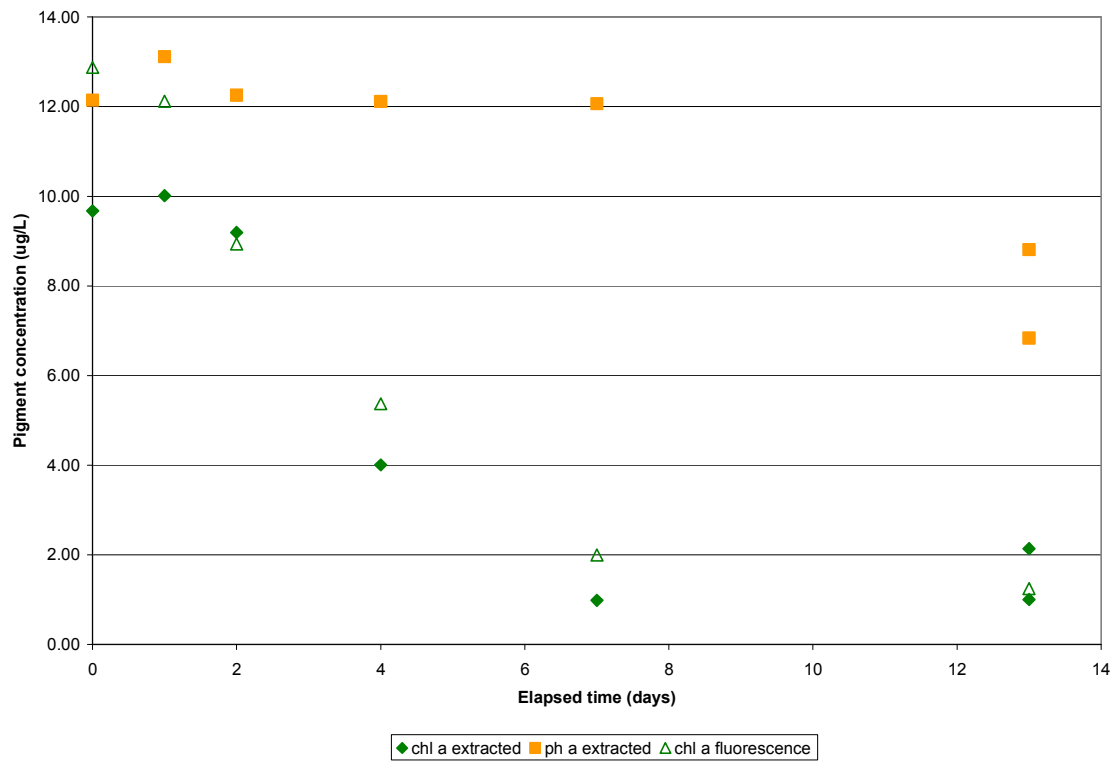


Figure 38: BOD, CBOD and NBOD measured for San Joaquin River water collected at SJR 3, July, 2005.

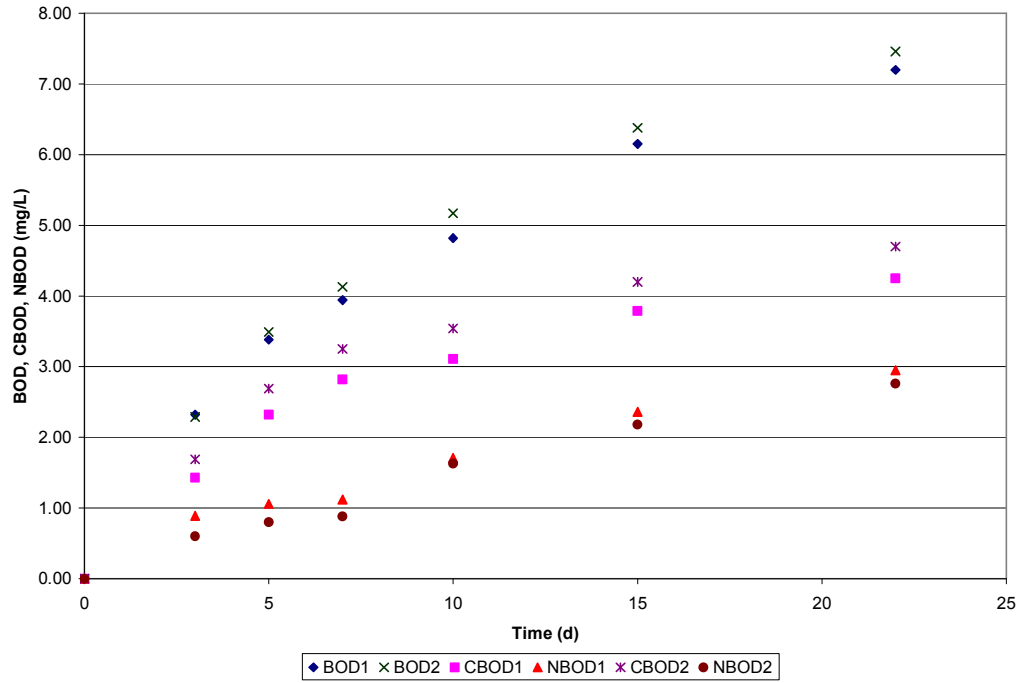


Figure 39: Correlation of BOD<sub>10</sub> to BOD<sub>ult</sub> for San Joaquin River samples collected in 2007.

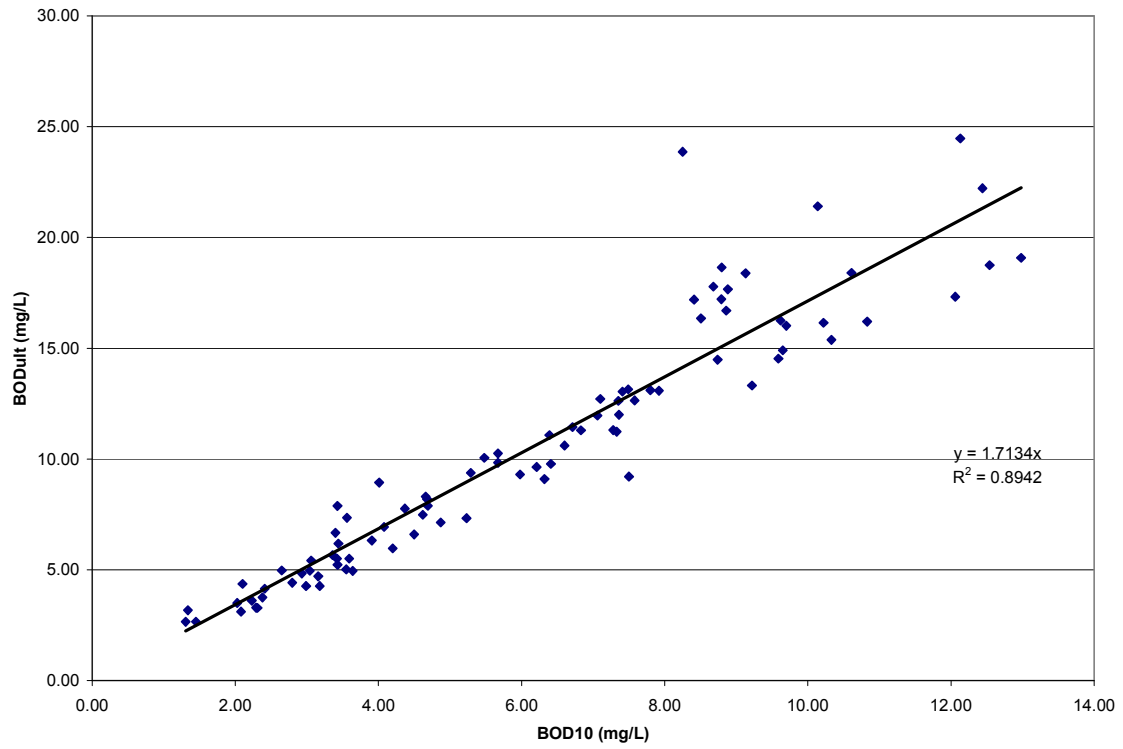


Figure 40: 20-day BOD concentrations for 2005 and 2006 monitoring.

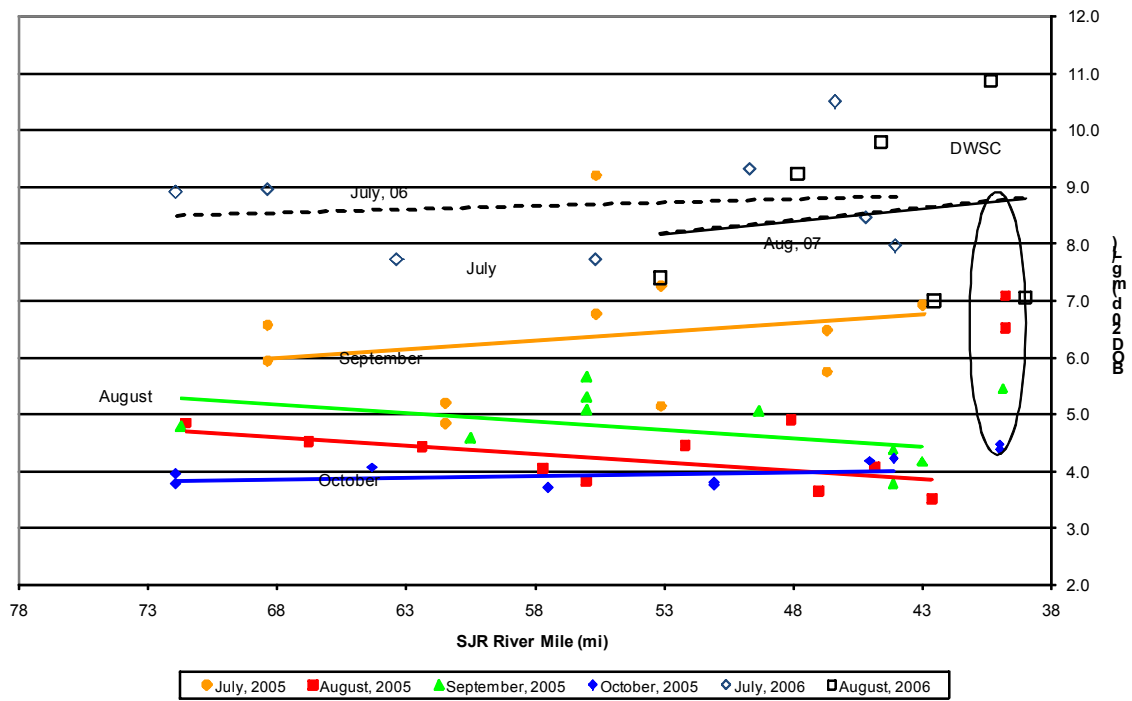


Figure 41: Longitudinal ultimate biochemical oxygen demands, ultimate carbonaceous BOD, and ultimate nitrogenous BOD for June 12-15, 2007 tracking.

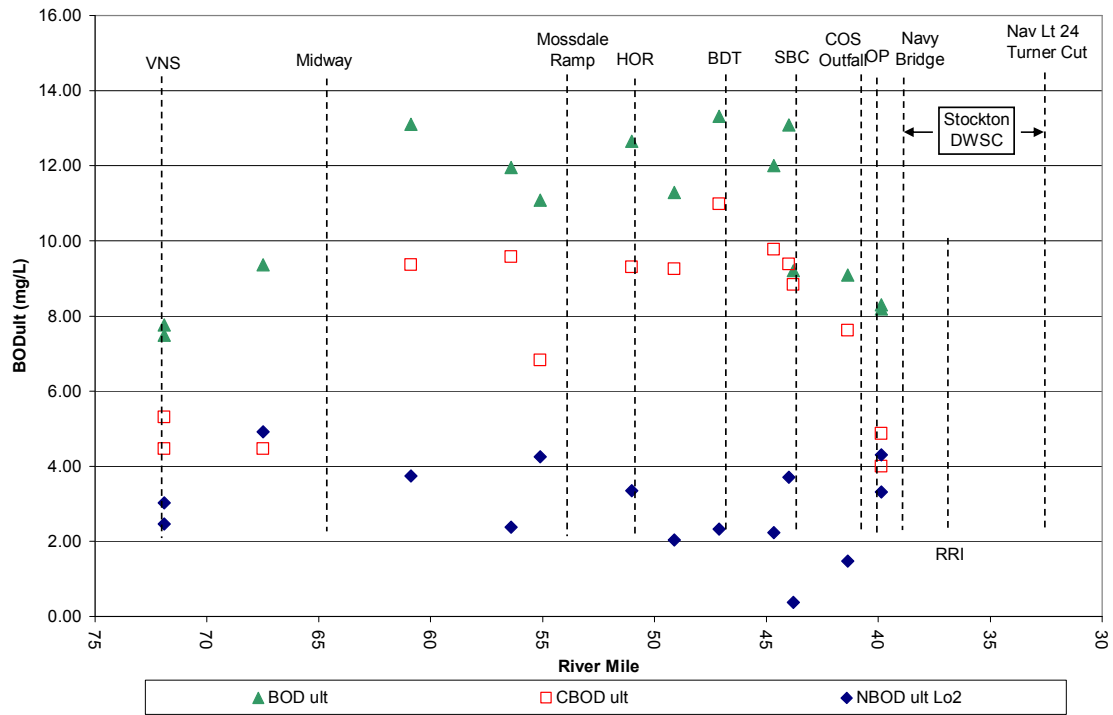


Figure 42: Dissolved oxygen production for measured light intensity at depths of 1, 2, and 3 feet.

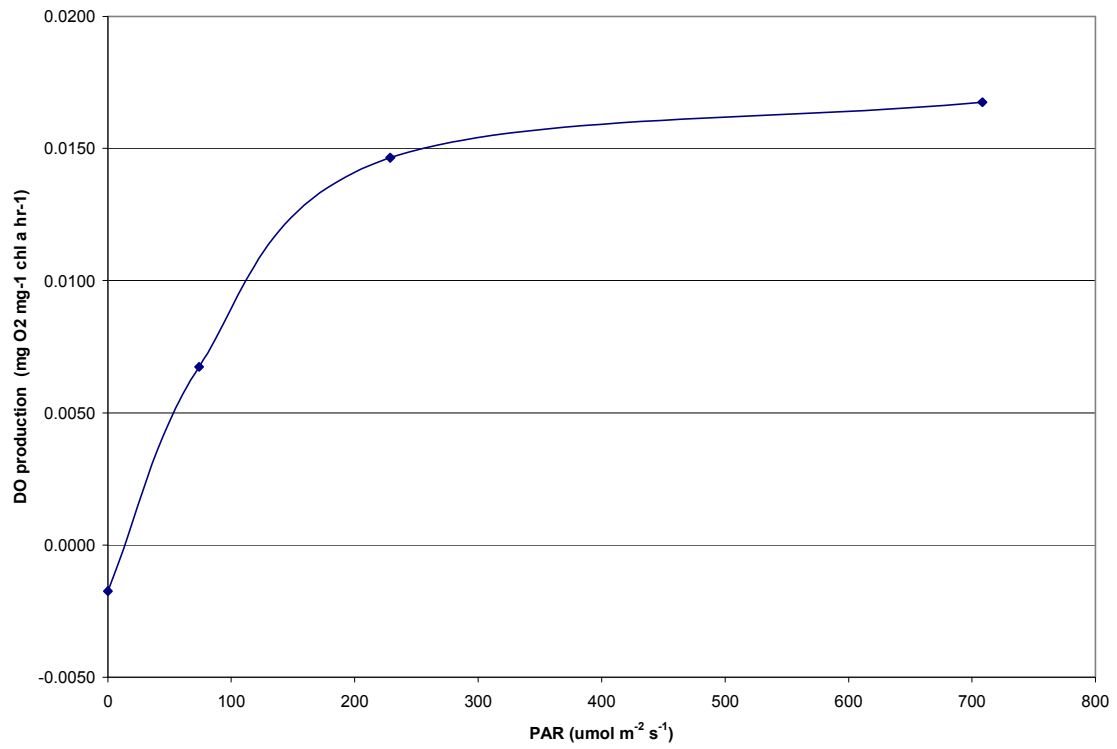


Figure 43: Measured and calculated chlorophyll a production in light-dark bottles deployed below Vernalis (River Mile 72 to 69).

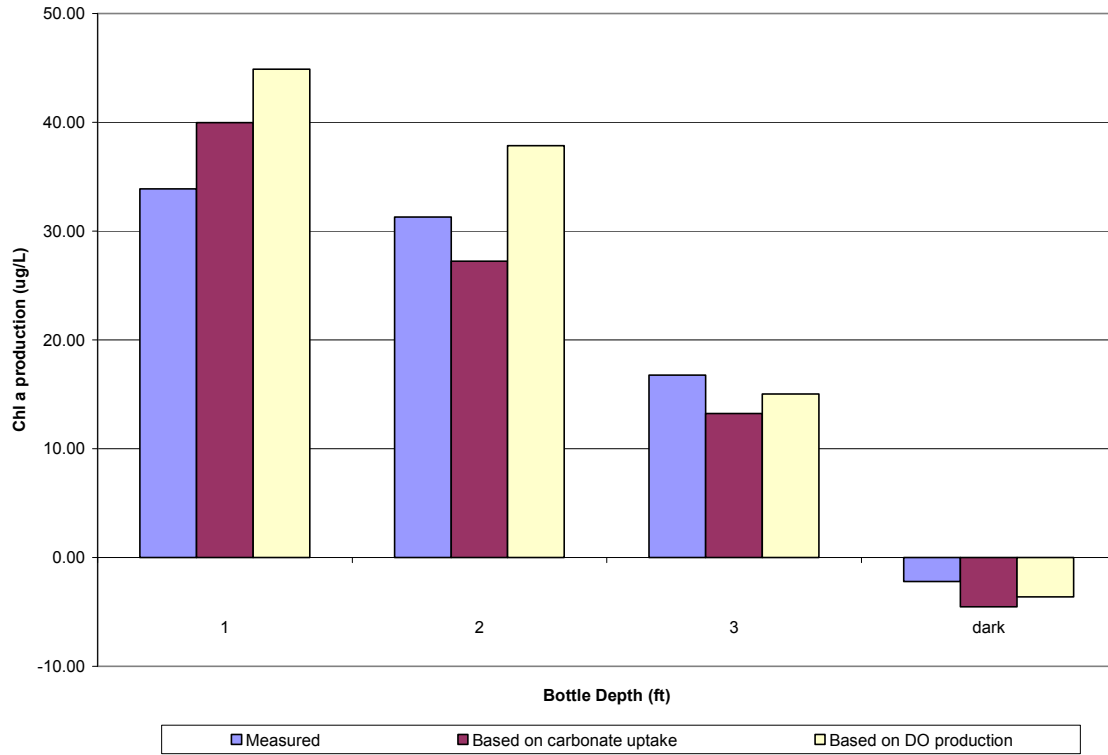


Figure 44: San Joaquin River bathymetry measured during the lagrangian monitoring.

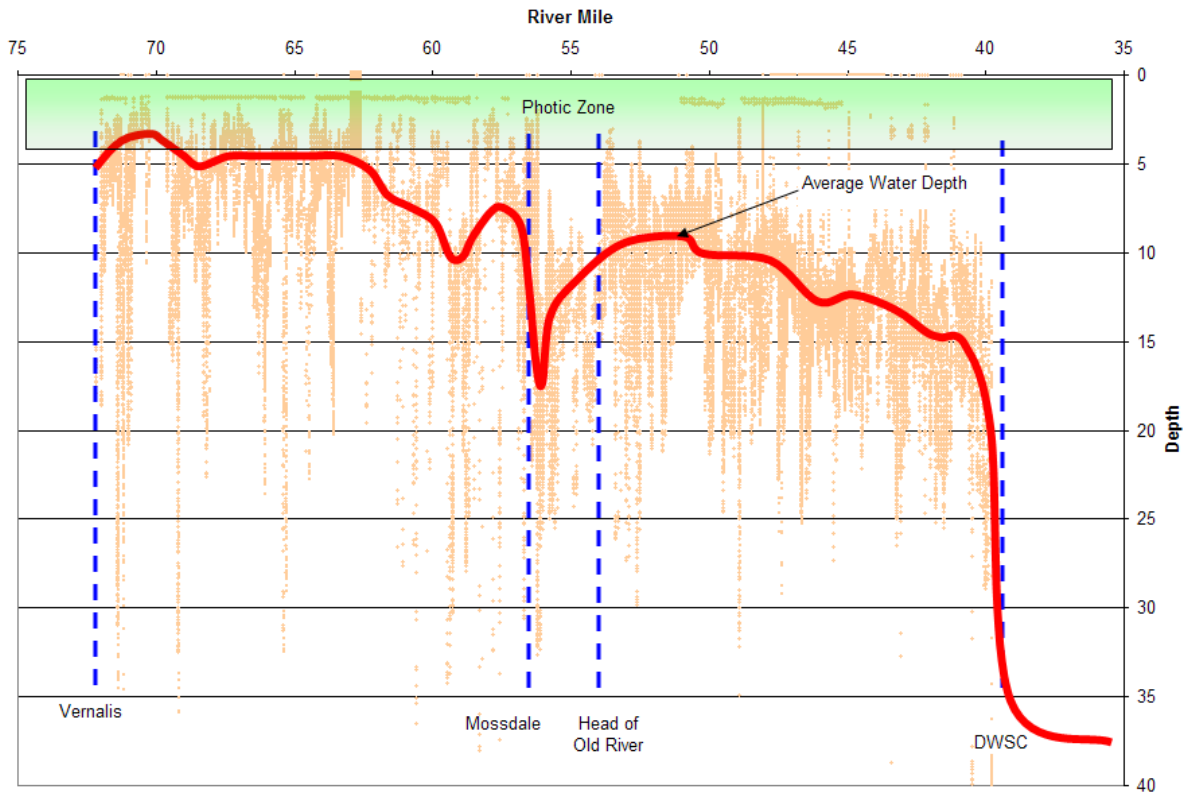


Figure 45: Attenuation fraction of the algal growth rate constant at water depths from 0 to 40 ft in the San Joaquin River. The example was generated with a Secchi-disk depth of 2 ft and optimal light intensity of 1300  $\mu\text{mol/L}$  and 2200  $\mu\text{mol/L}$  at the air-water interface.

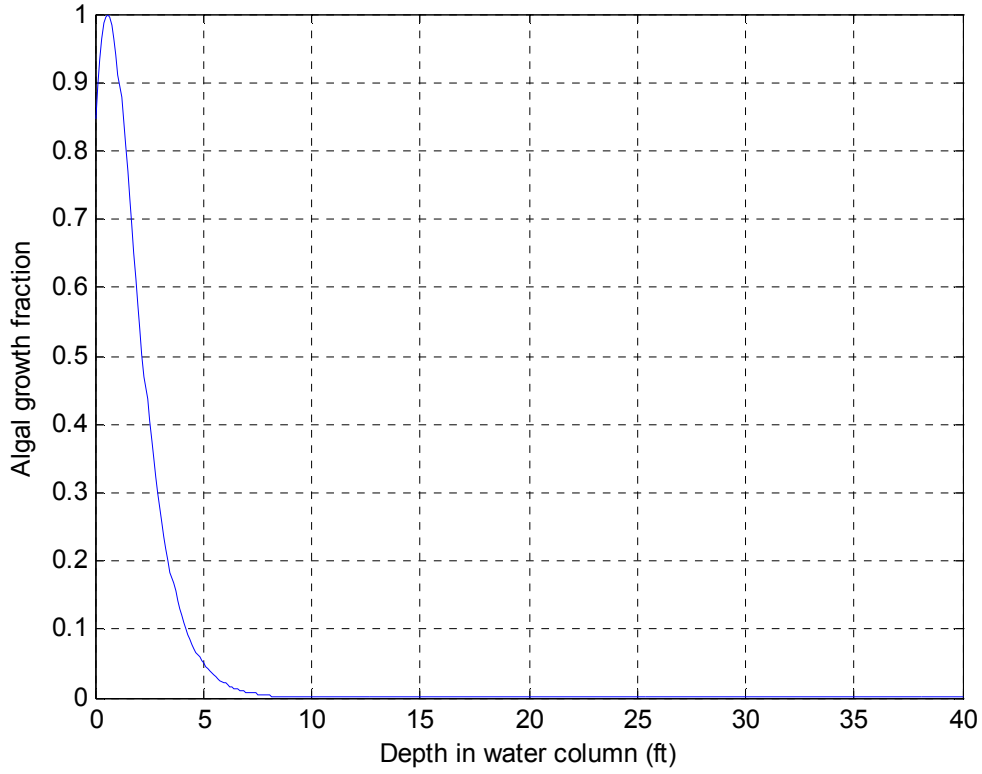


Figure 46: Response of the growth rate attenuation factor to the total water depth for the San Joaquin River. The example was generated with a Secchi-disk depth of 2 ft and optimal light intensity of 1300  $\mu\text{mol/L}$  and 2200  $\mu\text{mol/L}$  at the air-water interface.

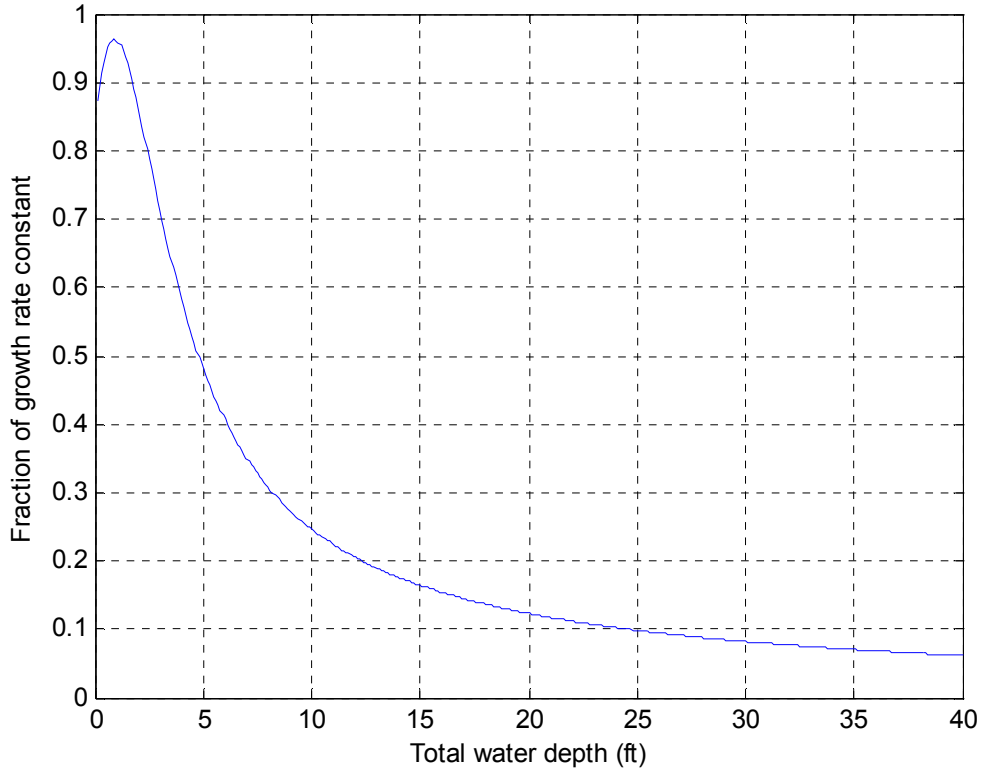


Figure 47: Half-sinusoid approximation of the normalized light intensity using a Fourier series ( $n=20$ ). The fraction of daylight during the 24-day was 0.6. Time was set to 0 at sunrise.

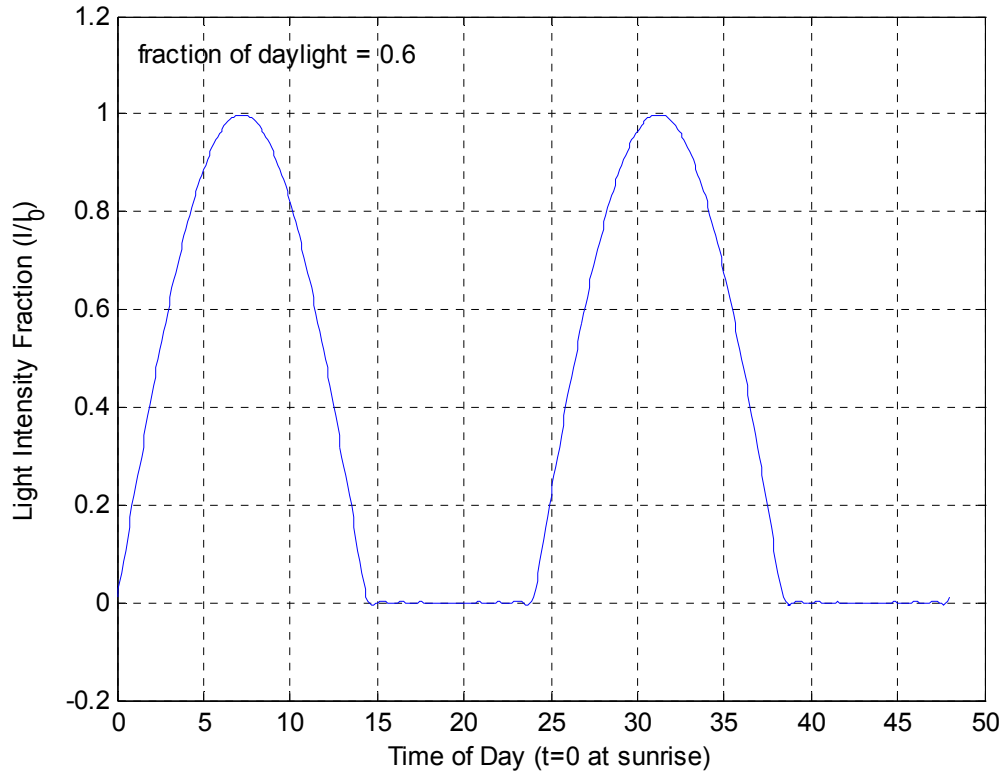


Figure 48: Simulated influence of river depth on chlorophyll *a* from Vernalis to the DWSC for flow conditions of September, 2005. Dye was released at 9:45 AM and tracked for the next 50 hours to the DWSC. The river depth was fixed at 5 feet and 20 feet for two of these simulations, the third line was calculated with the actual measured San Joaquin river depth in this reach. Parameters used in the simulations are presented in Table 3. Night is delineated with the shaded regions.

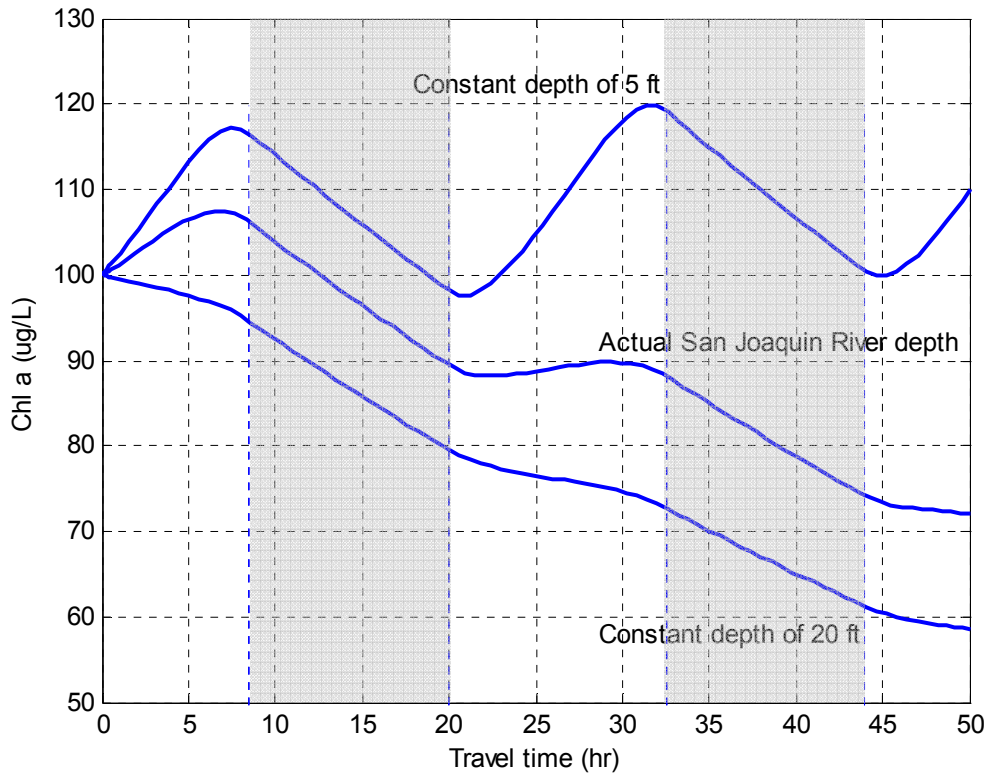


Figure 49: Simulations of chlorophyll a concentrations affected by light attenuation and zooplankton grazing for water traveling from Vernalis to the DWSC. Parameters used in the simulations are presented in Table 3. Night is delineated with the shaded regions.

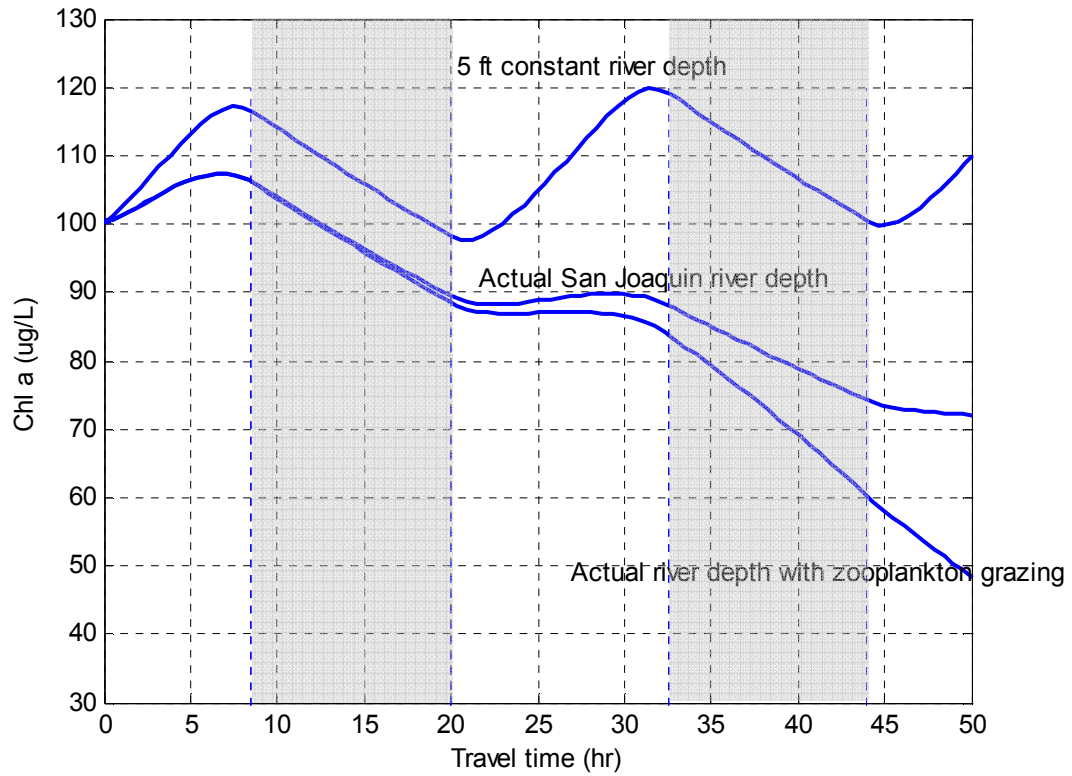


Figure 50: Simulations of the carbon concentrations associated with viable algae, decaying algae, and zooplankton for water flowing from Vernalis to the DWSC in 50 hours. Parameters used in the simulations are presented in Table 3. Night is delineated with the shaded regions.

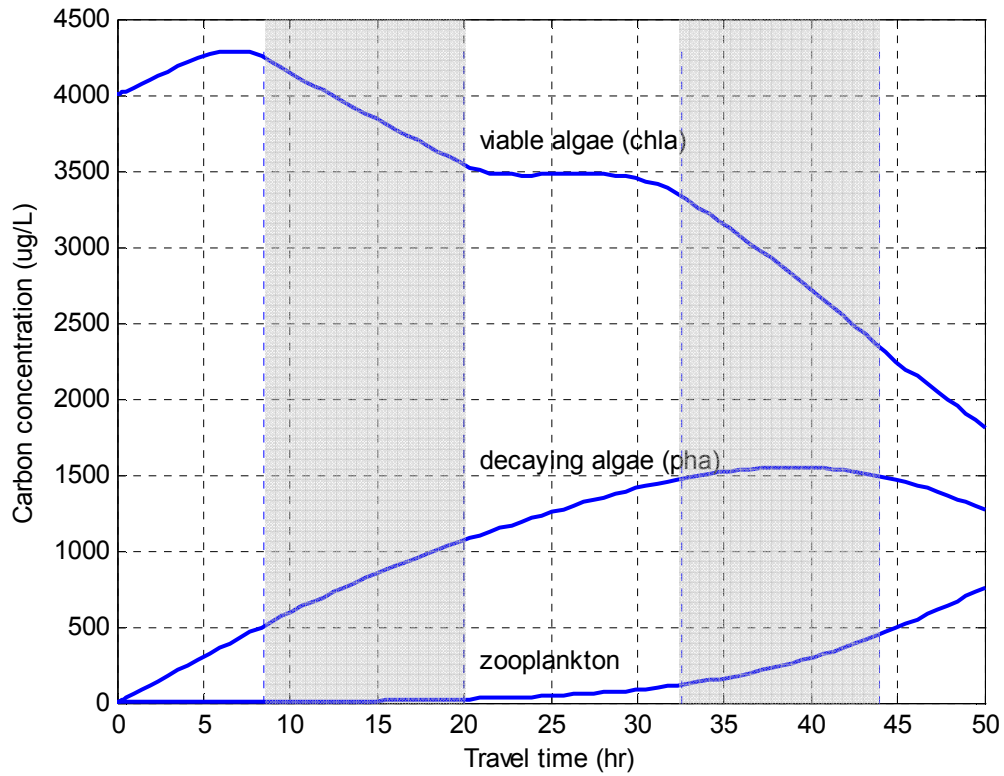


Figure 51: Comparison of observed and simulated chlorophyll a, pheophytin a, and zooplankton concentrations for the August, 2005 lagrangian monitoring.

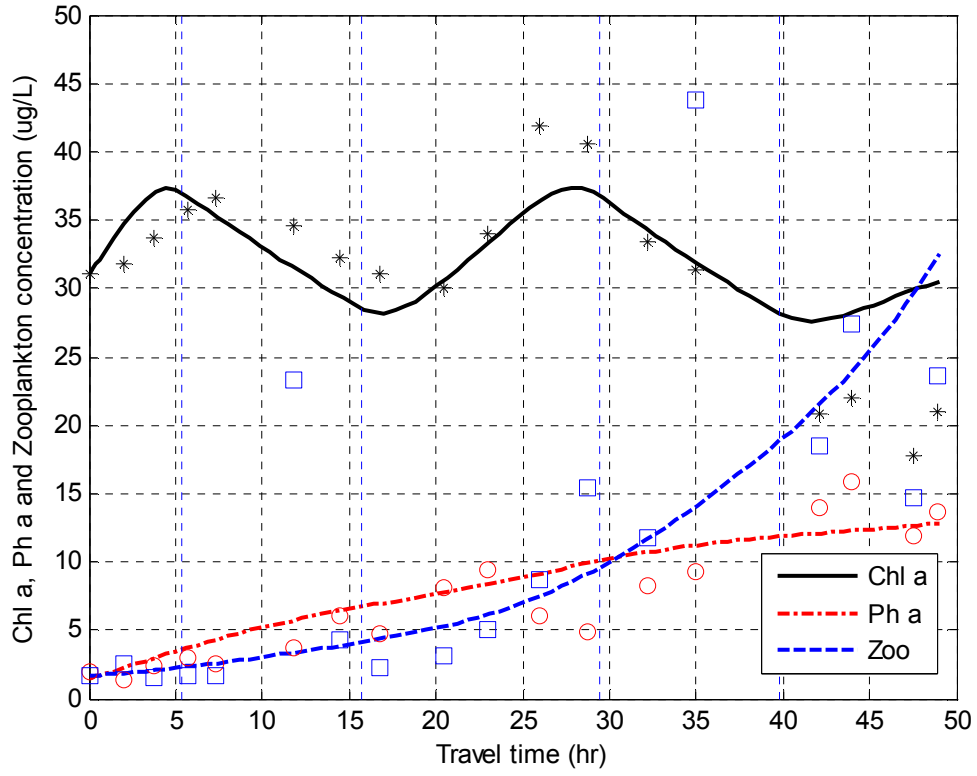


Figure 52: Comparison of observed and simulated chlorophyll a, pheophytin a, and zooplankton concentrations for the June, 2007 lagrangian monitoring.

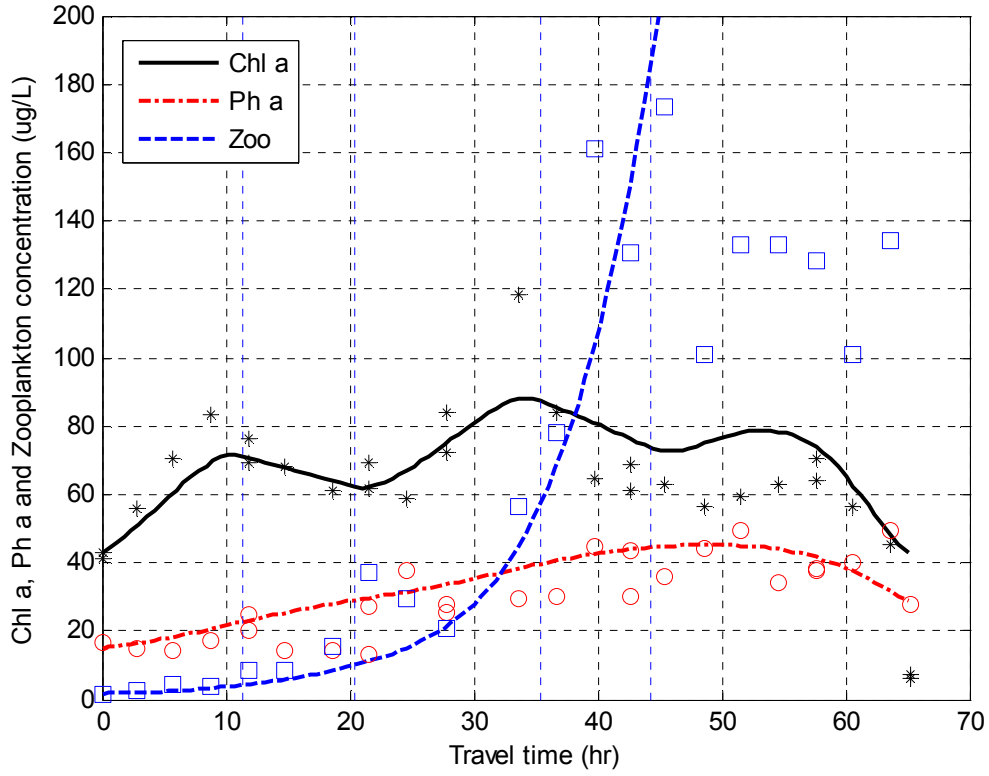


Figure Set A-1: Plots of BOD, CBOD, and NBOD vs. Time for the July 2005 Trial

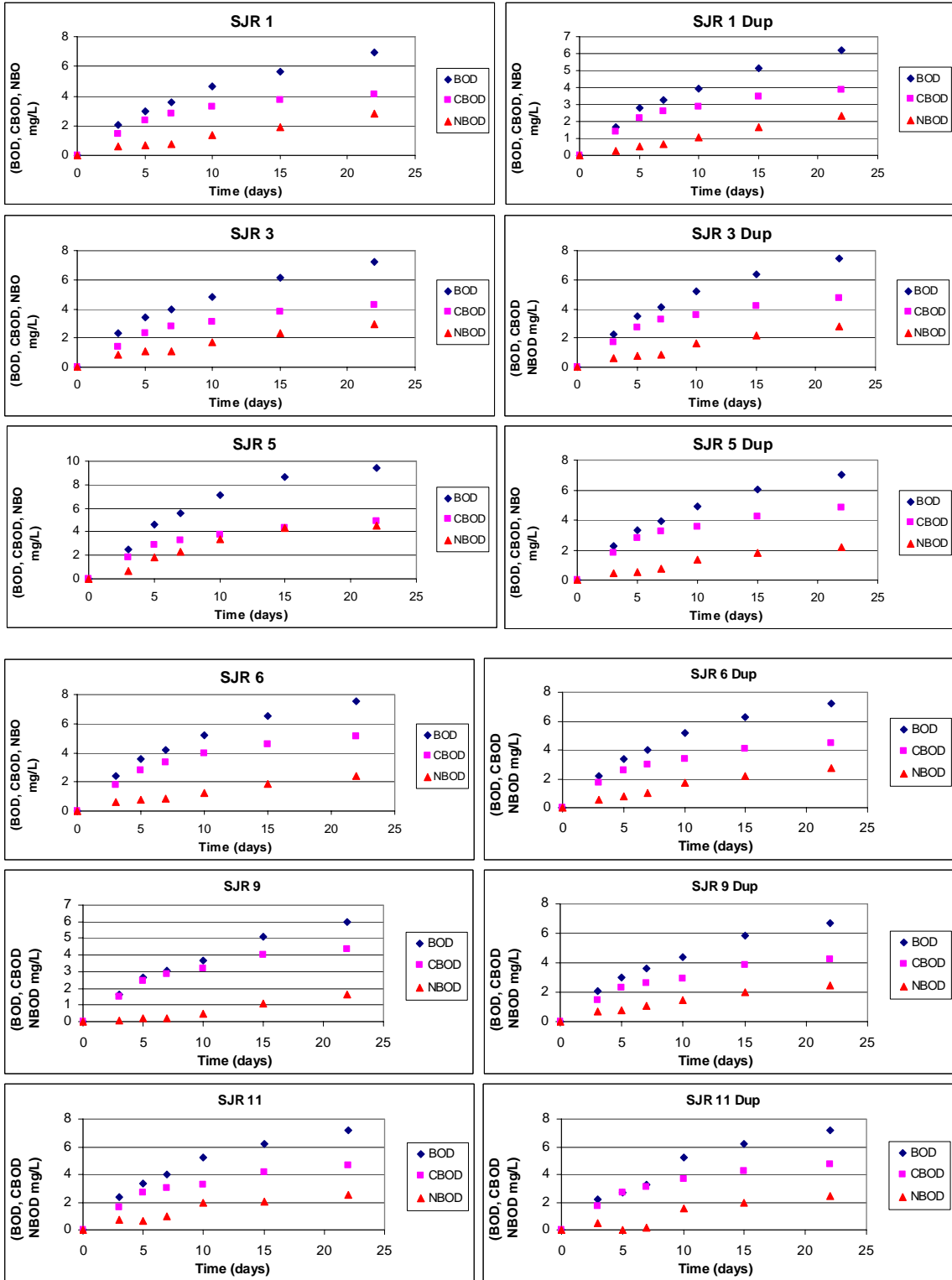


Figure Set A-2: Plots of BOD, CBOD, and NBOD vs. Time for the August 2005 Trial

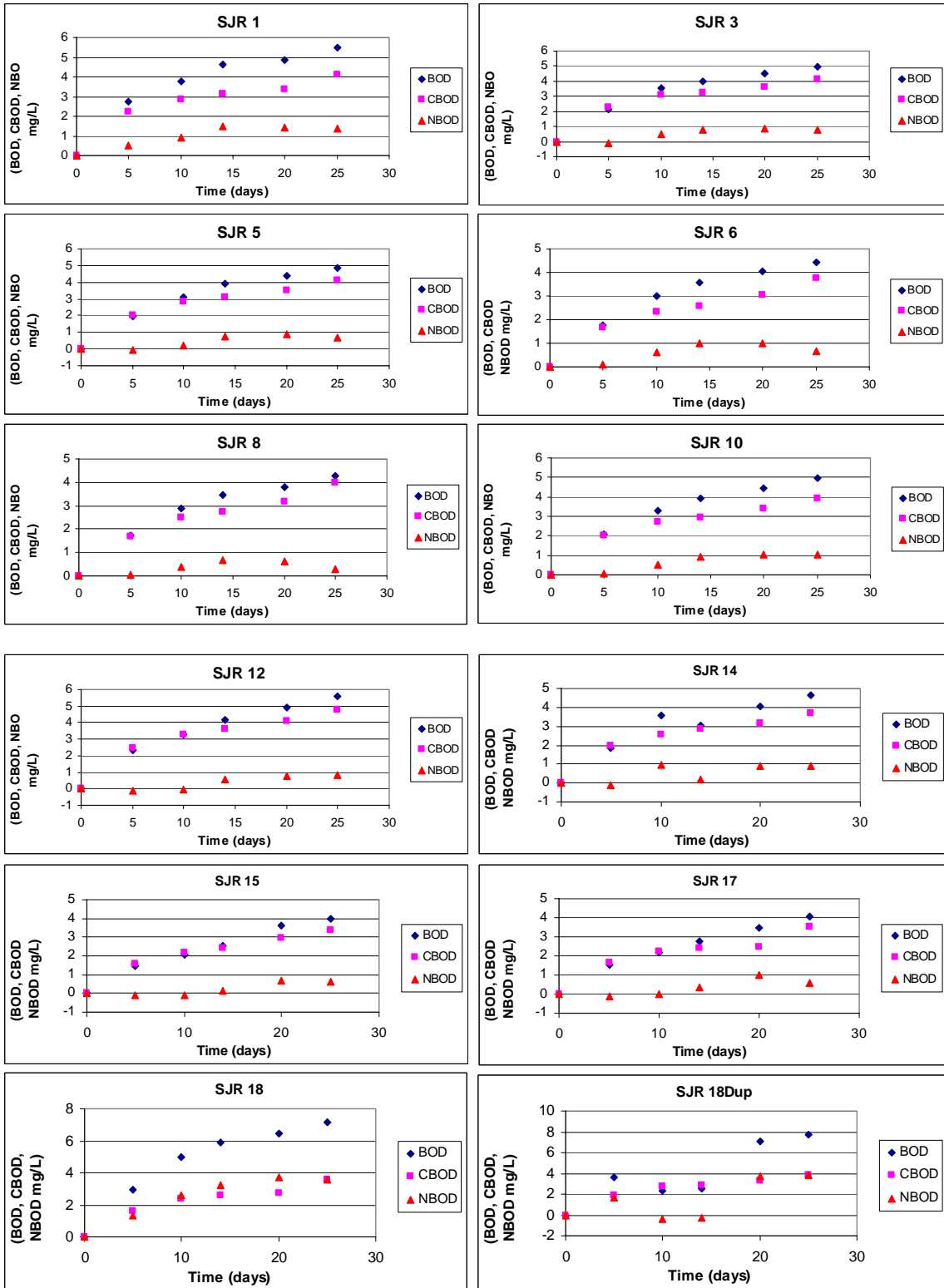


Figure Set A-3: Plots of BOD, CBOD, and NBOD vs. Time for the September 2005 Trial

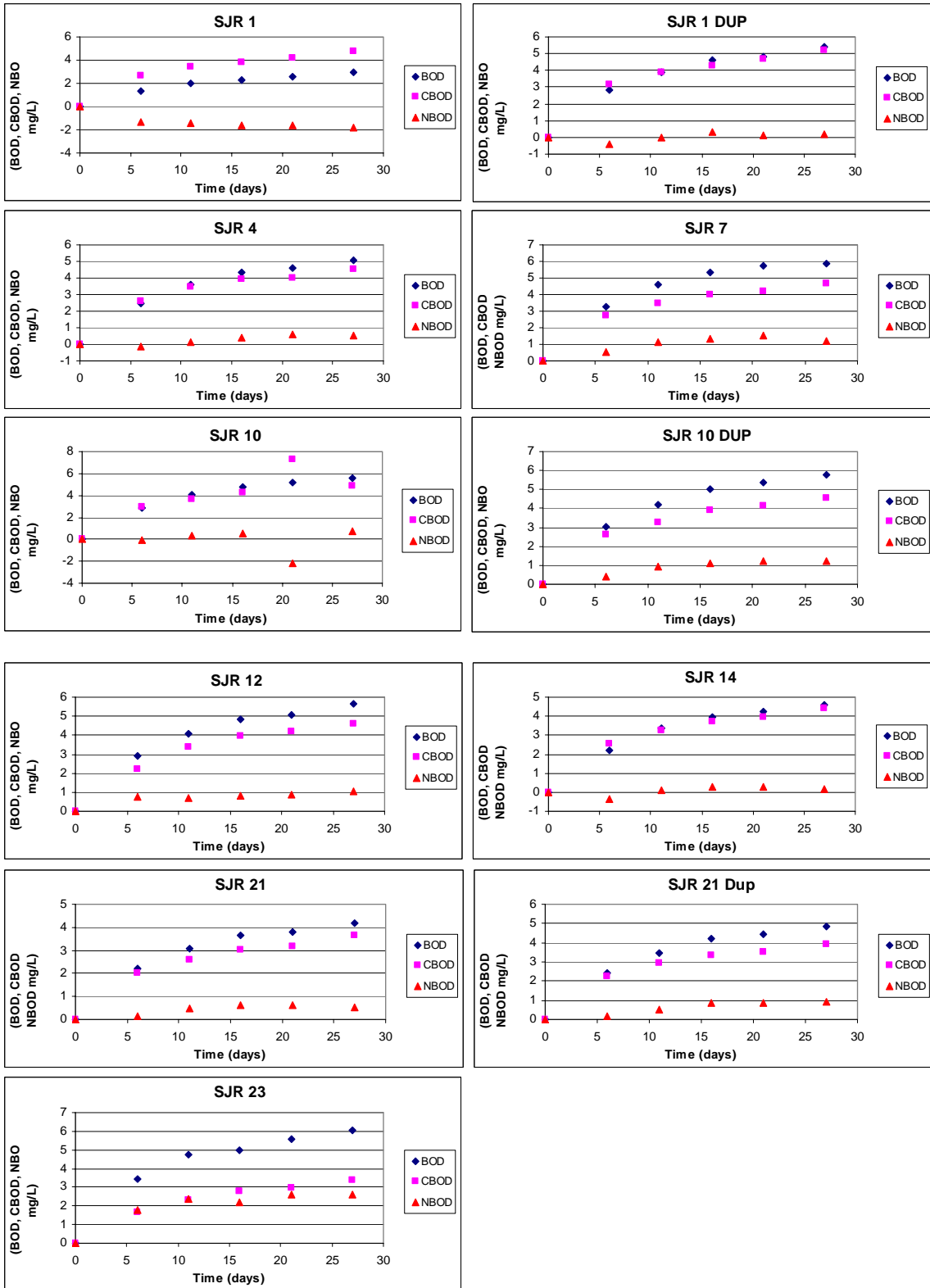


Figure Set A-4: Plots of BOD, CBOD, and NBOD vs. Time for the October 2005 Trial

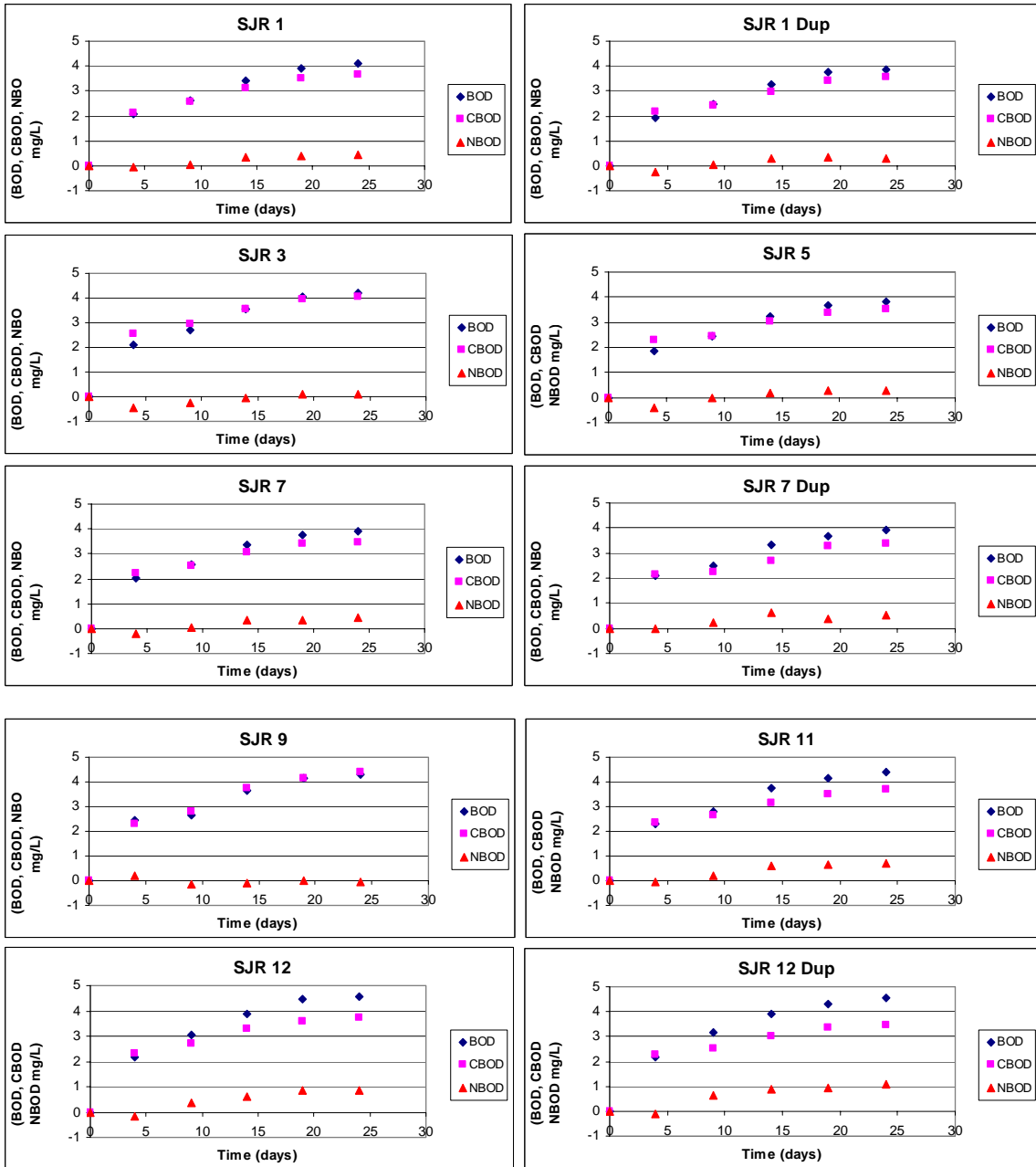


Figure Set A-5: Plots of BOD, CBOD, and NBOD vs. Time for the July 2006 Trial

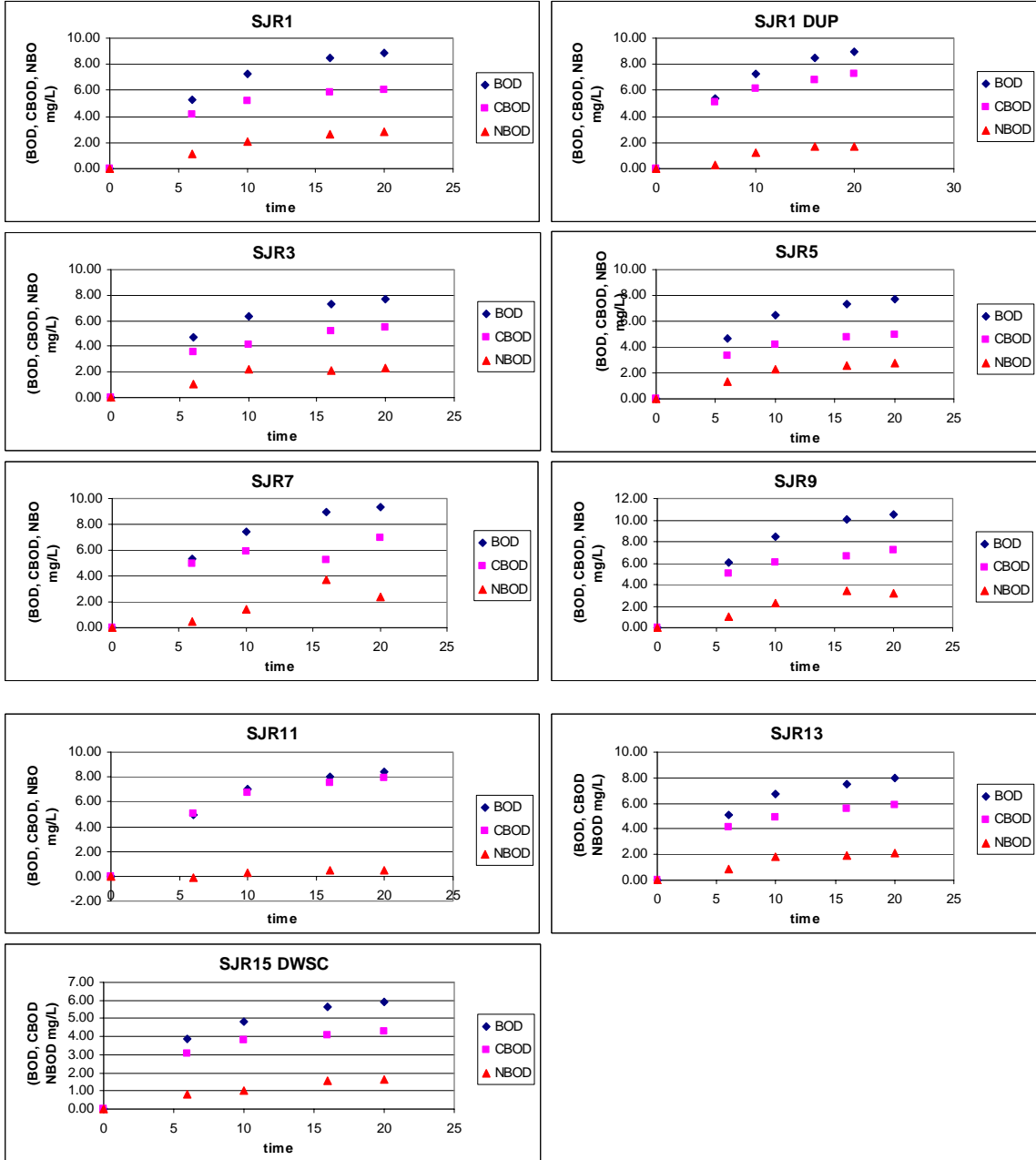


Figure Set A-6: Plots of BOD, CBOD, and NBOD vs. Time for the August 2006 Trial

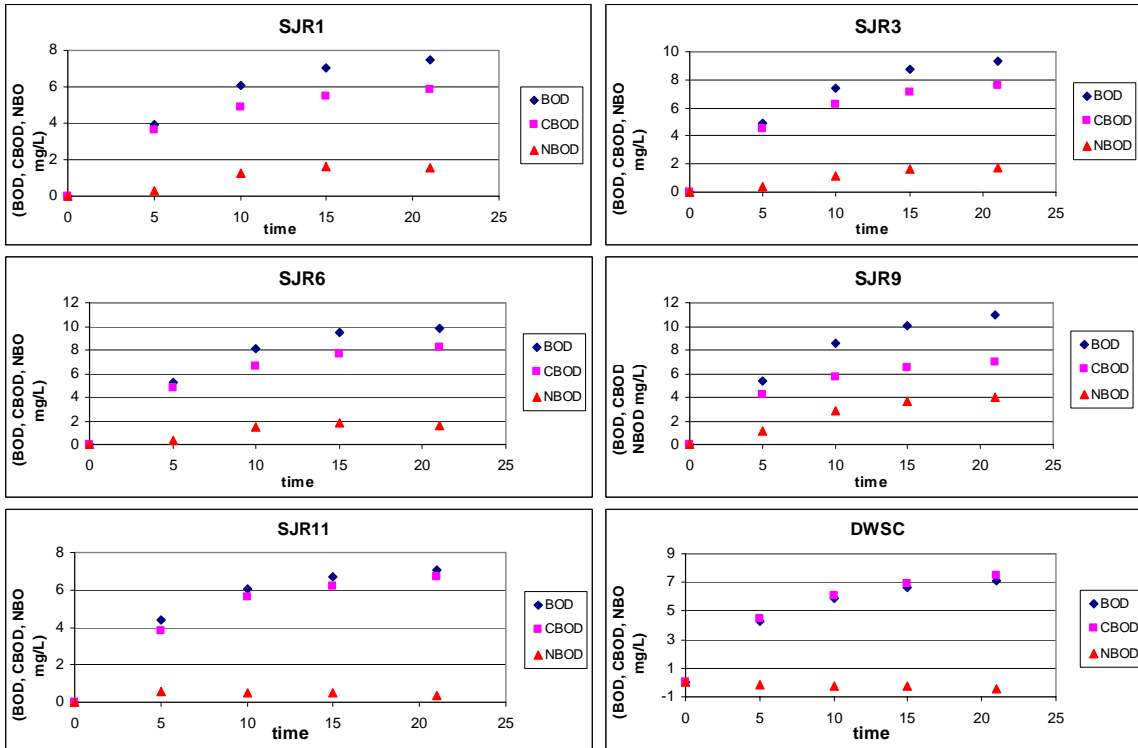


Figure Set A-7: Plots of BOD vs. River Mile for June 2007 Trial

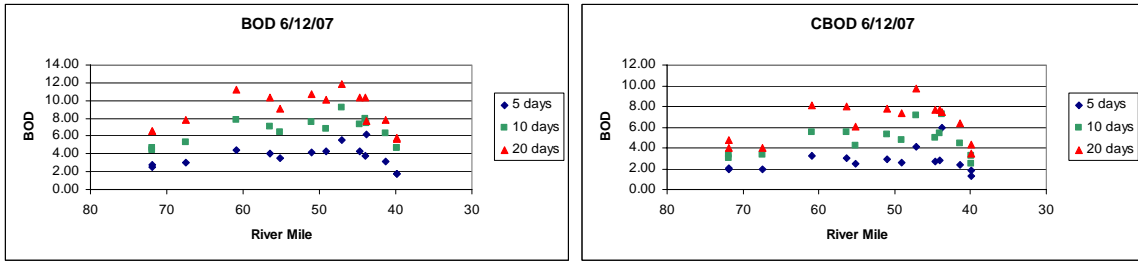


Figure Set A-8: Plots of BOD vs. River Mile for July 2007 Trial

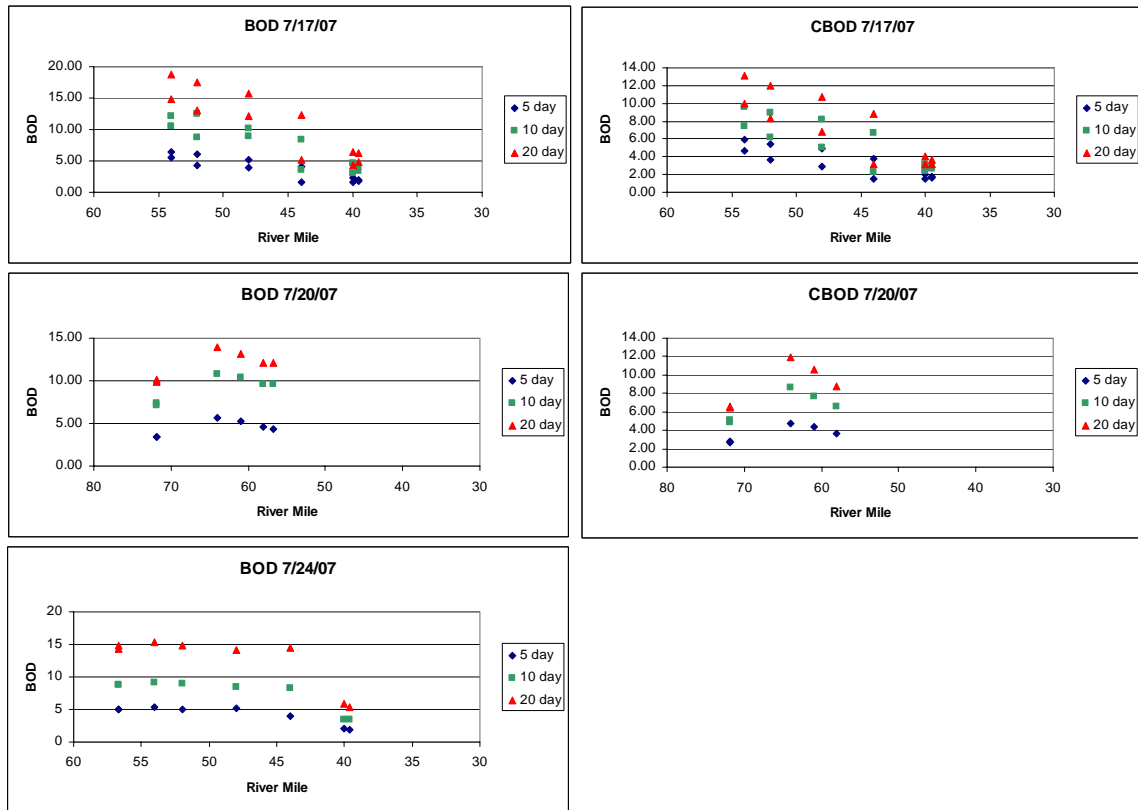


Figure Set A-9: Plots of BOD vs. River Mile for August 2007 Trial

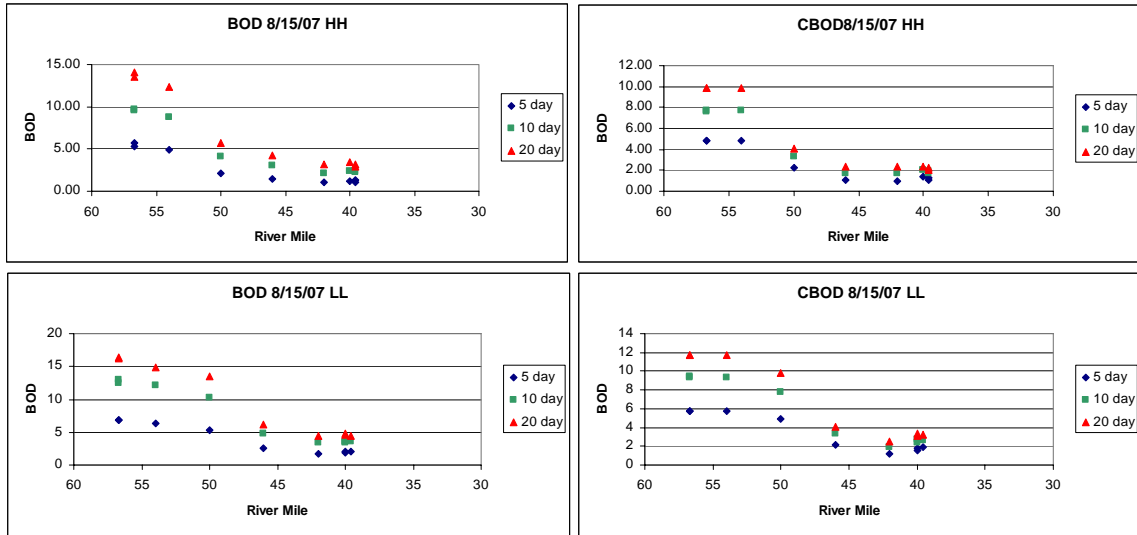


Figure Set A-10: Plots of BOD vs. River Mile for August 2007 Trial

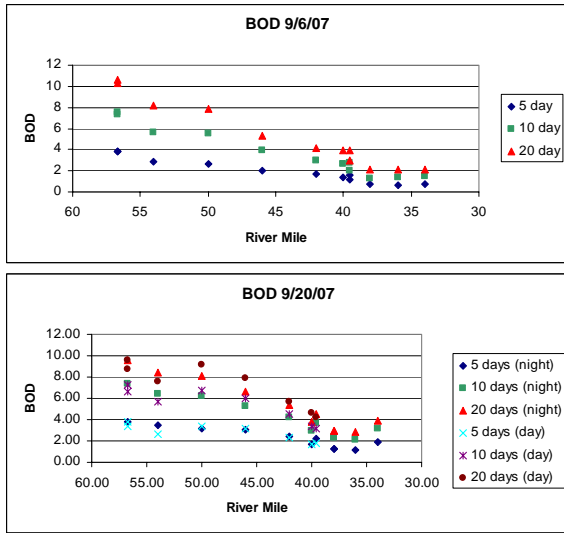


Table A-1: Summary of BOD for July 2005 Trial

Station	BOD						CBOD						NBOD						
	5 day	10 day	20 day	L <sub>0</sub>	k	R <sup>2</sup>	5 day	10 day	20 day	L <sub>0</sub>	k	R <sup>2</sup>	5 day	10 day	20 day	L <sub>0</sub> <sup>2</sup>	L <sub>0</sub> <sup>1</sup>	k	R <sup>2</sup>
SJR 1	3.0	4.7	6.5	6.9	0.11	0.980	2.3	3.3	4.0	4.4	0.14	0.987	0.7	1.4	2.6	2.5	3.6	0.05	0.195
SJR 1 dup	2.8	3.9	5.9	6.5	0.10	0.955	2.2	2.9	3.8	3.9	0.15	0.974	0.6	1.1	2.1	2.5	-7.0	-0.01	0.200
SJR 3	3.4	3.9	4.8	7.2	0.12	0.967	2.3	2.8	3.1	4.4	0.14	0.973	1.1	1.1	1.7	2.7	2.8	0.10	0.621
SJR 3 dup	3.5	4.1	5.2	7.8	0.12	0.987	2.7	3.3	3.5	4.8	0.15	0.980	0.8	0.9	1.6	3.0	5.2	0.03	0.211
SJR 5	4.7	7.1	9.2	12.7	0.08	0.868	2.8	3.8	4.7	4.9	0.16	0.991	1.8	3.4	4.5	7.8	-12.7	-0.02	0.062
SJR 5 dup	3.3	4.9	6.7	7.2	0.12	0.983	2.8	3.6	4.6	4.8	0.16	0.987	0.6	1.4	2.1	2.4	6.9	0.02	0.064
SJR 6	3.6	5.2	7.2	7.7	0.12	0.976	2.8	4.0	5.0	5.4	0.14	0.991	0.8	1.3	2.3	2.3	2.5	0.08	0.508
SJR 6 dup	3.4	4.0	5.1	7.9	0.11	0.989	2.6	3.0	3.4	4.6	0.15	0.986	0.8	1.0	1.8	3.3	10.5	0.02	0.178
SJR 9	2.6	3.6	5.7	6.5	0.09	0.903	2.4	3.2	4.3	4.6	0.14	0.968	0.2	0.5	1.5	1.9	-0.2	-0.12	0.792
SJR 9 dup	3.0	4.4	6.4	7.0	0.11	0.948	2.3	2.9	4.1	4.4	0.13	0.948	0.8	1.4	2.3	2.6	2.9	0.07	0.643
SJR 11	3.3	5.2	6.9	7.5	0.12	0.980	2.7	3.3	4.5	4.7	0.15	0.945	0.7	1.9	2.4	2.8	3.6	0.18	0.180
SJR 11 dup	2.7	5.2	6.9	8.8	0.08	0.694	2.7	3.6	4.6	4.9	0.14	0.986	0.0	1.6	2.3	3.8			

L<sub>0</sub><sup>1</sup>: Determined from differences of individual BOD and CBOD data

L<sub>0</sub><sup>2</sup>: Difference of BOD and CBOD Lo values

Table A-2: Summary of BOD for August 2005 Trial

Station	BOD						CBOD						NBOD						
	5 day	10 day	20 day	L <sub>0</sub>	k	R <sup>2</sup>	5 day	10 day	20 day	L <sub>0</sub>	k	R <sup>2</sup>	5 day	10 day	20 day	L <sub>0</sub> <sup>2</sup>	L <sub>0</sub> <sup>1</sup>	k	R <sup>2</sup>
SJR 1	2.7	3.8	4.9	5.9	0.11	0.979	2.2	2.9	3.4	4.2	4.18	0.936	0.50	0.94	1.45	1.7	1.9	0.07	0.750
SJR 3	2.2	3.6	4.5	5.5	0.10	0.993	2.3	3.1	3.7	4.3	4.34	0.954	-0.12	0.47	0.85	1.1	0.1	-0.69	0.540
SJR 5	2.0	3.1	4.4	5.6	0.09	0.995	2.1	2.9	3.5	4.3	0.11	0.951	-0.08	0.24	0.87	1.3	0.1	-0.68	0.469
SJR 6	1.8	3.0	4.0	5.1	0.09	0.997	1.7	2.4	3.0	3.9	0.10	0.905	0.09	0.63	1.00	1.2	-1.4	-0.02	0.025
SJR 8	1.8	2.9	3.8	4.8	0.09	0.991	1.7	2.5	3.2	4.2	0.09	0.915	0.05	0.38	0.61	0.7	-12.6	0.00	0.000
SJR 10	2.1	3.3	4.4	5.6	0.09	0.993	2.0	2.7	3.4	4.1	0.12	0.950	0.03	0.53	1.04	1.5	-0.1	-0.13	0.394
SJR 12	2.3	3.3	4.9	6.3	0.08	0.951	2.5	3.3	4.1	4.9	0.12	0.950	-0.14	-0.06	0.77	1.3	0.0	-0.41	0.629
SJR 14	1.9	3.6	4.1	5.0	0.09	0.863	2.0	2.6	3.2	3.8	0.12	0.947	-0.12	0.98	0.89	1.2	0.1	-0.75	0.463
SJR 15	1.5	2.1	3.6	5.0	0.06	0.825	1.6	2.2	2.9	3.6	0.10	0.930	-0.09	-0.07	0.68	1.4	0.0	-0.43	0.573
SJR 17	1.5	2.2	3.5	4.9	0.07	0.922	1.6	2.2	2.5	3.4	0.11	0.850	-0.12	-0.02	1.02	1.5	0.0	-0.39	0.542
SJR 18	2.9	5.0	6.5	8.1	0.09	0.994	1.6	2.4	2.8	3.6	0.11	0.918	1.32	2.61	3.74	4.5	4.7	0.08	0.909
SJR 18 Dup	3.6	2.4	7.1	10.0	-0.35	0.133	1.9	2.7	3.3	4.1	0.11	0.951	1.70	-0.36	3.76	5.9	0.3	-0.35	0.133

L<sub>0</sub><sup>1</sup>: Determined from differences of individual BOD and CBOD data

L<sub>0</sub><sup>2</sup>: Difference of BOD and CBOD Lo values

Table A-3: Summary of BOD for September 2005 Trial

Station	BOD						CBOD						NBOD						
	5 day	10 day	20 day	L <sub>0</sub>	k	R <sup>2</sup>	5 day	10 day	20 day	L <sub>0</sub>	k	R <sup>2</sup>	5 day	10 day	20 day	L <sub>0</sub> <sup>2</sup>	L <sub>0</sub> <sup>1</sup>	k	R <sup>2</sup>
SJR 1	4.4	3.2	2.5	3.3	0.08	0.971	8.9	4.9	4.1	5.0	0.11	0.969	-4.4	-1.7	-1.6	-1.8	-1.9	0.16	0.969
SJR 1 Dup	9.3	5.9	4.8	5.8	0.10	0.988	10.6	5.1	4.6	5.5	0.12	0.965	-1.3	0.8	0.2	0.3	20.4	7.67	0.240
SJR 4	8.2	5.7	4.6	5.6	0.09	0.996	8.6	5.0	4.0	4.9	0.12	0.983	-0.4	0.7	0.5	0.8	0.2	-0.79	0.425
SJR 7	10.8	7.0	5.6	6.6	0.11	1.000	9.1	4.9	4.2	5.0	0.12	0.978	1.7	2.2	1.5	1.6	1.6	0.08	0.709
SJR 10	9.6	6.2	5.1	6.1	0.10	0.995	9.7	5.1	6.7	6.2	0.10	0.715	-0.1	1.1	-1.6	-0.1	0.0	-0.40	0.256
SJR 10 Dup	10.1	6.3	5.3	6.4	0.10	0.995	8.7	4.5	4.1	4.9	0.11	0.978	1.4	1.8	1.2	1.5	1.8	0.05	0.698
SJR 12	9.8	6.2	5.0	6.1	0.10	0.991	7.3	5.5	4.2	5.2	0.09	0.996	2.4	0.7	0.9	1.0	1.0	0.14	0.910
SJR 14	7.3	5.5	4.2	5.2	0.09	0.996	8.6	4.5	3.9	4.7	0.12	0.974	-1.2	1.0	0.3	0.5	0.2	-1.12	0.549
SJR 21	7.3	4.7	3.8	4.6	0.10	0.992	6.8	3.6	3.1	3.9	0.11	0.965	0.5	1.1	0.6	0.7	1.0	0.04	0.211
SJR 21 Dup	8.0	5.4	4.4	5.4	0.10	0.994	7.5	4.2	3.5	4.2	0.12	0.979	0.5	1.2	0.9	1.2	-1.6	-0.02	0.088
SJR 23	11.5	7.0	5.5	6.5	0.12	0.978	5.5	3.5	2.9	3.7	0.09	0.978	6.0	3.5	2.5	2.8	2.9	0.15	0.966

L<sub>0</sub><sup>1</sup>: Determined from differences of individual BOD and CBOD data

L<sub>0</sub><sup>2</sup>: Difference of BOD and CBOD Lo values

Table A-4: Summary of BOD for October 2005 Trial

Station	BOD						CBOD						NBOD						
	5 day	10 day	20 day	L <sub>0</sub>	k	R <sup>2</sup>	5 day	10 day	20 day	L <sub>0</sub>	k	R <sup>2</sup>	5 day	10 day	20 day	L <sub>0</sub> <sup>2</sup>	L <sub>0</sub> <sup>1</sup>	k	R <sup>2</sup>
SJR 1	3.8	4.4	3.9	4.4	0.13	0.941	3.5	3.7	3.5	3.9	0.15	0.948	0.3	0.7	0.4	0.5	0.5	-1.36	0.323
SJR 1 Dup	3.6	4.2	3.8	4.2	0.12	0.941	3.0	3.6	3.5	3.8	0.16	0.926	0.6	0.6	0.3	0.4	26.2	7.52	0.248
SJR 3	4.0	4.5	4.1	4.5	0.13	0.946	3.8	4.3	4.0	4.4	0.17	0.951	0.2	0.2	0.1	0.1	0.0	-0.42	0.467
SJR 5	3.7	4.1	3.7	4.1	0.12	0.945	2.8	3.7	3.4	3.8	0.17	0.926	0.9	0.4	0.3	0.3	0.0	-0.44	0.471
SJR 7	3.7	4.3	3.8	4.2	0.14	0.949	3.1	3.7	3.4	3.8	0.17	0.945	0.6	0.6	0.4	0.4	2.7	-2.68	0.339
SJR 7 Dup	3.3	4.3	3.7	4.2	0.14	0.928	2.5	3.3	3.3	3.6	0.16	0.899	0.8	1.1	0.4	0.6	0.0	-0.60	0.537
SJR 9	3.1	4.8	4.2	4.6	0.14	0.898	4.0	4.9	4.2	4.7	0.13	0.939	-0.9	-0.1	0.0	-0.1	0.0	-1.16	0.763
SJR 11	4.0	4.9	4.2	4.7	0.13	0.939	3.2	3.8	3.5	4.0	0.17	0.940	0.7	1.1	0.7	0.7	0.2	-0.82	0.456
SJR 12	5.1	4.9	4.5	5.0	0.12	0.974	3.5	4.0	3.6	4.1	0.17	0.953	1.5	0.9	0.8	1.0	0.3	-0.94	0.515
SJR 12 Dup	5.3	4.8	4.4	4.9	0.13	0.981	3.1	3.6	3.4	3.8	0.17	0.944	2.2	1.2	1.0	1.1	0.1	-0.71	0.556

L<sub>0</sub><sup>1</sup>: Determined from differences of individual BOD and CBOD data

L<sub>0</sub><sup>2</sup>: Difference of BOD and CBOD Lo values

Table A-5: Summary of BOD for July 2006 Trial

Station	BOD						CBOD						NBOD						
	5 day	10 day	20 day	L <sub>0</sub>	k	R <sup>2</sup>	5 day	10 day	20 day	L <sub>0</sub>	k	R <sup>2</sup>	5 day	10 day	20 day	L <sub>0</sub> <sup>2</sup>	L <sub>0</sub> <sup>1</sup>	k	R <sup>2</sup>
SJR 1	4.4	7.3	8.9	10.1	0.13	0.999	3.5	5.2	6.1	6.7	0.16	0.998	0.9	2.1	2.8	3.4	4.5	0.05	0.746
SJR 1 Dup	4.5	7.3	8.9	10.1	0.13	0.999	4.3	6.1	7.2	7.9	0.16	0.991	0.2	1.2	1.7	2.2	-0.8	-0.07	0.292
SJR 3	3.9	6.4	7.7	8.7	0.13	0.999	3.0	4.1	5.5	6.0	0.14	0.974	0.9	2.2	2.3	2.7	2.7	0.11	0.758
SJR 5	3.9	6.5	7.7	8.7	0.13	0.997	2.8	4.2	5.0	5.5	0.15	0.997	1.1	2.3	2.8	3.2	3.5	0.09	0.885
SJR 7	4.5	7.4	9.3	10.7	0.12	0.999	4.1	5.9	6.9	7.0	0.19	0.903	0.4	1.5	2.4	3.7	-1.0	-0.07	0.323
SJR 9	5.1	8.4	10.5	12.1	0.12	0.999	4.2	6.1	7.3	7.9	0.16	0.987	0.9	2.3	3.2	4.2	15.6	0.01	0.055
SJR 11	4.1	7.0	8.5	9.6	0.13	0.996	4.2	6.7	8.0	8.8	0.14	0.997	-0.1	0.3	0.5	0.8	0.0	-0.60	0.578
SJR 13	4.2	6.7	8.0	8.8	0.14	0.997	3.5	4.9	5.9	6.4	0.16	0.990	0.8	1.8	2.1	2.4	2.8	0.08	0.717
DWSC	3.2	4.8	5.9	6.5	0.14	0.996	2.6	3.8	4.3	4.7	0.17	0.996	0.7	1.0	1.6	1.8	2.2	0.07	0.925

L<sub>0</sub><sup>1</sup>: Determined from differences of individual BOD and CBOD data

L<sub>0</sub><sup>2</sup>: Difference of BOD and CBOD Lo values

Table A-6: Summary of BOD for August 2006 Trial

Station	BOD						CBOD						NBOD						
	5 day	10 day	20 day	L <sub>0</sub>	k	R <sup>2</sup>	5 day	10 day	20 day	L <sub>0</sub>	k	R <sup>2</sup>	5 day	10 day	20 day	L <sub>0</sub> <sup>2</sup>	L <sub>0</sub> <sup>1</sup>	k	R <sup>2</sup>
SJR 1	3.9	6.1	7.4	8.5	0.13	0.999	3.6	4.9	5.8	6.5	0.16	0.993	0.29	1.23	1.58	2.0	-3.3	-0.02	0.056
SJR 3	4.9	7.5	9.2	10.5	0.13	1.000	4.5	6.3	7.5	8.4	0.15	0.996	0.40	1.16	1.72	2.1	2	0.07	0.925
SJR 6	5.2	8.2	9.8	11.2	0.13	0.998	4.8	6.7	8.1	9.1	0.14	0.994	0.40	1.48	1.65	2.1	7.3	0.02	0.025
SJR 9	5.4	8.6	10.8	12.6	0.11	0.999	4.2	5.8	6.9	7.7	0.15	0.993	1.18	2.85	3.94	4.9	8.4	0.03	0.450
SJR 11	4.4	6.1	7.0	7.8	0.16	0.996	3.8	5.6	6.6	7.4	0.14	0.996	0.58	0.48	0.37	0.4	0.6	0.46	0.986
DWSC	4.3	5.8	7.0	7.9	0.15	0.993	4.4	6.1	7.4	8.3	0.15	0.992	-0.17	-0.28	-0.38	-0.4	-0.4	0.10	0.806

L<sub>0</sub><sup>1</sup>: Determined from differences of individual BOD and CBOD data

L<sub>0</sub><sup>2</sup>: Difference of BOD and CBOD Lo values

Table A-7: Summary of BOD for June 12, 2007 Trial

Station	River Mile	BOD						CBOD					
		5	10	20	L <sub>0</sub>	k	R <sup>2</sup>	5	10	20	L <sub>0</sub>	k	R <sup>2</sup>
SJR 1	71.90	2.77	4.62	6.59	7.49	0.11	0.97	1.99	3.32	4.00	4.46	0.15	1.00
SJR 1 dup	71.90	2.51	4.37	6.52	7.76	0.09	0.97	2.01	3.07	4.74	5.30	0.11	0.91
SJR 2	67.50	3.03	5.29	7.88	9.37	0.09	0.97	1.99	3.32	4.00	4.46	0.15	1.00
SJR 4	60.88	4.48	7.80	11.20	13.11	0.10	0.98	3.26	5.53	8.13	9.37	0.10	0.97
SJR 6	56.40	4.08	7.06	10.28	11.96	0.10	0.97	3.08	5.47	8.00	9.58	0.09	0.98
SJR 8	55.10	3.52	6.39	9.08	11.08	0.09	0.98	2.47	4.18	6.06	6.83	0.11	0.96
SJR 10	51.00	4.21	7.58	10.68	12.65	0.10	0.99	2.89	5.25	7.73	9.30	0.09	0.98
SJR 12	47.10	5.54	9.22	11.85	13.32	0.13	0.99	4.13	7.18	9.78	10.99	0.11	0.99
SJR 14	44.67	4.26	7.36	10.33	12.00	0.11	0.98	2.73	5.02	7.70	9.77	0.08	0.97
SJR 16	49.10	4.33	6.83	10.04	11.30	0.11	0.94	2.57	4.74	7.32	9.26	0.08	0.97
SJR 18	44.00	3.75	7.92	10.39	13.09	0.09	0.98	2.84	5.38	7.69	9.38	0.09	1.00
SJR 20	43.80	6.16	7.50	7.74	9.21	0.27	0.98	5.91	7.19	7.42	8.83	0.27	0.98
SJR 22	41.36	3.20	6.32	7.80	9.09	0.11	0.99	2.41	4.45	6.35	7.62	0.09	0.99
SJR 23	39.86	1.74	4.66	5.73	8.30	0.07	0.75	1.33	2.51	3.41	3.99	0.10	1.00
SJR 23 dup	39.86	1.76	4.68	5.75	8.19	0.07	0.76	1.89	3.29	4.35	4.87	0.12	0.99

Table A-8: Summary of BOD for July 17, 2007 Trial

Station	River Mile	BOD						CBOD					
		5	10	20	L <sub>0</sub>	k	R <sup>2</sup>	5	10	20	L <sub>0</sub>	k	R <sup>2</sup>
Lt 48	39.50	1.73	3.44	4.87	6.18	0.08	1.00	1.63	2.68	3.18	3.53	0.15	0.99
SJR RM 40	40.00	1.69	3.04	4.22	4.96	0.10	0.99	1.57	2.42	3.20	3.58	0.14	0.97
SJR RM 44	44.00	1.68	3.56	5.25	7.35	0.07	0.99	1.51	2.30	3.14	3.47	0.13	0.96
SJR RM 48	48.00	3.95	8.86	12.17	16.70	0.07	0.95	2.90	5.01	6.76	7.72	0.11	0.99
SJR RM 52	52.00	4.33	8.68	12.99	17.79	0.07	0.97	3.60	6.17	8.35	9.49	0.11	0.98
SJR RM 54	54.00	5.52	10.61	14.84	18.40	0.09	0.99	4.68	7.41	9.93	11.04	0.13	0.97
Lt 48	39.50	2.02	4.01	6.28	8.94	0.06	0.98	1.71	2.77	3.60	4.03	0.13	0.99
SJR RM 40	40.00	2.36	4.69	6.41	7.89	0.09	1.00	2.00	3.13	4.03	4.48	0.14	0.98
SJR RM 44	44.00	4.03	8.41	12.40	17.20	0.07	0.99	3.81	6.67	8.86	10.09	0.12	0.99
SJR RM 48	48.00	5.18	10.14	15.64	21.41	0.07	0.98	4.88	8.21	10.71	12.01	0.13	0.99
SJR RM 52	52.00	6.06	12.44	17.42	22.22	0.08	1.00	5.44	8.99	12.03	13.51	0.12	0.98
SJR RM 54	54.00	6.40	12.13	18.75	24.47	0.07	0.97	5.88	9.64	13.14	14.74	0.12	0.97

Table A-9: Summary of BOD for July 20, 2007 Trial

Station	River Mile	BOD						CBOD					
		5	10	20	Lo	k	R <sup>2</sup>	5	10	20	Lo	k	R <sup>2</sup>
SJR 1	71.90	3.43	7.41	10.11	13.05	0.08	0.99	2.83	5.06	6.60	7.57	0.11	0.99
SJR 1 dup	71.90	3.38	7.10	9.89	12.71	0.08	0.99	2.68	4.83	6.44	7.45	0.11	0.99
SJR 3	64.00	5.61	10.83	13.95	16.20	0.11	0.96	4.72	8.70	11.97	14.12	0.10	0.98
SJR 5	61.00	5.22	10.33	13.19	15.38	0.10	0.95	4.39	7.68	10.57	12.22	0.11	0.98
SJR 7	58.00	4.55	9.59	12.15	14.53	0.10	0.95	3.67	6.57	8.75	10.09	0.11	0.99
SJR 8	56.70	4.29	9.65	12.12	14.91	0.09	0.93	n/a	n/a	n/a	n/a	n/a	n/a

Table A-10: Summary of BOD for July 24, 2007 Trial

Station	River Mile	BOD					
		5	10	20	Lo	k	R <sup>2</sup>
Lt 48	39.60	1.96	3.40	5.38	6.67	0.08	0.99
SJR RM 40	40.00	2.03	3.43	5.91	7.88	0.07	0.97
SJR RM 44	44.00	4.00	8.25	14.53	23.87	0.05	0.92
SJR RM 48	48.00	5.14	8.51	14.18	16.35	0.09	0.89
SJR RM 52	52.00	4.98	8.88	14.84	17.66	0.08	0.84
SJR RM 54	54.00	5.32	9.13	15.34	18.38	0.08	0.90
Mossdale	56.70	4.98	8.79	14.24	17.21	0.08	0.95
Mossdale dup	56.70	4.93	8.80	14.89	18.65	0.07	0.91

Table A-11: Summary of BOD for August 15, 2007 Trial

Station	River Mile	BOD						CBOD					
		5	10	20	Lo	k	R <sup>2</sup>	5	10	20	Lo	k	R <sup>2</sup>
Lt 48	39.60	1.02	2.23	2.87	3.61	0.09	0.97	1.12	1.72	2.04	2.31	0.16	0.99
Lt 48 dup	39.60	1.32	2.38	3.22	3.75	0.11	0.99	1.23	1.88	2.26	2.56	0.16	0.98
SJR RM 40	40.00	1.26	2.41	3.40	4.15	0.09	1.00	1.39	2.05	2.41	2.72	0.18	0.98
SJR RM 42	42.00	1.03	2.10	3.14	4.37	0.07	0.99	1.02	1.70	2.33	2.70	0.11	0.97
SJR RM 46	46.00	1.48	3.06	4.24	5.42	0.08	1.00	1.06	1.74	2.33	2.68	0.12	0.97
SJR RM 50	50.00	2.18	4.08	5.73	6.93	0.09	0.99	2.23	3.30	4.07	4.51	0.16	0.98
SJR RM 54	54.00	4.92	8.74	12.30	14.49	0.10	0.99	4.78	7.68	9.82	10.80	0.14	0.99
Mossdale	56.70	5.65	9.62	14.01	16.25	0.10	0.97	4.78	7.68	9.82	10.80	0.14	0.99
Mossdale dup	56.70	5.33	9.70	13.59	16.02	0.10	0.99	4.78	7.64	9.84	10.79	0.14	0.98
Lt 48	39.60	2.01	3.55	4.44	5.02	0.13	1.00	1.93	2.68	3.22	3.59	0.18	0.98
SJR RM 40	40.00	1.90	3.42	4.68	5.50	0.10	0.99	1.50	2.35	3.06	3.44	0.14	0.97
SJR RM 40 dup	40.00	2.04	3.59	4.79	5.50	0.11	0.99	1.78	2.71	3.32	3.72	0.16	0.98
SJR RM 42	42.00	1.72	3.43	4.39	5.23	0.10	1.00	1.14	1.94	2.49	2.85	0.13	0.99
SJR RM 46	46.00	2.60	4.87	6.19	7.14	0.12	1.00	2.10	3.35	4.04	4.49	0.16	0.99
SJR RM 50	50.00	5.34	10.22	13.53	16.15	0.10	1.00	4.85	7.75	9.80	10.74	0.15	0.99
SJR RM 54	54.00	6.36	12.06	14.95	17.33	0.12	1.00	5.69	9.36	11.75	12.94	0.14	0.99
Mossdale	56.70	6.78	12.54	16.27	18.75	0.11	1.00	5.69	9.36	11.75	12.94	0.14	0.99
Mossdale dup	56.70	6.88	12.98	16.49	19.08	0.11	1.00	5.80	9.41	11.74	12.88	0.15	0.99

Table A-12: Summary of BOD for September 6, 2007 Trial

Station	River Mile	BOD					
		5	10	20	Lo	k	R <sup>2</sup>
SJR RM 34	34.00	0.77	1.45	2.15	2.66	0.08	0.99
SJR RM 34 dup	36.00	0.63	1.34	2.10	3.17	0.06	0.99
SJR RM 36	38.00	0.73	1.31	2.09	2.65	0.08	0.96
SJR RM 38	39.50	1.12	2.03	2.95	3.50	0.09	0.99
Lt 48	39.50	1.63	2.80	3.88	4.42	0.11	0.99
SJR RM 40	40.00	1.35	2.65	3.90	4.98	0.08	1.00
SJR RM 42	42.00	1.65	2.93	4.15	4.84	0.10	0.99
SJR RM 46	46.00	2.04	3.91	5.29	6.32	0.10	1.00
SJR RM 50	50.00	2.69	5.48	7.86	10.05	0.08	0.98
SJR RM 54	54.00	2.85	5.67	8.13	10.26	0.08	0.99
Mossdale	56.70	3.80	7.35	10.28	12.63	0.09	1.00
Mossdale dup	56.70	3.87	7.49	10.60	13.15	0.09	1.00

Table A-13: Summary of BOD for September 20, 2007 Trial

Station	River Mile	BOD					
		5	10	20	Lo	k	R <sup>2</sup>
SJR RM 34	34.00	1.91	3.18	3.85	4.27	0.15	1.00
SJR RM 36	36.00	1.15	2.08	2.81	3.12	0.11	0.97
SJR RM 38	38.00	1.28	2.31	2.95	3.28	0.12	0.99
SJR RM 38 dup	38.00	1.25	2.29	2.93	3.29	0.12	1.00
Lt 48	39.60	2.18	3.64	4.51	4.95	0.14	0.99
SJR RM 40	40.00	1.65	2.99	3.82	4.27	0.12	0.99
SJR RM 42	42.00	2.41	4.20	5.39	5.97	0.13	0.99
SJR RM 46	46.00	3.03	5.23	6.59	7.33	0.13	1.00
SJR RM 50	50.00	3.18	6.21	8.14	9.64	0.10	1.00
SJR RM 54	54.00	3.48	6.41	8.44	9.79	0.11	1.00
Mossdale	56.70	3.82	7.33	9.56	11.23	0.11	1.00
Lt 48	39.60	1.83	3.16	4.17	4.70	0.12	0.99
SJR RM 40	40.00	1.66	3.36	4.58	5.66	0.09	1.00
SJR RM 42	42.00	2.29	4.50	5.69	6.60	0.11	1.00
SJR RM 46	46.00	3.16	5.98	7.90	9.31	0.10	1.00
SJR RM 50	50.00	3.39	6.71	9.17	11.44	0.09	0.99
SJR RM 54	54.00	2.68	5.67	7.59	9.83	0.08	0.97
Mossdale	56.70	3.35	6.60	8.72	10.61	0.10	0.99
Mossdale dup	56.70	3.83	7.28	9.60	11.31	0.10	1.00